



Introductory Lecture: The State of the Field: From Inception to Commercialization of Metal-Organic Frameworks

Journal:	<i>Faraday Discussions</i>
Manuscript ID	FD-ART-09-2020-000103.R1
Article Type:	Paper
Date Submitted by the Author:	02-Oct-2020
Complete List of Authors:	Farha, Omar; Northwestern University, Department of Chemistry Chen, Zhijie; Northwestern University, Chemistry Wasson, Megan; Northwestern University, Drout, Riki; Northwestern University, Department of Chemistry Robison, Lee; Northwestern University, Chemistry Idrees, Karam; Northwestern University, Department of Chemistry Knapp, Julia; Northwestern University, Chemistry Son, Florencia; Northwestern University, Department of Chemistry Zhang, Xuan; Northwestern University, Hierse, Wolfgang ; Merck KGaA Kühn, Clemens; Merck KGaA Marx, Stefan ; BASF SE Hernandez, Ben ; NuMat Technologies



The State of the Field: From Inception to Commercialization of Metal–Organic Frameworks

Zhijie Chen,¹ Megan C. Wasson,¹ Riki J. Drout,¹ Lee Robison,¹ Karam B. Idrees,¹ Julia G. Knapp,¹ Florencia A. Son,¹ Xuan Zhang,¹ Wolfgang Hierse,³ Clemens Kühn,³ Stefan Marx,⁴ Benjamin Hernandez,^{5,*} and Omar K. Farha^{1,2,*}

¹ Department of Chemistry and International Institute for Nanotechnology, Northwestern University, 2145 Sheridan Road, Evanston, Illinois 60208, United States

² Department of Chemical & Biological Engineering, Northwestern University, Evanston, Illinois 60208, United States

³ Merck KGaA, Darmstadt, Germany, Frankfurter Str. 250, 64293 Darmstadt, Germany

⁴ BASF SE, RC/OI - M300, Carl-Bosch-Strasse 38, 67056 Ludwigshafen am Rhein, Germany

⁵ NuMat Technologies, 8025 Lamon Avenue, Skokie, Illinois 60077, USA

*Corresponding author. Email: o-farha@northwestern.edu, ben@numat-tech.com

MAIN TEXT

ABSTRACT: As chemists and materials scientists, it is our duty to synthesize and utilize materials for a multitude of applications that promote the development of society and the well-being of its citizens. Since the inception of metal–organic frameworks (MOFs), researchers have proposed a variety of design strategies to rationally synthesize new MOF materials, studied their porosity and gas sorption performances, and integrated MOFs onto supports and into devices. Efforts have explored the relevance of MOFs for applications including, but not limited to, heterogeneous catalysis, guest delivery, water capture, destruction of nerve agents, gas storage, and separation. Recently, several start-up companies have undertaken MOF commercialization within industrial sectors. Herein, we provide a brief overview of the state of the MOF field from their design and synthesis to their potential applications, and finally, to their commercialization.

Introduction

Diverse industrial applications, including heterogeneous catalysis, adsorption, and water remediation rely on porous materials.¹⁻³ Porous materials exist in three types depending on their pore sizes: macroporous (> 50 nm), mesoporous (≤ 50 and ≥ 2 nm), and microporous (< 2 nm).⁴ Zeolites and activated carbons, two prominent classes of porous materials, are important industrial catalysts and sorbents.^{1,2,5,6} However, new porous materials will require high adsorption capacity and specificity, which the traditional porous materials lack. Owing to their many useful and attractive properties, metal–organic frameworks (MOFs) are promising next-generation porous materials with applicability in the aforementioned fields, among many others.⁷⁻¹³

MOFs, or porous coordination polymers (PCPs), comprise multitopic organic ligands and inorganic nodes (i.e. metal ions or clusters) that are assembled into porous coordination frameworks.^{7,14} Since the demonstration of permanent porosity within MOFs,^{15,16} the field has

flourished due to these materials' uniform and tunable pore sizes,¹⁷⁻²⁰ high surface areas,²¹⁻²⁵ adjustable structures, and programmable functionalities.²⁶⁻³⁷ Researchers have ultimately shown that MOFs are efficacious for heterogeneous catalysis,³⁸⁻⁴⁶ sensing,⁴⁷⁻⁵⁰ conductivity,⁵¹⁻⁵⁵ guest delivery,⁵⁶⁻⁶² water capture,⁶³⁻⁷⁵ nerve agent destruction,^{38, 76-79} toxic chemical removal,⁸⁰⁻⁸³ water purification,⁸⁴⁻⁸⁷ gas storage^{25, 88-101} and separation,¹⁰²⁻¹²¹ and as crystalline sponges.¹²²⁻¹²⁵ MOF commercialization has recently found a stronghold in targeted industries; for example, NuMat Technologies has developed ION-X for the semiconductor industry.^{126, 127}

Herein, we chronicle a historical overview of coordination chemistry with respect to porosity through highlighted studies. We also discuss an array of design approaches for MOF structures and further post-synthetic modification, including examples from serendipitous explorations that led to the discovery of important classes of MOFs. Furthermore, we feature thin films, membranes, and fiber composites based on MOF materials, while also detailing MOF porosity behavior and activation methodologies. Highlighted works throughout represent the many diverse applications of the studied MOFs. We summarize the status of the commercialization of MOF-based products and conclude with a perspective about the future directions of the MOF field.

Historical perspective

Yaghi first devised the term “metal–organic frameworks” in 1995 in his seminal report on the host-guest chemistry of MOFs.¹²⁸ However, the foundation of coordination chemistry—which studies the coordination of organic ligands to metal centers—dates back to 1893, when Alfred Werner established the basis of transition-metal coordination chemistry.¹²⁹ Werner proposed the structural configuration of the cobalt-ammine salt, which was previously formulated as $\text{CoCl}_3 \cdot 6\text{NH}_3$, to be $[\text{Co}(\text{NH}_3)_6]\text{Cl}_3$, wherein the Co(III) centers were 6-coordinated with neutral

ammonia molecules in an octahedral geometry (**Fig. 1**). In honor of his contributions, these cobalt-ammine and other closely related complexes are known as Werner complexes. The concepts of coordination number and coordination geometry first introduced by Werner provided guidelines for the experimental and theoretical development of coordination complexes, which were subsequently extended to other metal complexes such as hydrates, cyanides, thiocyanates and carbonyls.¹³⁰

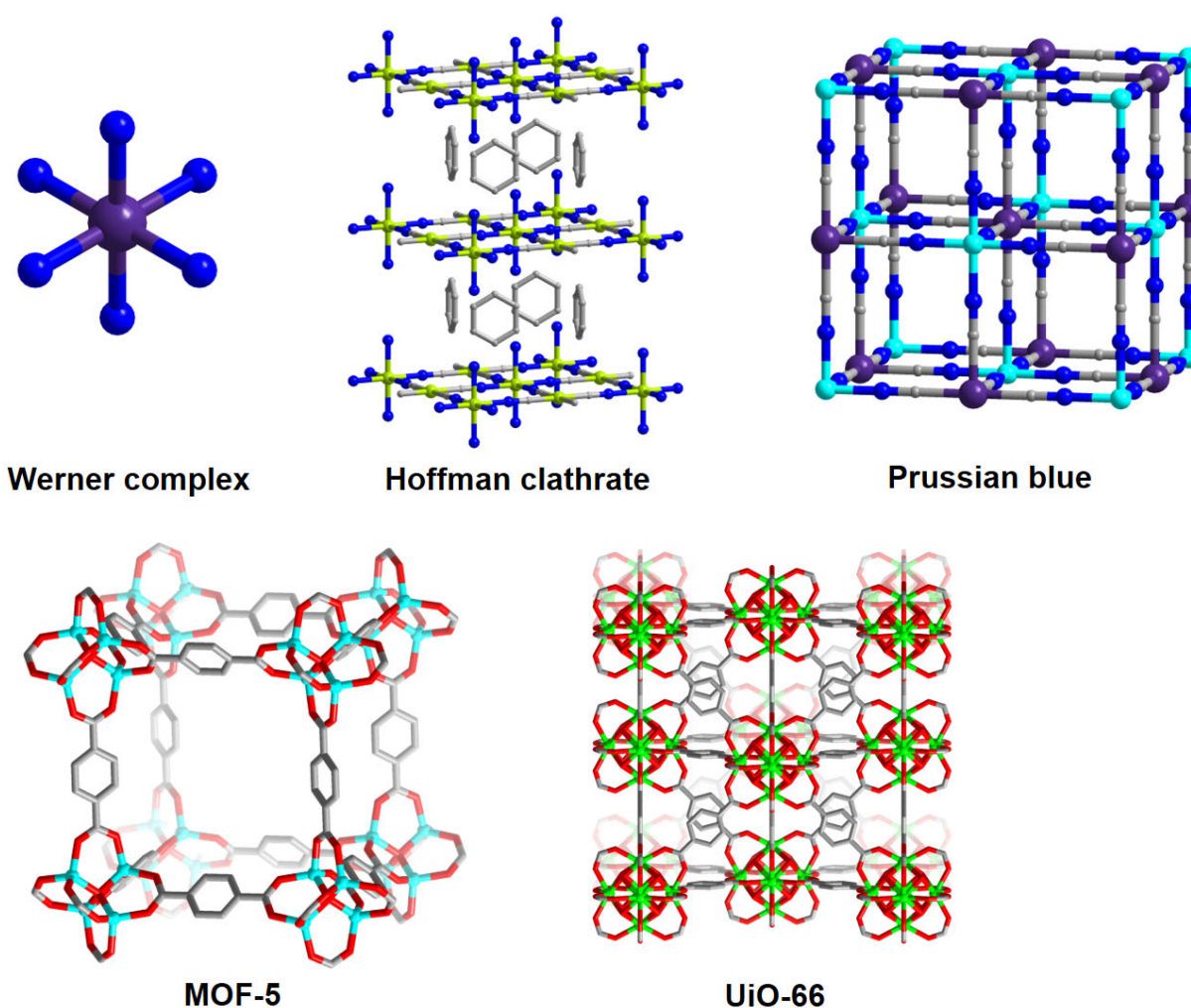


Fig. 1 Structures of a Werner complex, Hoffman clathrate, Prussian blue, and representative MOFs.

Figures were redrawn from the reported cifs.¹³¹⁻¹³⁶

The geometrical design and incorporation of chelating or bridging ligands—such as diamine-, bipyridine-, and cyanide-based ligands—into coordination complexes, allowed for the construction of other molecular architectures such as molecular polygons, polyhedrons, and even extended structures known as coordination polymers.^{8, 137-140} Hofmann clathrates and Prussian blue, formulated as $\text{Ni}(\text{NH}_3)_2\text{Ni}(\text{CN})_4 \cdot 2\text{C}_6\text{H}_6$ and $\text{Fe}^{\text{III}}_4[\text{Fe}^{\text{II}}(\text{CN})_6]_3$, respectively, are among the earliest examples of inorganic coordination polymers that exhibit 2-D and 3-D extended structures. Specifically, the cyanide group may serve as a bridging ligand coordinating to metal ions from both the -C and -N ends.¹³²⁻¹³⁵ However, in the early development of coordination polymers, the library of available ligands was limited to inorganic cyanides¹⁴¹, organic polynitriles¹⁴²⁻¹⁴⁶, and polypyridines.¹⁴⁷⁻¹⁵⁰ Due to the short linker length or stacking of linkers, resultant coordination polymers usually resulted in cavities too small to accommodate large guest molecules. Additionally, as many of these frameworks were positively charged, charge-balancing anions typically blocked the channels. One exceptional example is the synthesis of copper(I)-pyrazine honeycomb coordination polymers by Kitagawa group, and unprecedentedly, this network has organic molecules in the nanopores while the previous coordination networks have the counter ions in the pores.¹⁵¹ Of note, Zaworotko and Kitagawa groups reported $\text{Zn}(4,4'\text{-bipyridine})_2(\text{SiF}_6)]_n$ and $\text{Cu}(4,4'\text{-bipyridine})_2(\text{SiF}_6)]_n$ in 1995 and 2000, respectively.^{148, 152} Years later, this class of small-pore coordination polymers based on SiF_6^{2-} pillars turned out to be very useful for CO_2 capture.^{148, 153, 154}

The first reported MOFs with open structures and permanent porosity consisted of positively charged metal nodes and negatively charged carboxylate-based organic linkers, producing charge neutral frameworks that offered opportunities for the removal of neutral solvent guest molecules to open up the porosity.¹⁵⁵ The development of polynuclear secondary building

units (SBUs) tremendously enriched the MOF arsenal by introducing more complex building blocks which transcended the general guidelines of reticular chemistry.¹⁵⁶⁻¹⁶² These SBUs are predominantly metal-oxo clusters—binuclear paddle wheels, trinuclear clusters, hexanuclear clusters, and infinite rod-like chains,^{131, 136, 163-165}—with pendant carboxylate-terminated capping ligands as reactive handles that can be replaced by polytopic ligands to form extended MOF structures (**Fig. 2**).^{17, 155, 166-170} These findings established the molecular building-block approach and provided an immeasurable toolbox of reticular chemistry for the modular design of MOFs. As a result, the field of MOFs has burgeoned with an ever-increasing number of new structures and functionalities. The inorganic building blocks range from mononuclear to metal-cluster-based nodes, while the most common polytopic linkers are carboxylates, azolates, phosphonates, and sulfonates, due to their tailorable geometry and topicity. Thus, the integration of inorganic chemistry and organic chemistry expands access to new building blocks.¹⁷¹⁻¹⁷³ For a more detailed historical overview centered on the development of porosity in coordination chemistry and MOFs, we refer the readers to a review by Yaghi and coworkers.¹³⁰

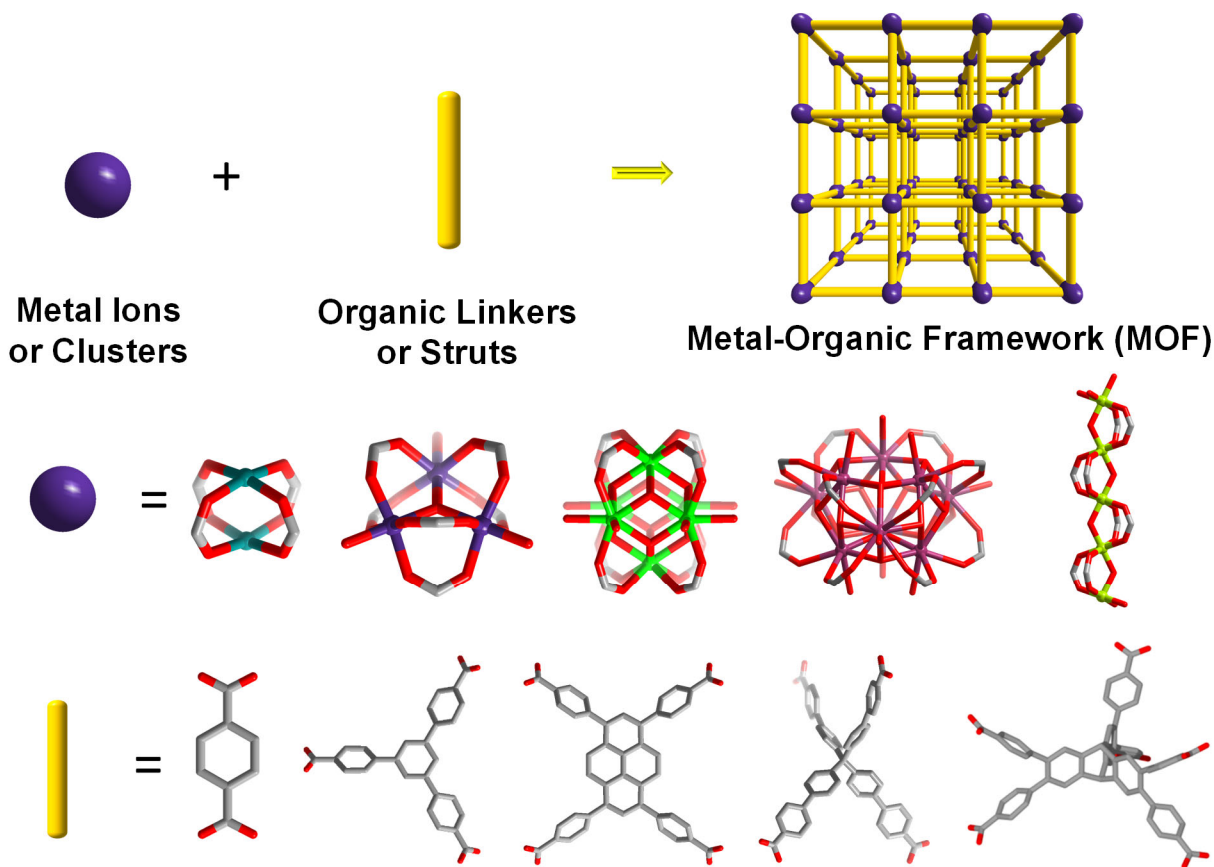


Fig. 2 Schematic representation of MOFs, which can be synthesized from diverse building units.

Design, discovery, and synthesis of metal–organic frameworks

Sir John Maddox once remarked, “*it remains in general impossible to predict the structure of even the simplest crystalline solids from a knowledge of their chemical composition,*” as contemporary scientists attempted to discover crystalline new materials.^{174, 175} The maturation of the MOF field is distinguished by the development of “designed syntheses”, for which “reticular chemistry”—pioneered by Yaghi—is essential.¹⁷⁶ Reticular chemistry relies on understanding topological nets and the ability to tailor node and linker structure to achieve a certain topology.^{17, 28, 130, 131, 155, 176-180} The iconic examples (**Fig. 3**) of reticular chemistry applied to MOF synthesis include MOF-5¹³¹ with a 6-connected **pcu** net, MOF-101¹⁸¹ with a 4-connected **nbo** net, **rht**-MOF-

1¹⁸² with a 3,24-connected **rht** net, and **alb**-MOF-1²⁷ with a 6,12-connected **alb** net. Moreover, this strategy allows for isorecticular expansion or contraction of MOF structures, functionalization of building blocks, and introduction of multivariate complexity.^{35, 102}

On the other hand, the serendipitous exploration of MOF structures is also vital for the discovery of interesting nets, which can then lead to the informed design and synthesis of isorecticular structures.^{24, 183, 184} The combination of 1,3,5-benzenetricarboxylate organic linkers and Zn₄O-based inorganic nodes yielded MOF-177²⁴ (**Fig. 3**), which exhibits a 3,6-connected **qom** net with a transitivity of [55] (i.e. 5 types of nodes and 5 types of edges); such rare transitivity is difficult to predict and account for in a designed synthesis. This fortuitous discovery led to the synthesis of a series of highly porous MOFs displaying the **qom** net such as MOF-177, MOF-180 and MOF-200.²³

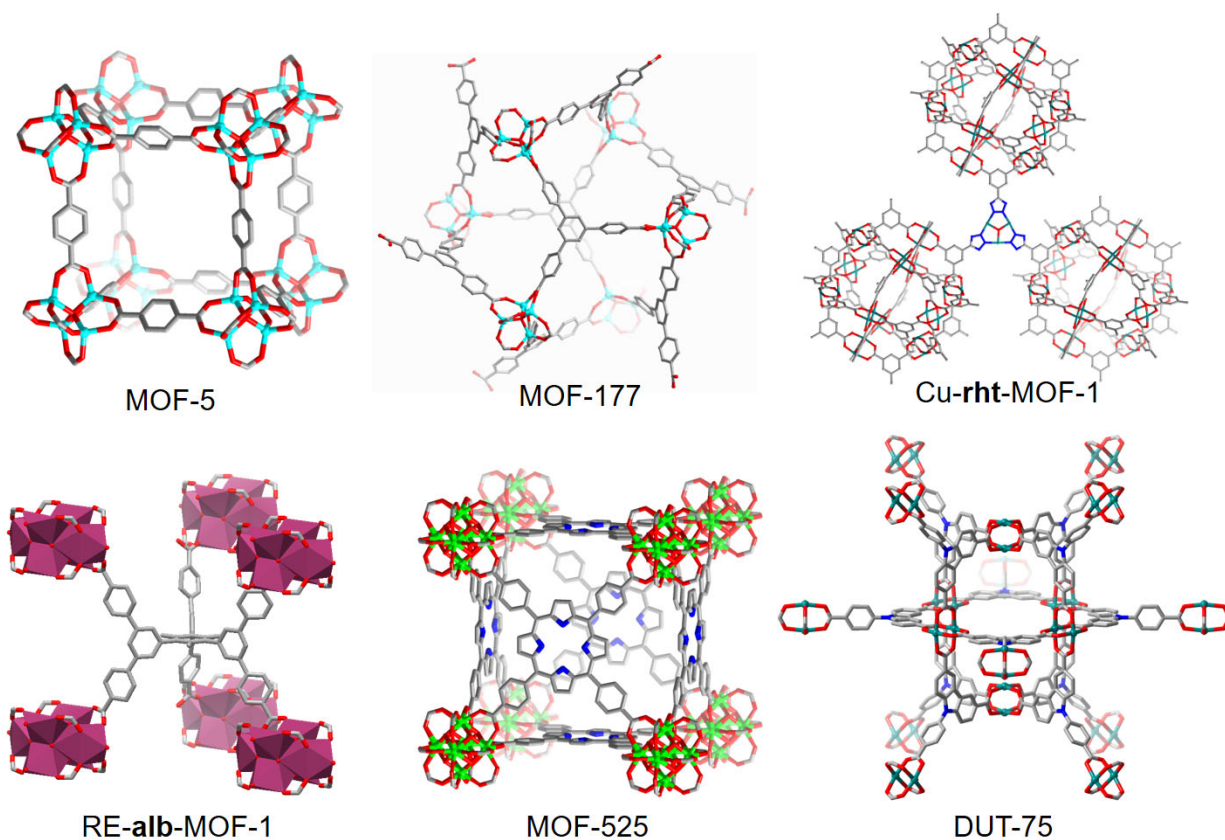


Fig. 3 Some examples of the design, discovery, and synthesis of MOFs. Figures were redrawn from the reported cifs.^{24, 27, 131, 182, 185, 186}

Stable MOFs based on high valent metal nodes and carboxylate linkers are important and attractive due to their stability and related properties.^{9, 26, 70, 93, 136, 168, 169, 185, 187-199} The first synthesis of UiO-66 in 2008 immediately ushered in a new sub-field of MOFs, zirconium-based MOFs (Zr-MOFs).^{26, 136, 185, 193, 194, 200} We recently reviewed the application of reticular chemistry to the design and synthesize diverse Zr-MOFs was covered in our recent review²⁰⁰ and employed such principles to rationally synthesize a series of Zr-MOFs with the highly connected **alB** net.²⁰¹ Isoreticular chemistry allows for the fine tuning of pore size and pore geometry via isoreticular contraction or expansion. Of note, the discovery of new inorganic building blocks, particularly highly stable ones, is crucial for further advancement of the MOF field.^{19, 168, 202}

In the past decades, researchers have employed several key synthetic approaches to attain new MOFs, including but not limited to, the molecular building block (MBB)^{17, 155, 166, 176} approach introduced by Yaghi and co-workers, the two-step crystal engineering²⁰³⁻²⁰⁵ method first reported by Zaworotko and collaborators, and the supermolecular building block (SBB)^{182, 206-210} approach established by Eddaoudi and colleagues. The SBB approach has yielded highly porous **rht**-MOFs, including the NU-100 series^{21, 92} reported by Farha and co-workers and PCN-68²¹¹ by Zhou and colleagues. Similarly, Kaskel and coworkers also relied on the SBB approach to isolate copper paddlewheel containing **ftw**-MOFs (i.e. DUT-49^{212, 213} and DUT-75¹⁸⁶).

Typically, the first step to MOF design involves targeting a specific network or topology tailored towards a chosen application. Edge-transitive or minimal edge-transitive nets are the best targets for the design and synthesis of MOFs.^{26, 161, 182, 200, 214-217} Augmentation of the parent net facilitates MOF design. Within the resulting augmented net, the vertex in the original net is

replaced by a vertex figure.²¹⁸ The relevant building units (i.e. organic, inorganic, or supermolecular building blocks) can feasibly be selected as a matching vertex figure of the augmented net. The final step, which is oftentimes most challenging, is identifying the optimal conditions to crystallize the building units into the targeted product. For example, to synthesize a 4,12-connected **ftw**-MOF, researchers should select chemical entities with the vertex figures of a cuboctahedron and a square as the starting materials. When the 12-connected cuboctahedral Zr_6 node and 4-connected square porphyrinic carboxylate ligand are combined, Zr-**ftw**-MOFs are one possible product.^{185, 219-222} Similarly, the combination of a 12-connected cuboctahedral SBB and 4-connected tetracarboxylate ligand yields **ftw**-MOFs as the preferred product, as evidenced with DUT-49.^{212, 213} As another example, the assembly of 3-connected carbazole-based carboxylate linkers and copper paddlewheels can also form **ftw**-MOFs as the carbazole moiety is able to form a 12-connected cuboctahedral SBB, while the carboxylate portion forms a 4-connected copper paddlewheel, as illustrated by DUT-75.¹⁸⁶

Postsynthetic Modification

Postsynthetic approaches permit unique structural features and cooperative functionalities in MOFs (**Fig. 4**).²²³⁻²⁴⁰ These stepwise synthetic methods provide alternative solutions for targeting desired functional MOF materials in addition to *de novo* syntheses. Here, we briefly review some examples of postsynthetic modifications, including the exchange of metal nodes or organic ligands, as well as solvent assisted linker incorporation (SALI).

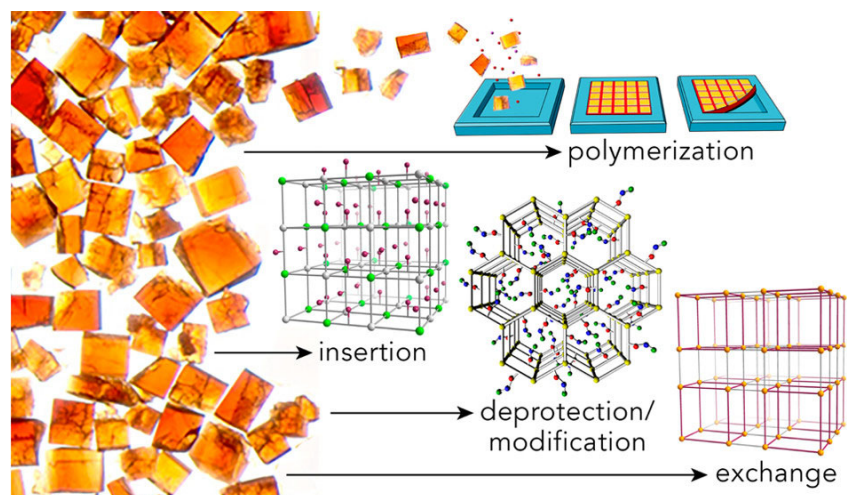


Fig. 4 A schematic representation of postsynthetic approaches in MOFs. Figure was reprinted with permission from ref²²³. Copyright 2017, American Chemical Society.

Metal-Node Exchange

The exchange of metal-nodes provides an alternative synthetic route to make synthetically challenging or inaccessible MOFs (**Fig. 5**).^{191, 241-250} An early example of metal-node exchange involved the complete exchange of Cd^{2+} for Pb^{2+} under mild conditions within the cubic MOF, $\text{Cd}_{1.5}(\text{H}_3\text{O})_3[(\text{Cd}_4\text{O})_3(\text{hett})_8] \cdot 6\text{H}_2\text{O}$, where H_3hett denotes an ethyl-substituted truxene tricarboxylic acid.²⁴¹ In the same work, Kim and co-workers demonstrated the transferability of the method to the lanthanide cations $\text{Nb}(\text{III})$ and $\text{Dy}(\text{III})$, illuminating a new synthetic route for synthesizing both d-block and non-d-block MOFs.²⁴¹ Our recent review provides additional insights regarding the trans-metalation of MOFs and details the use of this strategy to attain isostructural MOFs.²⁵¹ The Zhou group also recently summarized their progress towards stable MOFs via metal-node exchange.²⁵² This technique is essential for the synthesis of synthetically difficult to isolate MOFs. For example, metal-node exchange allows for the access of highly porous, stable Cr-MOFs for CO_2 adsorption,²⁵³ water capture,¹⁹² and methane hydration.²⁵⁴

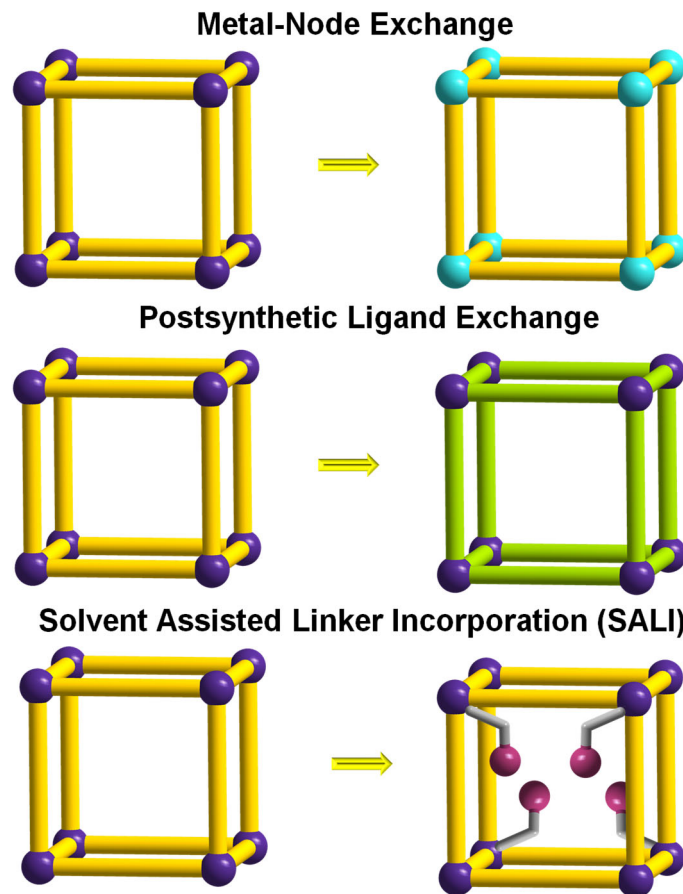


Fig. 5 Schematic illustration of postsynthetic modifications in MOFs.

Postsynthetic Ligand Exchange

Beyond altering the metal nodes, we can look toward postsynthetic ligand exchange (PSE),²⁴³ or solvent-assisted linker exchange (SALE), to synthesize MOFs which are unattainable via traditional *de novo* routes.^{226, 228, 233, 234, 243-245, 255-259} PSE may also be advantageous in tuning the pore sizes of MOFs, manipulating MOF reactivity, and furthermore controlling catenation.^{233, 260, 261} In a typical solvothermal synthesis, using organic linkers functionalized with electron-rich groups may result in the functional group coordinating to the metal rather than at the expected binding site, disrupting the crystallinity and uniform porosity within a MOF and possibly even preventing MOF formation. To circumvent this issue, Cohen and coworkers exchanged the

benzene dicarboxylate (BDC) linkers of UiO-66 with functionalized derivatives while maintaining overall crystallinity and porosity; of note, they synthesized UiO-66-OH and UiO-66-N₃, in spite of previous attempts via *de novo* methods.²⁵⁶ Postsynthetic ligand exchange functionalizes the parent MOFs to achieve better collective material performances for specific applications, such as catalysis,^{259, 262, 263} gas capture,^{228, 264, 265} or photodynamic therapy.²⁵⁷

Solvent Assisted Ligand Incorporation (SALI)

Certain node structures contain neutral or anionic moieties, such as hydroxyl groups and water molecules, that may be exchanged for more strongly binding ligands.²⁶⁶⁻²⁶⁸ SALI allows for functionalization of the node without sacrificing crystallinity. Attaching functional carboxylic acids to the nodes imparts additional properties to the pores beyond shape and size. One early example of SALI involved the binding of perfluoroalkyl carboxylic acids on the nodes of the zirconium-based NU-1000 for CO₂ capture based on polarizability.²⁶⁶ Recently, researchers have used SALI to tune the hydrophobicity of MOF surfaces for organic/water separation²⁶⁹ and to tailor the node environment for ethylene hydrogenation.²⁷⁰ Beyond providing an additional avenue to alter the reactivity of MOFs, we have demonstrated that by post-synthetically incorporating structural organic linkers, we can modify the bulk mechanical properties of MOF materials.²⁷¹ SALI serves as a valuable tool to not only introduce a variety of cooperative chemical reactivities to our materials, but also to enhance the mechanical stability of MOFs, which will be crucial for expanding industrial implementation of these nanomaterials.

MOFs on Supports

MOF thin films

The support of MOFs on thin films developed out of a necessity to understand MOF formation beyond the construction of SBUs and nucleation of crystallites.^{272, 273} Wöll, Fischer, and coworkers reported a synthetic route for MOF assembly on thin films in 2007.²⁷⁴ Using a step-by-step process, they exposed functionalized organic surfaces to node and linker solutions in an alternating fashion, rather than using a one-pot, solvothermal synthesis.²⁷⁴ This step-wise method allowed researchers to modulate MOF thickness by controlling the number of exposure cycles. Wöll and coworkers also utilized liquid-epitaxy to address interpenetration of MOFs; slower synthesis techniques and the coupling of MOF growth to a functionalized organic substrate selectively formed a MOF with only one orientation.²⁷⁵ Since then, researchers have implemented MOFs on thin films for specific applications. Hupp and co-workers utilized step-by-step layer deposition to synthesize luminescent, porphyrinic MOFs on the surface of silicon to investigate charge-transfer towards solar energy conversion applications.²⁷⁶ Synthesizing large-scale (i.e. wafer-scale) monolayer sheets remains challenging, but is of great importance for electrical applications. Park and coworkers have recently reported the large-scale synthesis of high-quality 2D porphyrinic MOF thin films with a technique called laminar assembly polymerization (**Fig. 6**).²⁷⁷ As made evident by these examples and many others, the growth of MOFs on thin films enables greater control over MOF assembly.^{272, 273}

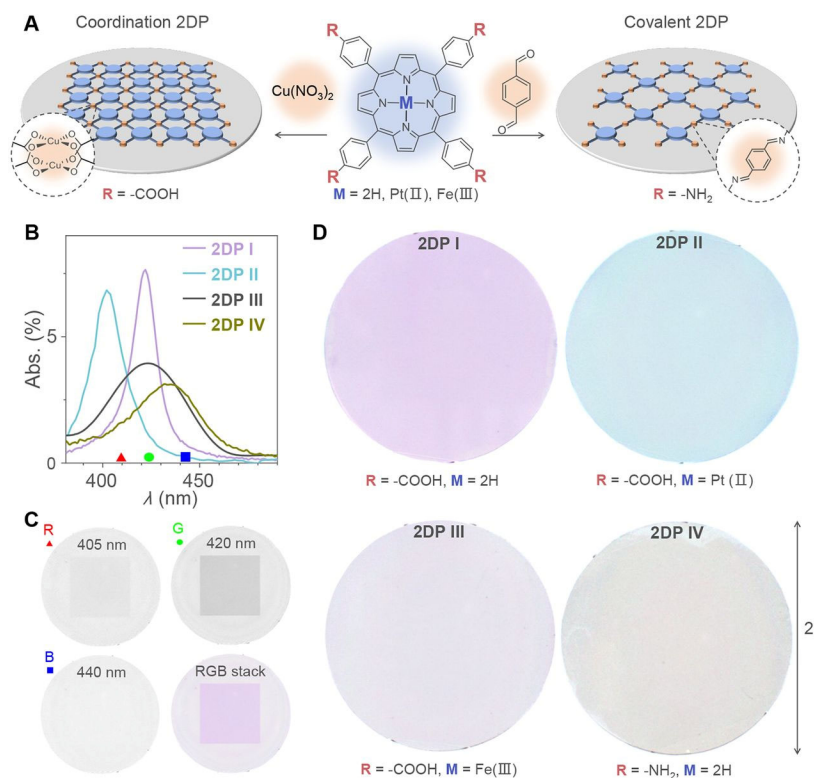


Fig. 6 Wafer-scale monolayer 2D MOFs. (A) assembly of 2D MOFs. (B) Absorption spectra of monolayer of 2D MOFs. (C-D) Hyperspectral transmission images at the wavelengths of 405, 420, and 440 nm, and resultant false-color images of 2D MOFs with sizes of 1-inch-square and 2-inch wafers. Reproduced from ref.²⁷⁷ with permission from the American Association for the Advancement of Science, Copyright 2019.

MOF Membranes

The uniform porosity of MOFs, coupled with their 2-D growth capabilities, motivates their incorporation onto membranes for molecular separations.²⁷⁸ One prevalent type of MOF membranes is based on zeolitic imidazolate framework (ZIF), favored for its stability and tunability. Seminal work by Jones, Nair, and coworkers successfully deposited ZIF-8 onto polymeric fibers for efficient alkane gas separation.²⁷⁹ By precisely alternating solvent exposure during the deposition, the authors achieved a high control over the orientation of ZIF-8, which is

promising for commercial synthesis.²⁷⁹ Tsapatsis, Ma, and coworkers expanded on this work with ZIF-based membranes and exposed ZIF-8 on alumina to additional 2-methylimidazole, which resulted in a porous material that achieved separations of propylene/propane (**Fig. 7**).²⁸⁰

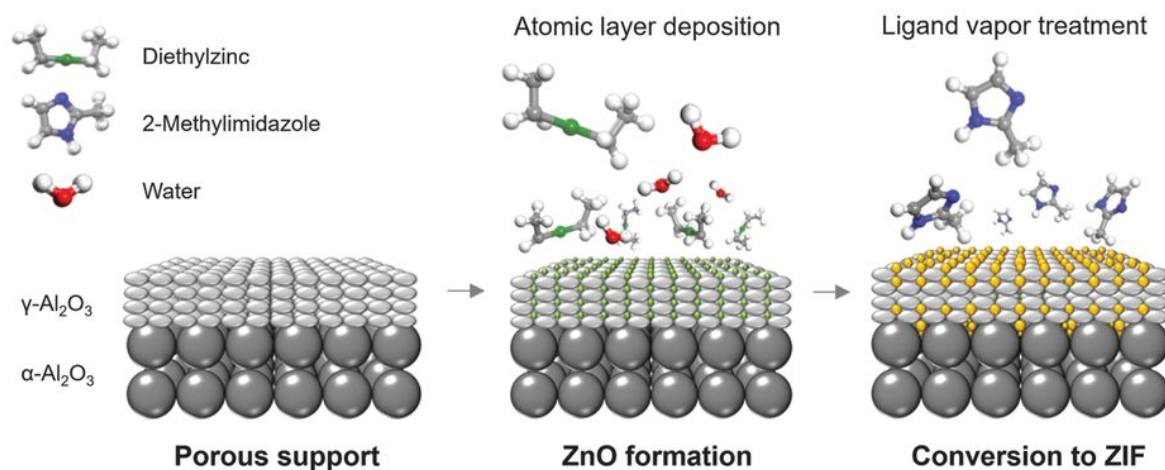


Fig. 7 A scheme of the all-vapor-phase ligand-induced membrane fabrication process for ZIF-8. Reproduced from ref.²⁸⁰ with permission from the American Association for the Advancement of Science, Copyright 2019.

MOFs on Fibers

Depositing MOFs on fibers enables their usage in suits and masks for the uptake, and sometimes detoxification, of various toxins.^{77, 281-285} By utilizing flexible fibrous substrates, we could mitigate engineering problems that arise when implementing MOFs in practical applications. Parsons and coworkers demonstrated that functionalized UiO-66 grown on fibers as a “nano-kebab” efficiently degrades chemical warfare agents (CWAs) and associated simulants.²⁸¹ Wang and coworkers reported that MOFs electro-spun onto polymeric fibers could efficiently, collectively, and selectively capture particulate matter and SO_2 when presented as a mixture with N_2 , indicating viability in pollution treatment (**Fig. 8**).²⁸² Additionally, we have recently integrated MOF-808 and

polyethylenimine (PEI) on the surface of cotton fibers for the efficient destruction of nerve agents.⁷⁷

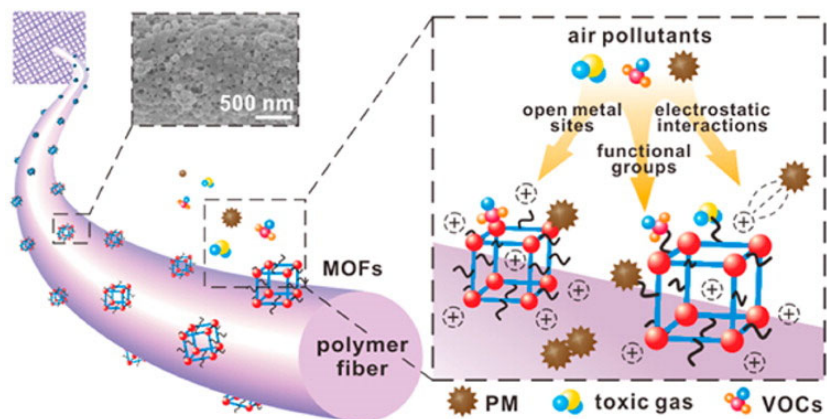


Fig. 8 A scheme of proposed capture mechanism of the MOF/fiber composites for air pollutants. Reproduced from ref.²⁸² with permission from the American Chemical Society, Copyright 2016.

Porosity and activation procedures of MOFs

Despite having large pore sizes, the permanent porosity of MOFs was not achieved until the late 1990s.^{15, 16, 286} Large channels or cavities in MOFs are of great interest because they provide the high porosity and diffusion capability necessary for countless applications. Permanent porosity, however, is also required for MOFs to be considered viable materials. In 1997, Kitagawa and coworkers demonstrated gas uptake at high pressures and room temperature using $\{[M_2(4, 4'$ -bpy) $_3(NO_3)_4] \cdot xH_2O\}_n$ ($M = Co, Ni, Zn$) with microporous channel-type cavities (**Fig. 9**).¹⁵ The unique 3-D structures showed a rapid increase in gas uptake up to 5 atm, mainly due to the diffusion of gases into the framework cavities; structural deformation was not observed. Yaghi and coworkers demonstrated the permanent porosity and surface area of MOF-2, Zn(BDC), through gas uptake measurements at low temperatures and low pressure.¹⁶ This distinction is very important when determining porosity of MOFs because structural deformation becomes more

apparent in this region. Along with low temperature and low pressure, IUPAC recommends using the Brunauer-Emmett-Teller (BET)²⁸⁷ method to determine porosity and surface area. Importantly, the BET method should be applied in the low-pressure region of $0.05 < p/p_0 < 0.3$ at the boiling temperature of the gas. Considering microporous MOFs, researcher may perform the calculation over a much smaller low-pressure region. To obtain apparent BET areas from gas adsorption isotherms of porous materials, four BET consistency criteria should be satisfied.^{288, 289}

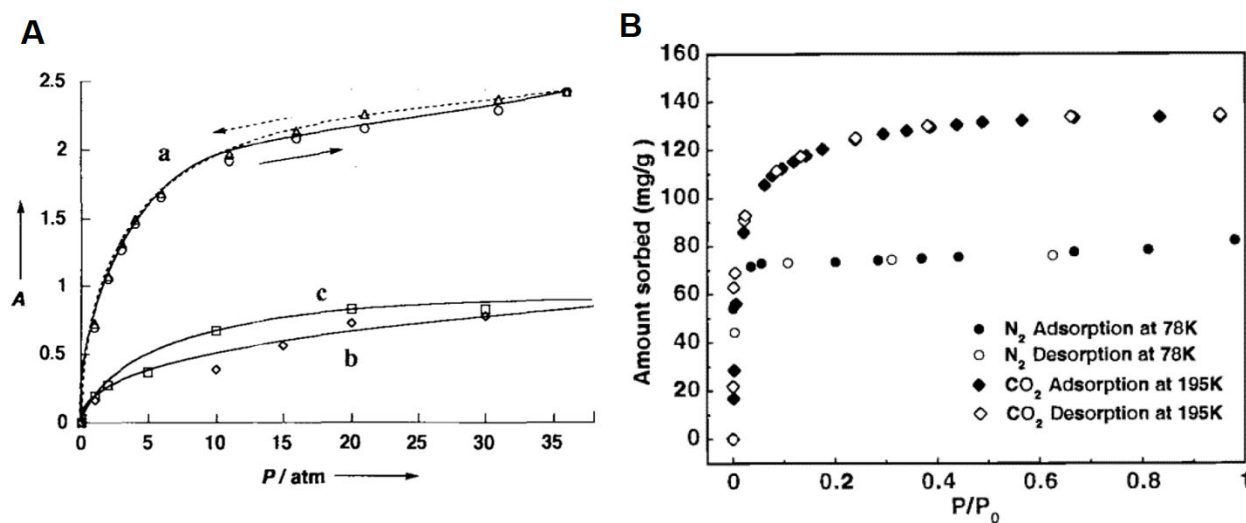


Fig. 9 (A) High pressure sorption of $[\text{Co}_2(4,4'\text{-bipyridine})_3(\text{NO}_3)_4] \cdot x\text{H}_2\text{O}$ at 298K. CH₄ (a), N₂ (b), and O₂ (c). Reproduced from ref.¹⁵ with permission from the John Wiley & Sons Inc (Copyright 1997). (B) Gas adsorption isotherms of MOF-2, Zn(BDC). Reproduced from ref.¹⁶ with permission from the American Chemical Society (Copyright 1998).

Nonetheless, preserving permanent porosity remains a challenge for certain flexible MOFs, which are inherently fragile and/or highly porous. Typically, thermal activation under dynamic vacuum thoroughly removes solvent molecules from the pores of a MOF.^{21, 92, 290} On occasion, such conditions are not adequate to remove all solvent molecules from the channels. Alternatively, these harsh activation conditions could induce channel collapse, both of which yield different

surface areas than what is theoretically calculated based on single crystal structures. To overcome this, Yaghi and colleagues cleverly demonstrated a method of exchanging the synthesis solvent to a lower boiling point solvent with low surface tension.¹⁷ This strategy decreased activation time, permitted milder activation conditions, and minimized framework collapse. While this method successfully addressed the permanent porosity problem in certain MOFs, it was not applicable for highly delicate MOFs. Therefore, researchers have since developed alternative physical methods to preserve a structure's porosity and prevent pore collapse. One example developed by Farha, Hupp, and coworkers utilized supercritical carbon dioxide, traditionally used to activate of polymers or aerogels.^{290, 291} By first exchanging the solvent with liquid CO₂ and subsequently achieving the supercritical phase, activation proceeds without pore collapse during solvent removal. The use of a supercritical fluid avoids the liquid to gas phase transformation, thereby eliminating surface tension and capillary forces that often induce pore collapse under traditional activation conditions. This technique has allowed for the activation of a series of highly porous materials with ultrahigh porosity and surface area.^{21, 92, 292} Another example by Lin and coworkers successfully demonstrated a freeze-drying activation method that significantly enhanced the surface areas of certain MOFs.²⁹³ This method involved solvent exchange to benzene, followed by benzene removal by freeze-drying; however, due to the toxicity of benzene, researchers employing this method must exercise utmost caution.

Flexibility

Flexibility in MOFs, pioneered by Kitagawa and coworkers, is highly desirable for gas storage and delivery.²⁹⁴⁻³⁰⁵ Much like conformational changes within enzymes, the flexible structure of MOFs enhances cooperative guest interactions through channel and cavity modifications. More rigid materials, such as zeolites, cannot demonstrate such behavior. External

stimuli such as light, heat, electric fields, pressure, or guests can influence the structure of MOFs without sacrificing MOF crystallinity.^{164, 189, 295, 297, 306-309} Moreover, reversible flexibility and retained crystallinity in MOFs, combined with their high porosity and surface area, further extend their practical applications into separation and storage.^{90, 112, 310, 311} Researchers have reported several different modes of flexibility in MOFs such as breathing, swelling, linker rotation, and subnetwork displacement, and Fischer, Kaskel, and coworkers have reviewed these extensively (Fig. 10).²⁹⁵

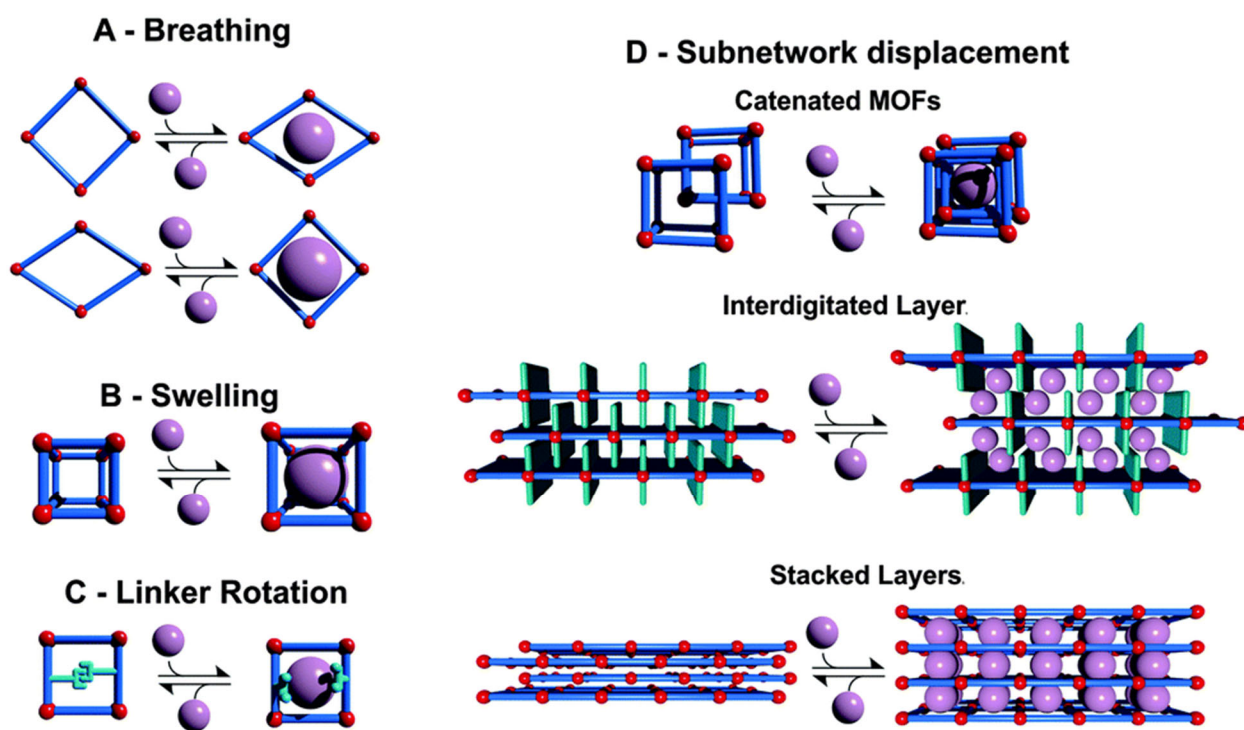


Fig. 10 Different modes of flexible MOFs. Reproduced from ref.²⁹⁵ with permission from The Royal Society of Chemistry, Copyright 2014.

Flexibility in MOFs also allows for dynamic control of pore and aperture dimensionality. This tunability regulates diffusion in these porous materials, rendering them important for separation and storage.^{300, 302, 312-317} The design and control of diffusion processes in MOFs poses

challenges due to the need for contracted pore apertures alongside accessible channels that can regulate the flow of guest molecules. Taking advantage of the reversible structural changes inherent to flexible MOFs, Kitagawa and colleagues designed a diffusion regulated porous material with kinetic gate functionality that enables efficient gas separation and storage (**Fig. 11**).³¹⁸ They used temperature as an external stimulus to control the pore and aperture dimensionality, thereby facilitating kinetic-based cooperative gas separation of oxygen/argon and ethylene/ethane with high selectivity.

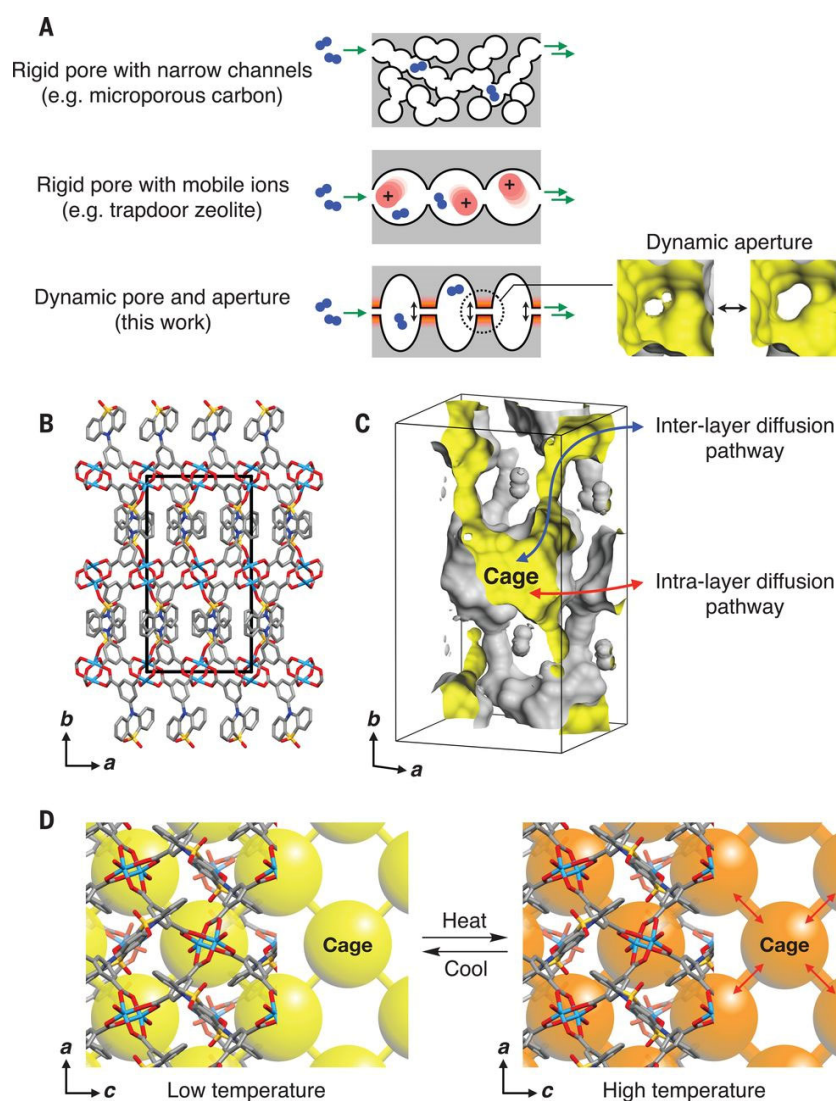


Fig. 11 Schematic diagram of a diffusion-regulatory PCP. Reproduced from ref.³¹⁸ with permission from The American Association for the Advancement of Science, Copyright 2019.

In addition to temperature, external stimuli such as guest interactions with a flexible framework can impart desirable adsorption phenomena, such as improved gas uptake at higher pressure points. Kaskel and colleagues reported an interesting case of negative gas adsorption transitions (**Fig. 12**).²¹² DUT-49 showed spontaneous gas desorption after reaching a certain pressure point. This negative gas adsorption resulted from structural deformation and pore contraction, which forced guest molecules to spontaneously desorb from the framework. In collaboration with Coudert group, they performed quantum chemistry calculations to support that adsorption triggered the structural transition. This counterintuitive phenomenon holds great potential in technologies requiring pressure amplification in micro- and macroscopic system engineering.

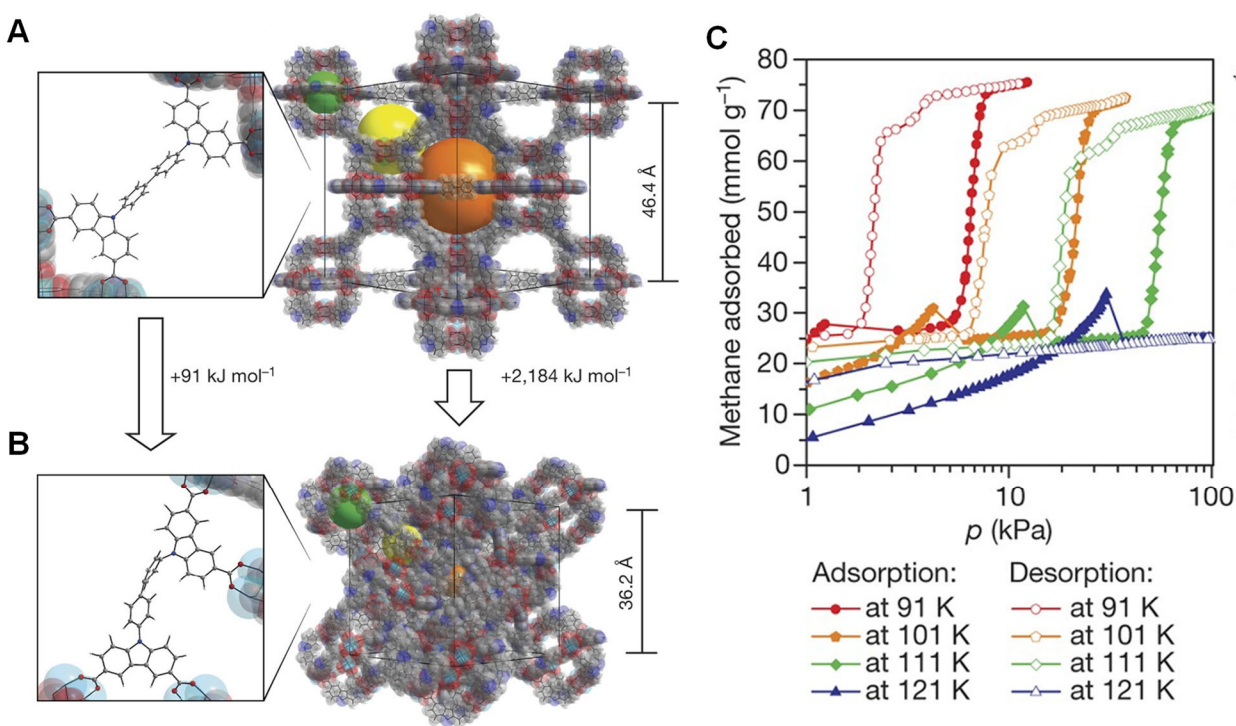


Fig. 12 Structure of DUT-49*op* (A) and DUT-49*cp* (B). Methane adsorption isotherms at different temperatures (C). Reproduced from ref.²¹² with permission from Springer Nature (Copyright 2016).

Integrating flexible MOFs into thin films can further harness their structural flexibility, expanding their applicability into solid-state and microelectronic devices. Fischer and colleagues developed Cu-based layered-pillared frameworks anchored at surfaces using liquid-phase epitaxy with such aforementioned applications in mind (**Fig. 13**).³¹⁹ These frameworks displayed unique structural flexibility and transformations during methanol sorption. Interestingly, the structural responsiveness of the surface-anchored framework differed from the bulk material. With this observation, they systematically controlled structural transformations by varying crystallite dimensions and orientation. Such tunable flexibility is highly sought after in the design of thin-film selective sensors.

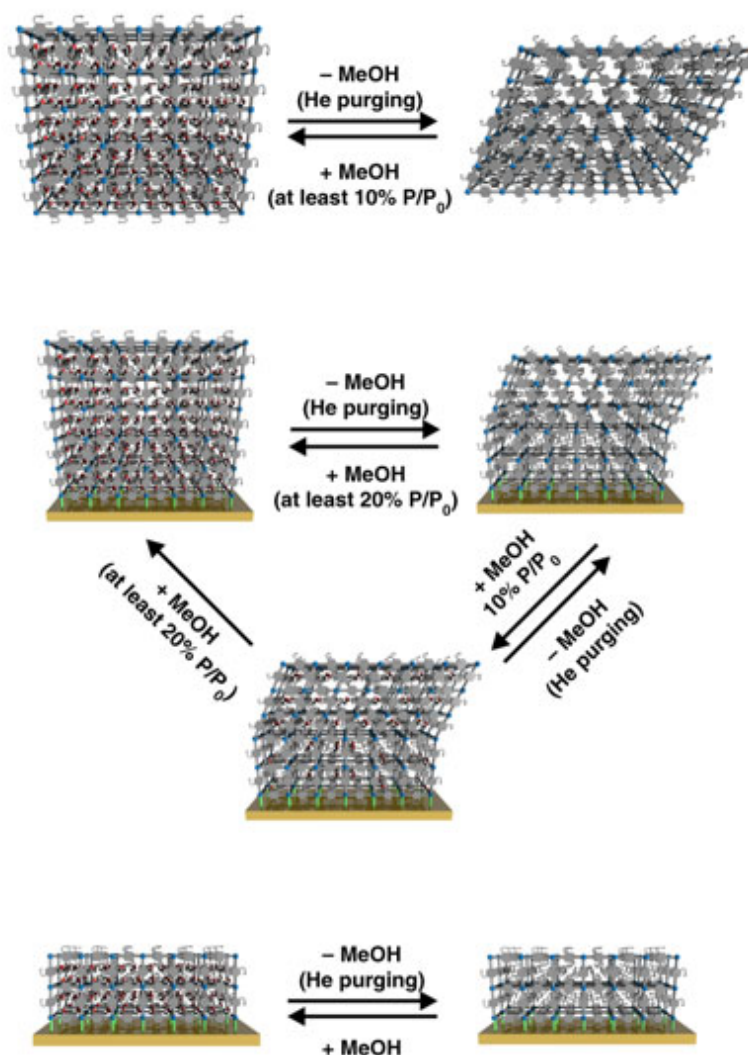


Fig. 13 Illustration of controlled structural flexibility of Cu-based layered-pillared MOFs anchored at surfaces. Reproduced from ref.³¹⁹ with permission from Springer Nature (Copyright 2019).

Applications

The ease of design and synthesis of MOFs through reticular chemistry and their inherent permanent porosity and crystallinity allow researchers to design MOFs for specific purposes. For instance, we can synthesize MOFs to exhibit specific pore sizes and shapes, withstand increased thermal temperatures, aqueous media, acidic or basic conditions, or display affinity for a specific

toxin. Researchers have demonstrated the utility of MOFs in many applications such as gas storage, separation and capture, catalysis, drug storage and delivery, and chemical sensing, among others. In the following sections, we focus on noteworthy results in catalysis and gas separation, and briefly discuss their potential for further development in these areas. While several other potential applications exist, a comprehensive review of all of these would become exhaustive.

Gas Storage

Methane storage

Methane gas is an attractive alternative transitional fuel to gasoline because it emits significantly less CO₂ upon combustion. However, the operation of methane powered vehicles would require high pressure compression (250 bar), which is costly and unsafe for vehicular on-board storage tanks.³²⁰ Since MOFs are porous and lightweight hybrid materials, they could potentially physisorb methane at high density and low pressure, allowing for the storage of methane to power vehicles. MOF-based methane storage technologies may even enable methane to power vehicles under lower pressures (e.g. 100 bar) than is needed, if no porous material is used in the tank.^{23, 88-91, 93, 213, 320-327} Of note, the cooperative gas sorption phenomena in flexible MOFs could lead to sigmoidal sorption profiles, thus resulting in a higher working capacity for gas storage than that of rigid MOFs.^{300, 304, 328-330} The US Department of Energy (DOE) established a gravimetric storage capacity of 0.5 g/g at room temperature and a volumetric storage capacity of 263 cm³ (STP) cm⁻³ as targets for the development of on-board storage and delivery systems. Farha, Yildirim and coworkers assessed the volumetric and gravimetric storage capacities in addition to the working capacities of several of the most promising MOF adsorbents.⁸⁹ They surprisingly discovered that of the six candidates tested -- PCN-14, UTSA-20, HKUST-1, Ni-MOF-74, NU-111, and NU-125 -- HKUST-1 exhibited a high volumetric methane uptake (230 cm³ (STP) cm⁻³

at 35 bar and $270 \text{ cm}^3 \text{ (STP) cm}^{-3}$ at 65 bar) at room temperature. The authors suggested that HKUST-1 should become the new methane storage benchmark material against which all potential MOF candidates should be tested. However, the authors stress that the working capacity, defined as the difference in uptake at two pressures (65 and 5 bar), is the most important metric by which a material should be evaluated as a potential adsorbent for methane, rather than either volumetric or gravimetric uptake. The working capacity ultimately determines how far a car can drive when powered by methane gas. In this regard, HKUST-1 ($190 \text{ cm}^3 \text{ (STP) cm}^{-3}$), NU-125 ($183 \text{ cm}^3 \text{ (STP) cm}^{-3}$), and NU-111 ($180 \text{ cm}^3 \text{ (STP) cm}^{-3}$) all displayed competitive working capacities.

A seminal example of MOFs applied to gas storage, specifically methane storage, is Al-**soc**-MOF-1 (**Fig. 14**).⁹³ Eddaoudi and coworkers demonstrated elegant reticular chemistry in synthesizing this MOF, which comprised aluminum trinuclear clusters and tetratopic ligands and displayed very high surface area and porosity. Due to the unique sizes and shapes of the MOF pores, the researchers achieved the best compromise between volumetric and gravimetric methane uptake.

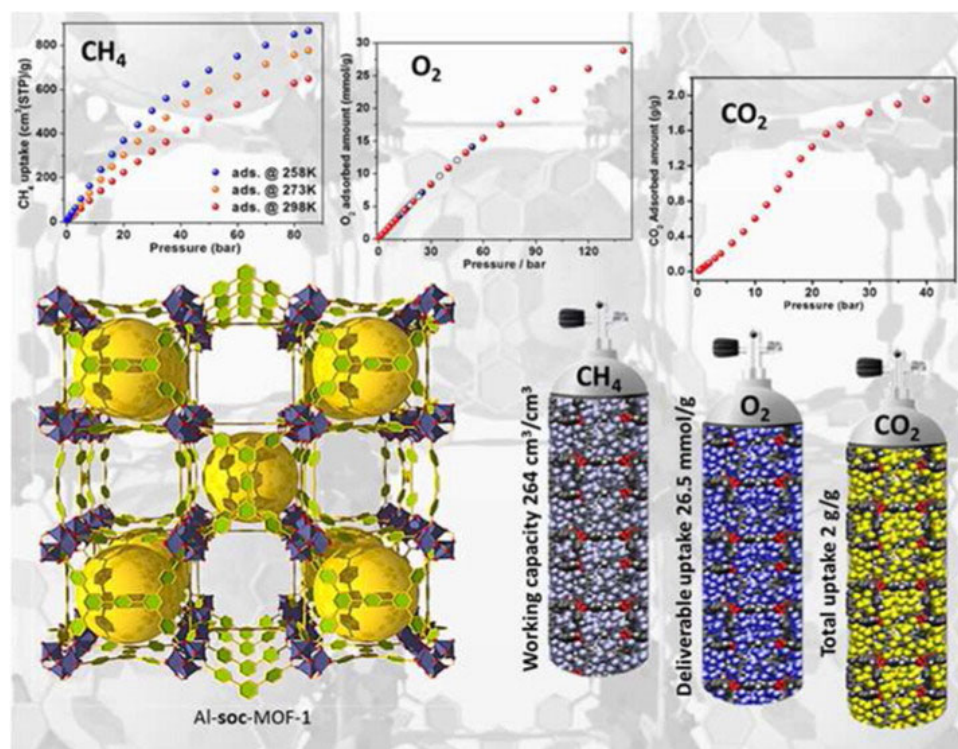


Fig. 14 Al-soc-MOF-1 for gas storage of methane, oxygen, and carbon dioxide. Reproduced from ref.⁹³ with permission from the American Chemical Society (Copyright 2015).

We recently reported the simulation-motivated synthesis of a class of highly porous MOFs, NU-1501-M (M = Al or Fe), based on the assembly of metal trinuclear clusters and trigonal prismatic hexacarboxylate linkers.²⁵ NU-1501 is an extended isorecticular structure of NU-1500 (**Fig. 15**)¹⁷⁹ and shows concurrently high gravimetric and volumetric surface areas. High-pressure gas sorption measurements revealed that NU-1501 has notable balanced gravimetric and volumetric storage performance. For example, at 100 bar, NU-1501-Al displays impressive gravimetric methane uptakes of $\sim 0.54 \text{ g g}^{-1}$ and $\sim 0.66 \text{ g g}^{-1}$ at 296 K and 270 K, respectively. The 5-100 bar deliverable capacities at 296 K and 270 K for NU-1501-Al are 0.50 g g^{-1} and $\sim 0.60 \text{ g g}^{-1}$ while having balanced high volumetric methane working capacities. NU-1501-Fe has a comparable methane storage performance to NU-1501-Al.

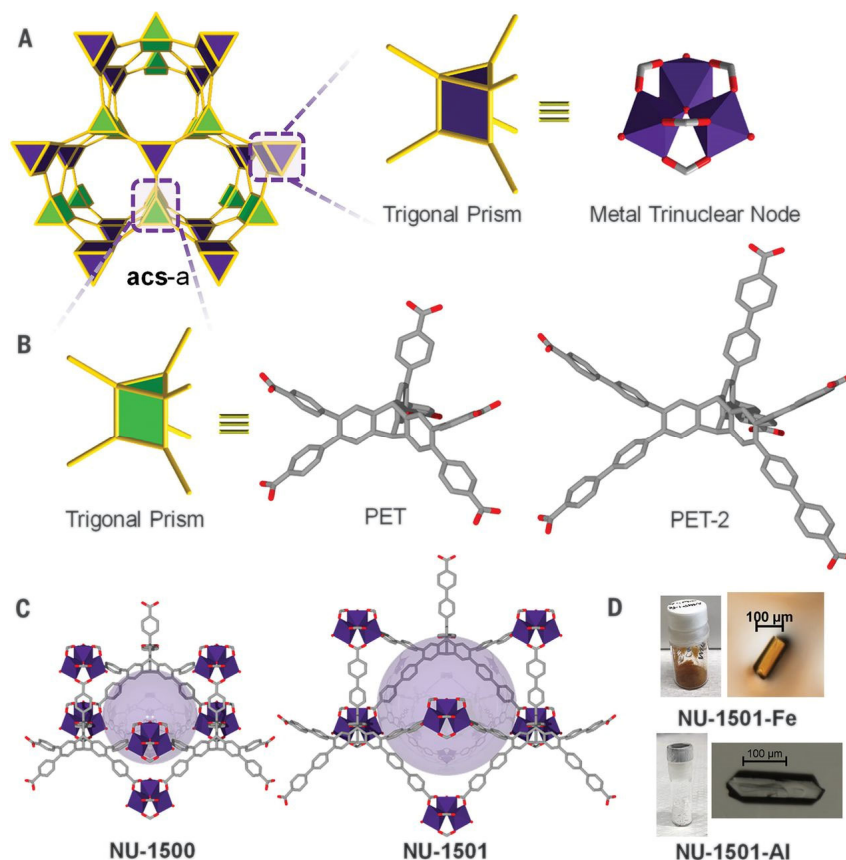


Fig. 15 Schematic representation of the design and synthesis of NU-1501. Reproduced from ref.²⁵ with permission from The American Association for the Advancement of Science, Copyright 2020.

Hydrogen storage

Hydrogen (H₂) gas is a clean alternative fuel because water is the only byproduct of the fuel cell cycle.³³¹ Fuel cell electric vehicles (FCEVs) use a propulsion system like that of electric vehicles whereby a fuel cell converts energy stored as H₂ into electricity. In contrast to conventional combustion engines, FCEVs do not produce greenhouse gas emissions.³³² The current drawback to this technology lies in the storage of H₂ onboard the vehicle; H₂ is only weakly interacting at ambient pressures and temperatures. Thus, the onboard storage of hydrogen requires low temperatures and high pressures in order to store enough fuel to drive the vehicle reasonable distances. Adsorbent materials, such as MOFs, that can store the gas at ambient pressure and

temperature are an alternative to these energy intensive and potentially unsafe cooling and compressive storage systems.³²⁰

The DOE has also established metrics for the development of on-board storage and delivery systems for H₂ gas. The 2020 DOE targets comprise a gravimetric storage capacity of 4.5 wt.% and a volumetric storage capacity of 30 g/L.³³³ To date, no adsorbents have reached these targets. The volumetric usable capacity (**Fig. 16**), defined as the total amount of H₂ adsorbed between 5 and 100 bar in the total adsorption isotherm, is the most important factor when evaluating MOF materials for H₂ storage. Striving to reach these targets, Kapelewski, Long and collaborators assessed several high-performing MOFs for H₂ adsorption.⁹⁵ They reported Ni₂(m-dobdc) as the top-performing material with a usable volumetric capacity between 100 and 5 bar of 11.0 g/L at 25 °C and 23.0 g/L using a temperature swing between -75 and 25 °C. The highly polarizing open-metal Ni²⁺ adsorption sites of the MOF produced the optimal binding enthalpies and led to dense packing of H₂ within the framework. The authors suggested that these results provide benchmark data to compare with future generations of MOF adsorbents designed for H₂ storage.

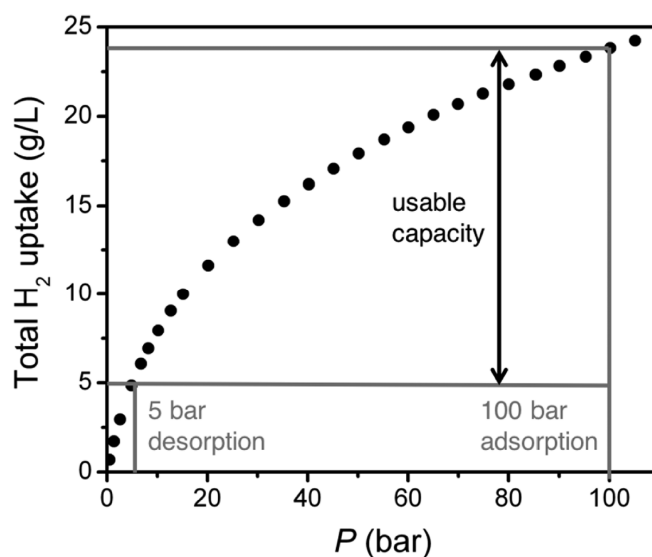


Fig. 16 Usable capacity is calculated by considering adsorption at 100 bar and desorption at 5 bar. Usable volumetric capacity is determined from the total uptake and crystallographic density. Reproduced from ref.⁹⁵ with permission from the American Chemical Society (Copyright 2018).

Combined temperature and pressure swing conditions (e.g. 77 K/100 bar → 160 K/5 bar) have achieved high uptake for hydrogen in a commercially feasible setup. Some MOFs record much higher hydrogen uptake under a combined temperature and pressure swing of 77 K/100 bar → 160 K/5 bar compared to a sole pressure swing condition. For example, NU-125 (49 g/L, 8.5 wt.%), NU-1000 (48 g/L, 8.3 wt.%), and UiO-68-Ant (47 g/L, 7.8 wt.%), NU-1103 (43 g/L, 12.6 wt.%), IRMOF-20 (51 g/L, 9.1 wt.%), NU-100 (47.6 g/L, 13.9 wt.%), and NU-1501-Al (46.2 g/L, 14 wt.%) show both significant volumetric and gravimetric deliverable capacity for hydrogen under this combined temperature and pressure swing condition.^{96 334 25, 94, 335}

NH₃ capture

Ammonia (NH₃) is a colorless, toxic, reactive, and corrosive gas,³³⁶ but is also a chemical feedstock for the global agricultural industry whose yearly production reaches 140 million metric tons.³³⁷ While ammonia emissions from point sources such as oil refineries, textile plants, and wastewater treatment plants are common, industrial agricultural operations are the main global source of NH₃ emissions.³³⁸ Ammonia is a greenhouse gas precursor in the formation of N₂O in the atmosphere; therefore, adsorbents that capture NH₃ at industrial sites which release significant amounts of NH₃ are necessary to mitigate emissions. In 2018, Dincă and colleagues investigated the NH₃ sorption properties of two series of triazolate frameworks, M₂Cl₂BBTA (M = Co, Ni, Cu; BBTA = 1H,5H-benzo(1,2-d),(4,5-d')bistriazole) and M₂Cl₂(BTDD) (M = Mn, Co, Ni, Cu; BTDD = bis(1H-1,2,3-triazolo[4,5-b],[4',5'-i])dibenzo[1,4]dioxin).³³⁹ These MOFs contain a high density of open metal sites (OMS), and several of these frameworks exhibited record static and dynamic NH₃ capacities.

Under equilibrium conditions at 1 bar, $\text{Cu}_2\text{Cl}_2\text{BBTA}$ adsorbed $19.79 \text{ mmol NH}_3 \text{ g}^{-1}$ (**Fig. 17**), more than twice the capacity of activated carbon. Additionally, when investigating the kinetics of adsorption in each MOF, they observed a dynamic NH_3 capacity for CoCl_2BBTA at 1000 ppm of 8.56 mmol g^{-1} , which is 27% greater than the ability of HKUST-1, a leading MOF in the capture of NH_3 . These findings emphasized that increasing the density of OMS yields a systematic increase in the performance in dry conditions. Several reviews in the field delve further into the gas storage applications of MOFs.^{81, 82, 88, 97, 98, 340}

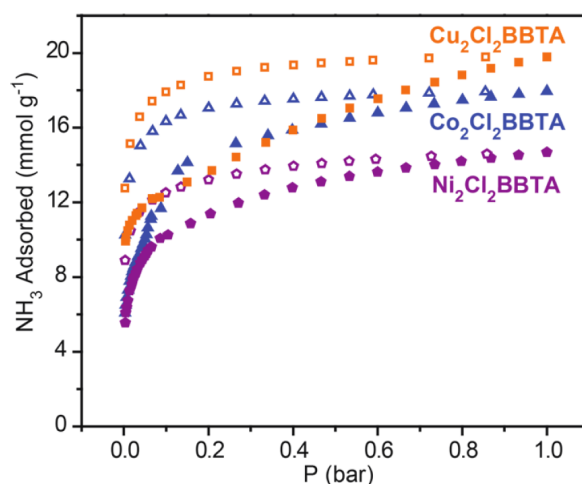


Fig. 17 NH_3 adsorption and desorption of $\text{Co}_2\text{Cl}_2\text{BBTA}$, $\text{Ni}_2\text{Cl}_2\text{BBTA}$, and $\text{Cu}_2\text{Cl}_2\text{BBTA}$ at 298 K. Reproduced from ref.³³⁹ with permission from the American Chemical Society (Copyright 2018).

Gas Separation

Separation and purification of chemical commodities including, but not limited to, gases, fine chemicals, and fresh water consume approximately 15 percent of energy produced annually.^{341, 342} Current projections anticipate that this value will triple by 2050.¹⁵³ The inherent chemical and structural diversity of MOFs affords scientists with a platform material with which they can

capitalize on equilibrium and kinetic selectivity, size selectivity, and molecular recognition among other strategies to efficiently separate chemical species. Beyond the examples we highlight below, several reviews explore MOFs for gas separation.^{102, 118, 119, 343-346}

CO₂ Separation

To ensure the safe transportation of gaseous energy streams including natural gas, refinery-off-gas, and syngas, it is necessary to remove trace amount of acidic gases such as CO₂ and H₂S which pose several operational risks.³⁴⁷ Traditional sorbents such as amines, modified carbons, and polymers suffer from corrosion, poisoning, and high energy consumption.³⁴⁸ The ideal CO₂ adsorbent must display favorable sorption kinetics and thermodynamics over a broad CO₂ loading range. High surface area MOFs often afford high gravimetric uptake; however, such loadings are difficult to attain under practical conditions.

Eddaoudi, Zaworotko, and coworkers delineated MOF design rules with which they pinpointed the “sweet spot” where kinetic and thermodynamic adsorption driving forces balance each other and afford high volumetric CO₂ uptake at low partial pressures (< 0.15 bar).¹⁵³ They employed reticular chemistry to control the chemical functionality and size of pores in a series of isostructural MOFs with periodically ordered hexafluorosilicate (SiF₆⁻, SIFSIX) anions, namely, SIFSIX-2-Cu, SIFSIX-2-Cu-i, and SIFSIX-3-Zn.^{148, 153, 154} Catenated SIFSIX-2-Cu-i recorded one of the highest gravimetric CO₂ uptakes reported (121.2 cm³ g⁻¹, 5.41 mmol g⁻¹, 238 mg g⁻¹) at 298K and 1 bar. Additionally, this MOF displayed a higher isosteric heat of adsorption (Q_{st}) and higher selectivity for CO₂ from CO₂/CH₄:50/50 v/v (33 vs. 5.3) and CO₂/N₂:10/90 v/v (140 vs. 13.7) mixtures compared to SIFSIX-2-Cu as determined by ideal adsorbed solution theory (IAST) calculations. These selectivity values, which agreed well with column breakthrough experiments, surpassed those of any MOF that lacked OMS or amino groups. Moreover, given its high

selectivity (240) for CO₂ over H₂S from a 30/70 mixture, SIFSIX-2-Cu-i is promising for CO₂ separation from syngas. Alternately, SIFSIX-3-Zn is a promising candidate for post-combustion CO₂ capture as seen through its CO₂ isotherm. The material's CO₂ adsorption profile displayed a sharp increase at low pressures (11 wt.% at 0.1 bar) due to pore contraction and similarly plateaued at relatively low pressures. Further breakthrough experiments with SIFSIX-3-Zn displayed CO₂ elution after longer times, indicating the material's higher selectivity for CO₂ over methane and nitrogen as compared to SIFSIX-2-Cu-i. Additionally, IAST calculations yielded unprecedented values, exceeding benchmarks set by Mg-dobdc³⁴⁹ and UTSA-16,³⁵⁰ suggesting that SIFSIX-3-Zn is suitable for pre-combustion CO₂ capture. Non-equilibrium kinetic adsorption experiments demonstrated that CO₂ adsorbs onto SIFSIX-3-Zn more strongly and faster than N₂, O₂, CH₄, and H₂. SIFSIX-2-Cu-i retained its CO₂ affinity and selectivity in the presence of water (up to 74% relative humidity in a CO₂/H₂:30/70 mixture); however, high humidity levels induced a reversible phase change in SIFSIX-3-Zn. Within this elegant work, the authors capitalized on reticular chemistry and electrostatic interactions to design a series of stable porous materials which displayed unprecedented affinity for CO₂ under industrially relevant conditions.

Motivated by the exceptional performance of SIFSIX-3-Zn, Eddaoudi and coworkers investigated its isostructural counterpart SIFSIX-3-Cu¹⁰⁷ for CO₂ adsorption. The Cu-based material showed a steeper CO₂ adsorption isotherm within the low-pressure region at room temperature (**Fig. 18**) as compared to SIFSIX-3-Zn. This change is a consequence of the contracted pore environment, due to Jahn-Teller distortions of the Cu²⁺ ion. Building on work established by Poeppelmeier and coworkers using [NbOF₅]²⁻ as a building block,^{351, 352} Eddaoudi and colleagues explored a more hydrolytically stable MOF, NbOFFIVE-1-Ni, to study trace CO₂ removal.³⁵³ Importantly, single-crystal X-ray diffraction (SCXRD) clearly localized the CO₂ molecules inside

the pore of NbOFFIVE-1-Ni. The distance between the electropositive carbon of CO₂ and the electronegative fluorine atoms of the [NbOF₅]²⁻ pillar is smaller than the sum of van der Waals radii of carbon and fluorine, demonstrating the origin of the strong interactions between CO₂ and the MOF host.

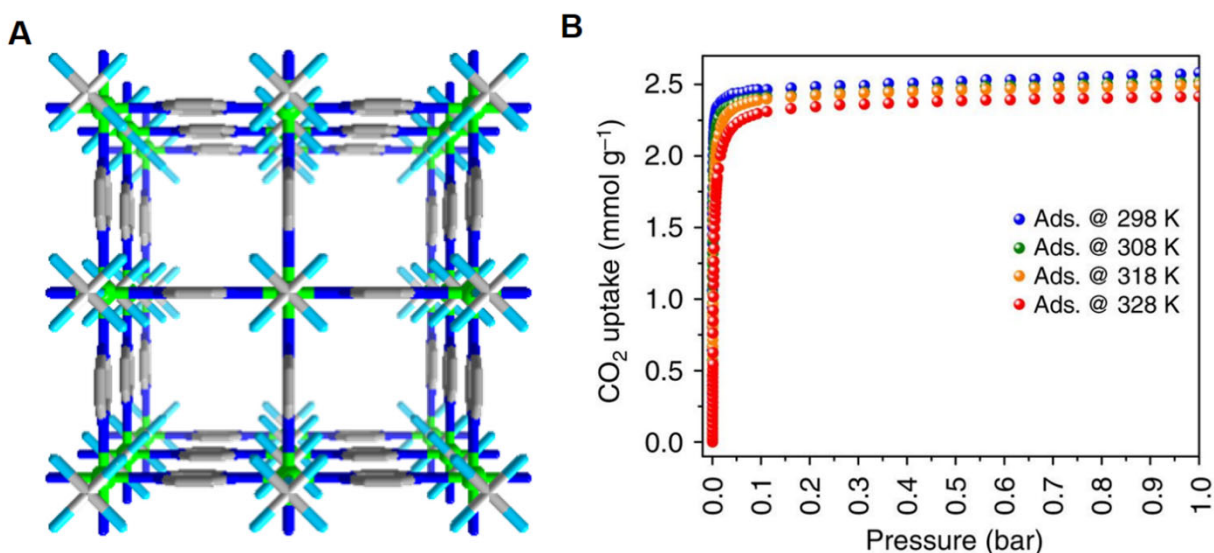


Fig. 18 (A) A structural representation of SIFSIX-3-Cu. (B) CO₂ adsorption isotherms at variable temperatures for SIFSIX-3-Cu. The isotherms are reproduced from ref.¹⁰⁷ with permission from Springer Nature, Copyright 2014.

In several other MOFs, OMS serve as well-defined binding sites for selective CO₂ capture. One prominent example of this is rod-packing MOF—MOF-74, also known as CPO-27.^{354,355} Mg-MOF-74 features open magnesium sites that efficiently extract CO₂ from gaseous mixtures and requires only mild regeneration conditions.³⁵⁶ Moreover, the incorporation of amine-based molecules at these OMS can further enhance CO₂ selectivity. Long and coworkers introduced diverse amine-containing guest molecules into M₂(dobpdc) (dobpdc⁴⁻ = 4,4'-dioxidobiphenyl-3,3'-dicarboxylate), an expanded structure of MOF-74, and observed excellent CO₂ uptake

capacities.^{330, 357-359} Specifically, they demonstrated the cooperative insertion of CO₂ molecules in mmen-Mn₂(dobpdc) (mmen = *N,N'*-dimethylethylenediamine), affording both remarkable CO₂ separation capacity and energy-efficient regeneration (**Fig. 19**).³³⁰

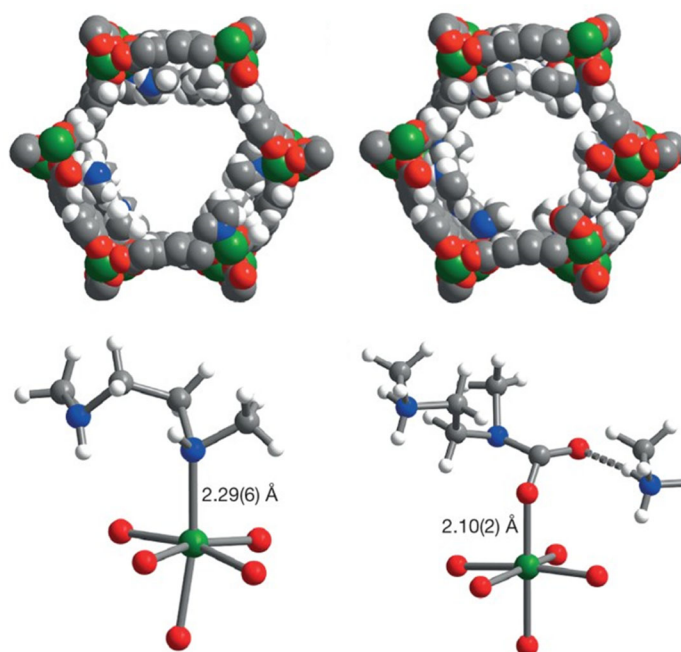


Fig. 19 Structures of mmen-Mn₂(dobpdc) and CO₂-mmen-Mn₂(dobpdc). Reproduced from ref.³³⁰ with permission from Springer Nature (Copyright 2015).

CO₂ and H₂S Separation

Eager to concomitantly remove multiple acidic gases *via* a single method, researchers have sought to isolate a MOF with equivalent affinity for CO₂ and H₂S and an H₂S/CO₂ selectivity ratio of 1. Eddaoudi and coworkers undertook a systematic study to propel the field's understanding of structure-property relationships that govern the adsorption of CO₂ and H₂S from methane-rich gas streams.³⁶⁰ The presence of fluorine atoms in the cavities of SIFSIX-2-Ni-i tuned localized charge density and increased the framework's affinity for CO₂ without sacrificing its selectivity for H₂S.

SIFSIX-3-Ni, with shorter linkers, and therefore narrower cavities, displayed an inversion of selectivity, favoring CO₂ over H₂S in column breakthrough experiments (H₂S/CO₂/CH₄:5/5/90). Alternatively, NbOFFIVE-1-Ni, a MOF which efficiently adsorbs CO₂ even at low concentrations, also displayed a greater affinity for CO₂ compared to H₂S in breakthrough experiments. Upon increasing the temperature to 50 °C, the retention time of H₂S decreased while that of CO₂ remained unchanged. Moreover, the CO₂ retention time in dual-component (CO₂/CH₄) and triple-component (CO₂/H₂S/CH₄) experiments were identical, suggesting H₂S does not interfere with CO₂ adsorption. Density-functional theory (DFT) calculations revealed that although the CO₂ and H₂S adsorption sites were unique, only one molecule of CO₂ or H₂S could occupy the area due to the sites' proximity. Moreover, CO₂ possesses a slightly more favorable host-guest interaction energy compared to H₂S (-57 kJ/mol vs. -55 kJ/mol). SCXRD measurements of gas-loaded samples confirmed this data.

AlFFIVE-1-Ni, the aluminum-based analogue of NbOFFIVE-1-Ni, is uniquely capable of hosting OMS. Compared to the Nb analogue, AlFFIVE-1-Ni displayed a much steeper H₂S isotherm, suggesting specific sites in the framework favor H₂S adsorption. DFT calculations revealed strong interactions between the hydrogen atoms of H₂S and two neighboring fluorine atoms. Additionally, while a CO₂ molecule can interact with four fluorine atoms in NbOFFIVE-1-Ni, it can only interact with two fluorine atoms in the Al analogue due to the presence of OMS, thereby reducing the framework's CO₂ affinity. Uniquely, in breakthrough experiments, the retention times and adsorbed molar amounts of CO₂ and H₂S were nearly identical. DFT calculations revealed that upon the adsorption of one guest molecule in a cavity, there is insufficient space to allow another molecule to occupy the site. Regeneration at 105 °C affords 100% recycling efficiency. Through iterative design, Eddaoudi and coworkers isolated AlFFIVE-

1-Ni which displays nearly equivalent affinity for CO₂ and H₂S and an H₂S/CO₂ selectivity ratio equivalent to 1.

Water Vapor Capture

The amount of water vapor in the atmosphere is equivalent to ~10% of all fresh water in lakes and its capture could serve to lessen the world's pressing water shortage.³⁶¹ Unfortunately, conventional water adsorbents such as zeolites and silica gels suffer from low water uptake capacities and/or require energy-intensive processes to desorb water.

Wang, Yaghi, and coworkers capitalized on the three distinct cavities of MOF-801, which can accommodate and promote the aggregation of water molecules, to prepare a highly efficient MOF-based device for water harvesting (**Fig. 20**).⁶³ When monitoring the temperature and pressure of a vessel containing the device during the adsorption of water vapor at 35 °C, the temperature of the MOF increased rapidly before decreasing to equilibrate with the surroundings. Under these conditions, the experimental water harvesting data agreed well with the potential harvestable water. The team developed a theoretical model to optimize the water-harvesting process and ultimately, performed iterative experiments to interrogate the effects of packing porosity and MOF layer thickness to determine the amount of water harvested under 1 sun of solar flux (100 mW cm⁻²). In simulations, MOF-801 equilibrated first in an environment with 20% RH at 25 °C. Upon solar irradiation, the relative humidity of the air-vapor mixture adjacent to the MOF layer increased rapidly from 20% to 100% indicating water desorption. A device equipped with a 1 mm MOF-801 layer yielded 2.8 L of water per kilogram per day under continuous harvesting with low-grade heat (1 kW m⁻²). These results suggested that designing MOF-based devices with high sorption capacity and intracrystalline diffusivity could further increase the amount of water harvested daily. A prototype device was designed that relied on the daily natural temperature swing

to adsorb water during the night and to desorb water during the day requiring no active cooling. Although the structure of the device exhibited a slightly delayed desorption step, the water harvesting results matched the aforementioned predictions based on isotherms.

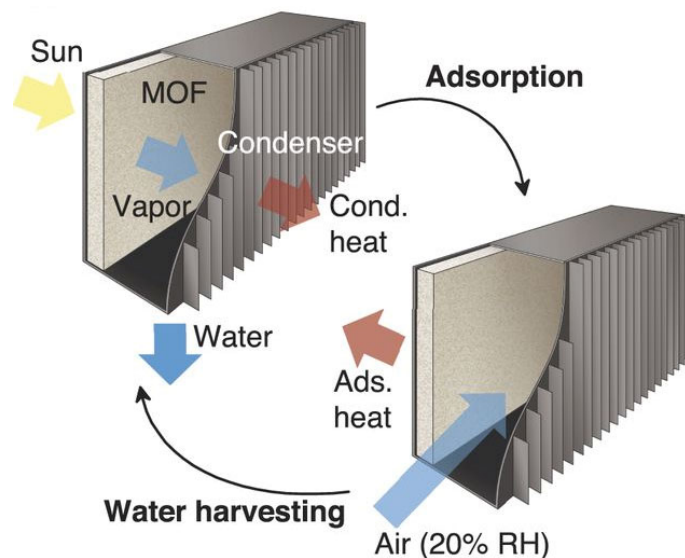


Fig. 20 Schematic of a MOF-based device for water harvesting. Reproduced from ref.⁶³ with permission from The American Association for the Advancement of Science, Copyright 2017.

More recently, Yaghi and coworkers reported a microporous aluminum-based MOF, MOF-303, which displays high water uptake at low relative humidity, a low isosteric heat of adsorption, and, rapid sorption kinetics.⁶⁴ Notably, a water harvesting device based on MOF-303 shows dramatically improved performance compared to previously reported devices in both indoor arid environments and the real desert. This work represents a significant step toward applying MOFs for commercial applications of water harvesting.

Another strategy to develop better water adsorbent focuses on developing MOFs comprised of water-stable metal-azolate building blocks.^{66, 179, 192, 362-364} Dincă and coworkers sought to take advantage of the water-stability of early transition metals and azolates by assessing a series of

azolate-based MOFs for water adsorption.^{66, 362, 363} These MOFs achieve high uptake capacities for water and their water sorption behaviors can be further tuned by altering the composition of the metal nodes. For more comprehensive summaries of MOFs as water adsorbents, one can refer to these reviews.⁶⁵⁻⁶⁹

Heterogeneous Catalysis

Manufacturing chemical commodities relies on the development and implementation of highly efficient catalytic processes. Homogenous catalysts are highly tunable and demonstrate record activities due to their molecular nature; however, they are less practical for industrial scale manufacturing given the difficulty of separating such species from product streams.³⁶⁵ To circumvent this issue, many processes employ thermally robust and recyclable heterogeneous catalysts.^{366, 367} Often, ill-defined heterogeneous supports result in multiple catalytically active sites, thereby complicating delineation of design rules.³⁶⁸⁻³⁷⁰

The long-range order of MOFs enables the isolation and characterization of single-site heterogeneous catalysts (SSHCs) through crystallographic and other atomically precise methods.^{371, 372} SSHCs feature only one type of active site distributed throughout the bulk material and, consequently, must exist within or be deposited onto a well-defined, uniform support.^{373, 374} Within MOF-based heterogeneous catalysts, SSHCs can exist as structural elements anchored on the node or linker, or as guests within the pore.³⁷⁵⁻³⁷⁷ The aforementioned development of MOF activation procedures allows for the removal of labile solvent molecules from MOF nodes to expose highly reactive open metal sites which function as collective well-defined SSHCs.¹⁶⁷ As an example, the self-assembly of a tritopic linker, benzene-1,3,5-tricarboxylate, with Fe(III) carboxylate trimers yields the thermally robust, MIL-100(Fe).³⁷⁸ Intriguingly, each iron trimer displayed two OMS upon thermal activation which proved efficient at benzylation of benzene with

benzyl chloride, resulting in the nearly quantitative yield of the desired diphenylmethane product (**Fig. 21**). The OMS and the high redox activity of Fe(III) to Fe(II) promote reactivity and account for MIL-100(Fe) exceeding the activity of its isostructural Cr(III) analogue as well as HBEA and HY zeolites. These trimer-based MOF systems including MIL-100(Fe)³⁷⁸ and M-**so**c-MOF³⁷⁹⁻³⁸⁵ (also known as PCN-250 and MIL-127) also show catalytic behavior in more complex reactions such as light alkane oxidation using N₂O as the oxidant.^{386, 387}

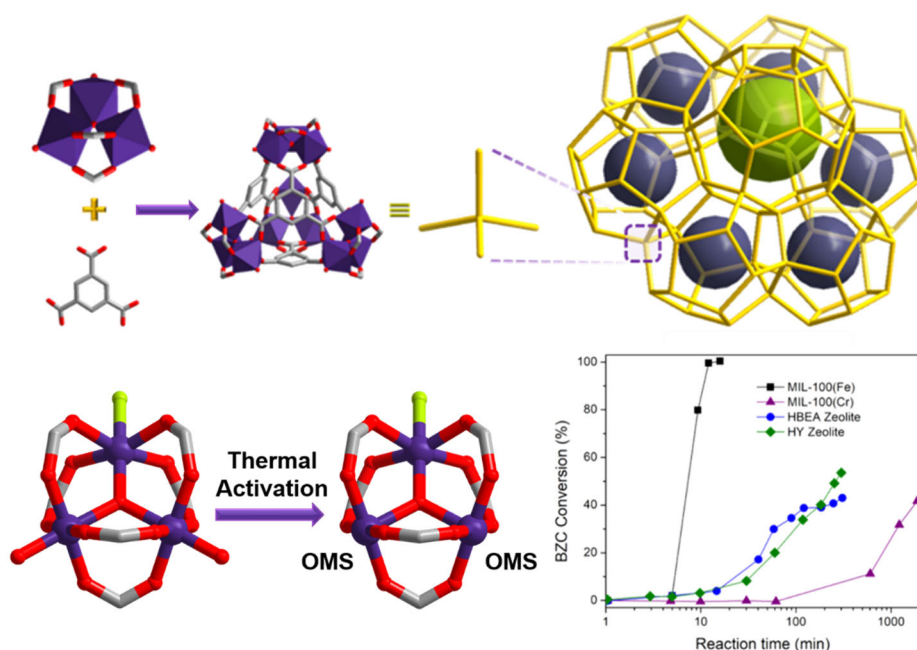


Fig. 21 MOFs with open metal sites as well-defined SSHCs.¹⁶⁷ Reproduced from ref.³⁷⁴ with permission from the Elsevier (Copyright 2019).

Extending beyond incorporating OMS to enhance reactivity, cluster connectivity can similarly affect catalytic activity. Specifically, the versatile nature of the $[\text{Zr}_6(\mu_3\text{O})_4(\mu_3\text{-OH})_4]^{12+}$ cluster allows for a wide range of linker connectivities which results in differing amounts of terminal $\text{-OH/-H}_2\text{O}$ ligands. The Zr-OH-Zr motif present within this cluster resembles the Zn-OH-Zn active site of the phosphotriesterase enzyme, responsible for hydrolyzing

phosphotriesters.³⁸⁸ This similarity prompted the investigation of Zr-MOFs for the detoxification of organophosphorus nerve agents (**Fig. 22**).^{76, 389} Our group probed NU-1000, a MOF comprising 8-connected Zr₆ nodes and 1,3,6,8-tetrakis(p-benzoate)pyrene (H₄TBAPy) linkers, for the hydrolysis of dimethyl 4-nitrophenyl phosphate (DMNP), a nerve agent simulant.³⁸ This MOF recorded a half-life of 15 min, owing to its large mesoporous channels that facilitate substrate diffusion and the spatial isolation of the Zr₆ node active sites. In contrast, the free Zr₆ node and Zr salt showed poor catalytic activity under the same conditions in solution. DFT calculations suggested an incoming simulant molecule displaces a terminal water present on a node. Thorough thermal activation of NU-1000 fully dehydrated the node as demonstrated by diffuse reflectance infrared Fourier transform spectroscopy (DRIFTS) and the resulting material achieved an impressive half-life of only 1.5 min. In follow-up work, we have observed that varying the linker connectivity of a Zr₆ node further influences catalytic activity.^{39, 390}

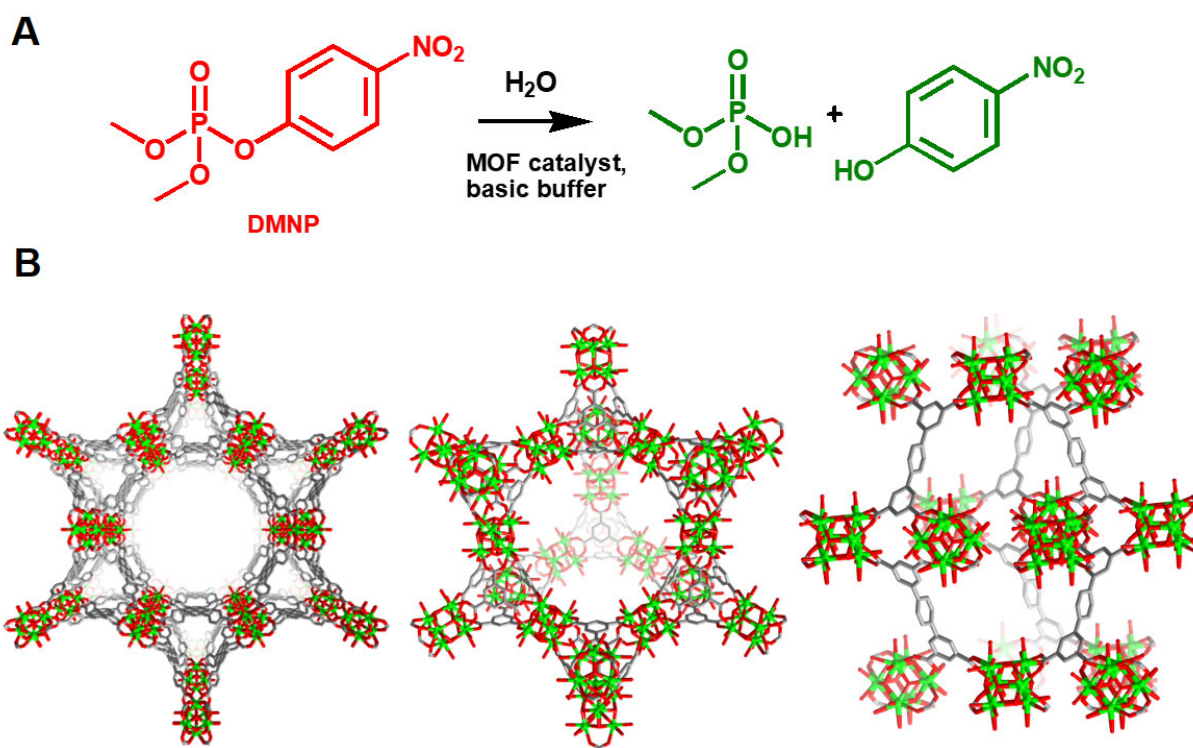


Fig. 22 (A) Scheme depicting the hydrolysis of chemical warfare agents using MOF catalysts. (B) Representative Zr-MOFs such as NU-1000^{38, 194}, MOF-808³⁹¹, and NU-1400³⁹⁰ for destruction of CWAs.

Beyond CWA degradation, MOF-based catalysts are efficient in several other chemical transformations relevant to the energy sector.^{371, 392, 393} Interest in electrochemical conversion of CO₂, an atmospheric greenhouse gas, to more useful compounds has prompted researchers to design new catalysts.³⁹⁴⁻³⁹⁹ Most efforts to realize electrocatalysts that favor high CO product selectivity rely on earth abundant elements.⁴⁰⁰⁻⁴⁰² For example, Yaghi, Yang, and coworkers impressively designed nano-sized MOF-based thin film electrocatalysts for cooperative CO₂ conversion (**Fig. 23**).⁴³ They synthesized their materials from free-base and metallated porphyrin linkers, which assemble with alumina deposited onto conductive carbon disk electrodes by atomic layer deposition (ALD). Within the [Al₂(OH)₂TCPP-M'] thin film series, the Co metallated system exhibited the highest relative increase in current density following exposure to a solution saturated with CO₂. Increasing the scan rates of the voltammograms resulted in a cathodic wave at -0.5 V versus the reversible hydrogen electrode (RHE), commonly associated with the reduction of Co(II) to Co(I). The authors inferred that a majority of the catalytically active centers in this substrate were redox active. Moreover, they precisely controlled the thickness of the thin film by varying the number of ALD cycles, thereby tuning both charge transport and reactant diffusion. A MOF thin film with a thickness of 30–70 nm achieved the highest charge density; however, increasing MOF thickness beyond this regime decreased catalytic activity, despite a higher active site loading. Authors attributed this phenomenon to either charge transport limitations from the electrode to the MOF surface or possible incomplete MOF formation that instead yielded a highly insulating alumina phase. Further optimization of thin film growth conditions resulted in a highly active

catalyst with a 76% selectivity for CO production maintained for 7 h with a turnover number (TON) of 1400.

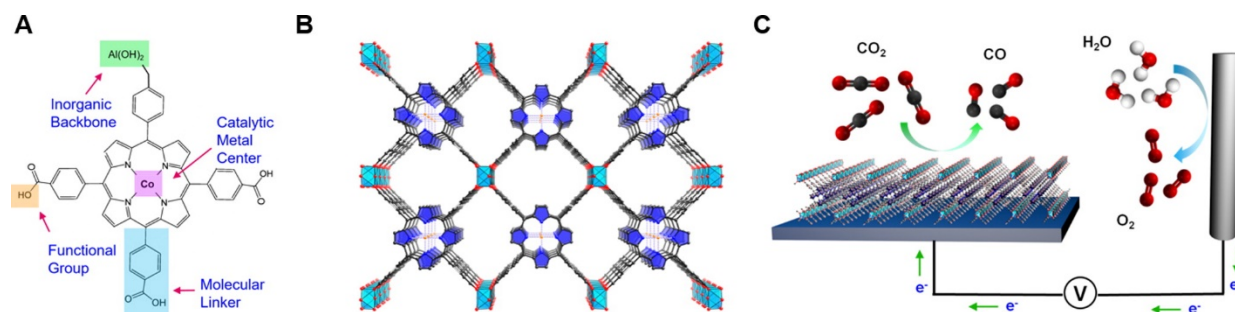


Fig. 23 Nano-sized MOF-based thin films electrocatalysts for CO₂ conversion. Reproduced from ref.⁴³ with permission from the American Chemical Society (Copyright 2015).

Drawing inspiration from nature, transforming solar energy into chemical energy through the generation of chemical bonds has motivated the development of photochemically active catalysts.⁴⁰³⁻⁴⁰⁵ Such systems generally require the incorporation of a variety of components to ensure visible light absorption, charge separation with negligible recombination, and charge mobility.⁴⁰⁶⁻⁴⁰⁹ The modularity of MOFs has afforded the design of multiple sophisticated photocatalysts.⁴¹⁰⁻⁴¹³ Lin and coworkers demonstrated such tunability through the assembly of six different mixed linker MOFs based on UiO-67 , $\text{Zr}_6(\mu_3\text{-O})_4(\mu_3\text{-OH})_4(\text{bpdc})_{6-x}(\text{L})_x$, with **L1-L6** containing either Ir, Re, or Ru complexes and each framework is named **MOF 1-6** accordingly (**Fig. 24**).⁴¹⁴ MOFs comprising **L1-L3** were effective for catalytic water oxidation with cerium ammonium nitrate (CAN) used as an oxidant. Surprisingly though, transformations catalyzed by the bare ligands in solution reported a TOF at least one order of magnitude higher than their MOF counterparts. Surface poisoning experiments suggested that the MOF catalysis was limited to the surface because CAN could not diffuse through the MOF pores. The installation of **L4**, which contains a Re complex, enabled the reduction of CO₂ with the use of triethylamine (TEA) as a

sacrificial reducing agent. The authors initially observed higher catalytic activity with homogenous **L4** over MOF **4**, but the heterogenous catalyst ultimately exhibited higher activity and TON as the reaction progressed, attributed to stabilization of the active catalyst in the MOF. Unfortunately, the recyclability of MOF **4** was poor and leaching studies and post-catalysis IR measurements suggested the decomposition of **L4** within the framework. The addition of **L5-L6**, which contain Ir and Ru complexes, respectively, produced materials that catalyzed a series of useful organic transformations. Photochemical aza-Henry reactions with tetrahydroisoquinoline derivatives in the presence of nitromethane reached high conversions with repeated cyclability. MOF **6** also catalyzed aerobic amine coupling and sulfide photo-oxidations with comparable performance to the homogenous ligand. Interested readers may consider delving into one of the several reviews published on MOF-based catalysts.^{40, 374, 375, 415-420}

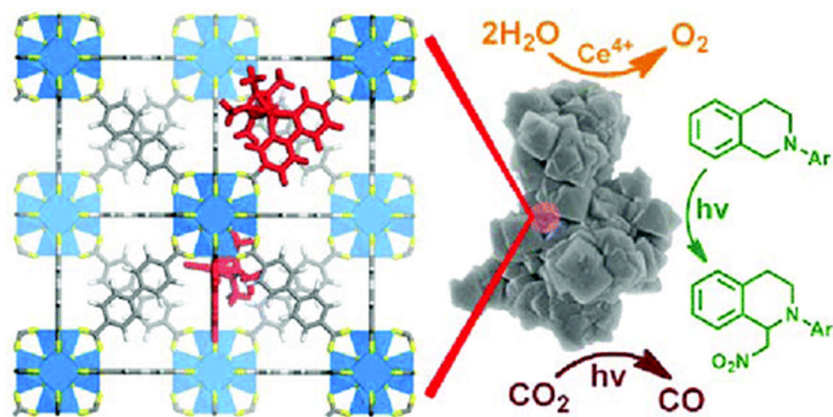


Fig. 24 Mixed linker MOFs based on UiO-67 for water oxidation, CO₂ reduction, and organic photocatalysis. Reproduced from ref.⁴¹⁴ with permission from the American Chemical Society (Copyright 2011).

Enzyme encapsulation

Beyond tuning the affinity of MOFs for the uptake of toxic moieties, these modular frameworks have demonstrated the capacity to encapsulate, stabilize, and retain precious guests within their pores. For example, to limit drug degradation *in vivo*, facilitate targeted delivery, and develop less painful and more convenient drug administration processes, researchers have begun examining MOFs as drug delivery vehicles.^{56, 59, 60, 421-424} Alternatively, enzymes are another important class of guest molecules. While attractive for transformations relevant to the pharmaceutical sector, the practical use of enzymes in commercial applications such as catalysis requires their stabilization to prevent denaturation in harsh conditions. MOFs offer a unique platform for enzyme encapsulation. Due to their intriguing hybrid organic-inorganic nature, one can envision a multitude of potential interactions between enzyme guests and MOF hosts, such as van der Waals forces, dispersion forces, covalent and/or coordinative bonding. Additionally, the tunable pore structure and crystalline nature of MOFs position them as a class of emerging hosts for immobilizing enzymes. Typically, *de novo* and post-synthetic methods are efficient strategies to encapsulate enzymes in MOFs. Liu, Ge, and coworkers reported the *de novo* encapsulation of an enzyme, Cyt c, in ZIF-8 for the detection of explosive organic peroxides in solution (**Fig. 25**).⁴²⁵ The embedded Cyt c showed a 10-fold enhancement of peroxidase activity compared to the free enzyme. The authors proposed that the immobilization of the Cyt c inside the framework changed its structural conformation and made the heme group more accessible, ultimately, increasing substrate affinity.

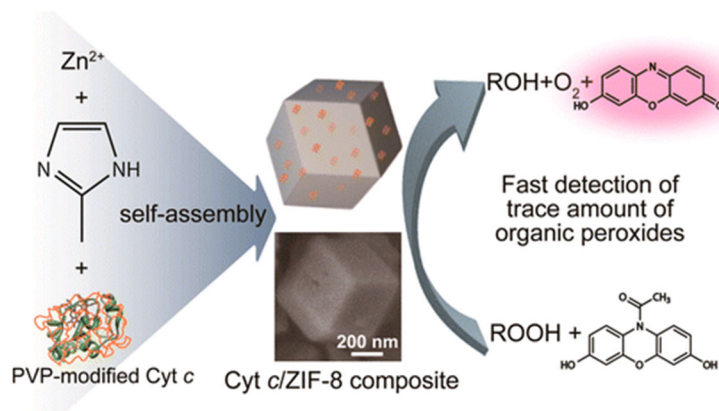


Fig. 25 De novo encapsulation of Cyt c in ZIF-8 for the detection of organic peroxides. Reproduced from ref.⁴²⁵ with permission from the American Chemical Society (Copyright 2014).

Ma and coworkers reported the post-synthetic encapsulation of an enzyme, microperoxidase-11 ($3.3 \times 1.7 \times 1.1$ nm) in the cage-type Tb-mesoMOF for catalytic oxidation.⁴²⁶ The modest cages of Tb-mesoMOF (3.9 and 4.7 nm) limit the size of enzymes that may be immobilized. Moreover, enzymes must undergo conformational changes to enter the cages *via* small pore apertures of 1.3 and 1.7 nm.^{427, 428} Cage-type MOFs with larger mesopores such as PCN-333 and PCN-888, developed by Zhou and coworkers, can accommodate larger enzymes such as horseradish peroxidase (4.0×4.4 nm \times 6.8 nm) and glucose oxidase ($6.0 \times 5.2 \times 7.7$ nm).^{429, 430}

Our group post-synthetically encapsulated insulin, a protein traditionally administered to patients through direct injections, in acid-resistant NU-1000 as a strategy for oral-delivery of insulin.⁵⁸ NU-1000 achieved a high insulin loading and retained the cargo even under highly acidic conditions resembling those of the stomach. Under physiological conditions (pH = 7.0), NU-1000 released the insulin, suggesting the payload could be effectively released within the bloodstream as desired. After its release, the once-encapsulated insulin retained its activity under physiological

conditions. Readers can learn more about enzyme encapsulation in MOFs in one of several reviews in the field.⁴³¹⁻⁴³⁵

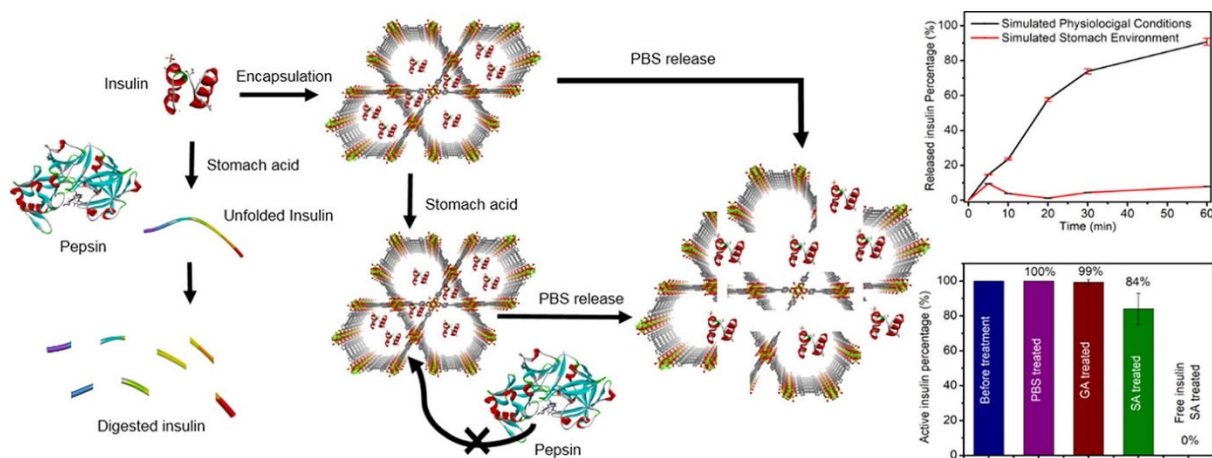


Fig. 26 Acid-resistant mesoporous MOF toward oral Insulin delivery. Reproduced from ref.⁵⁸ with permission from the American Chemical Society (Copyright 2018).

MOF Commercialization: A Strengthened Industrial Base Driving Commercial Adoption

New patent filings are a leading indicator of future commercial activity. They highlight innovation cadence, focus, and the activity of a field. Since 2011, the field of MOF research has witnessed a nearly 9 times increase in annual patent filings, from approximately 78 in 2011 to 665 in 2019 (**Fig. 27A**). Approximately 50% of assignees are from the private sector (**Fig. 27B**). Furthermore, a vast majority of this innovation is occurring in China and the United States, as evidenced by the location of filings (**Fig. 27C**). Private sector filings in the field are diverse, ranging from MOFs as battery materials, to chemical separations, and packaging applications (**Fig. 28A**). In the last few years, many companies have begun pursuing commercialization of MOFs for a wide range of applications. These companies include small spinoffs from academic labs, startup companies focused specifically on MOFs, and large multinational companies adding MOF capabilities to their existing R&D organizations (**Fig. 28B**).

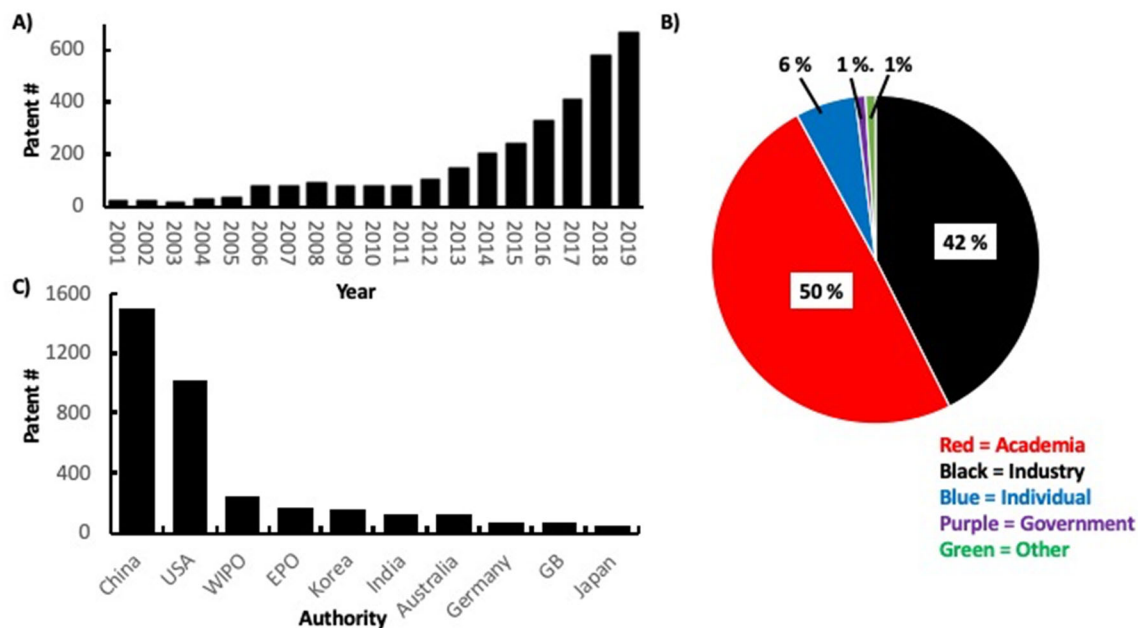


Fig. 27 A) Global patent application trend by year where “MOFs” or “Metal Organic Framework” are mentioned in the Title, Abstract or Claims (Source: PatSnap), B) Standard Patent Assignee by Type for 3,885 active patents and patent applications globally where “MOFs” or “Metal Organic Framework” are mentioned in the Title, Abstract or Claims (Source: PatSnap), and C) Top authorities for patents between 2011-2019, where “MOFs” or “Metal Organic Framework” are mentioned in the Title, Abstract or Claims (Source: PatSnap).

A

Publication Number	Title	Publication Date	Current Assignee
IN201917051020A	Use of type v adsorbent and gas concentration for c02 adsorption and capture	2020-01-24	EXXONMOBIL RESEARCH AND ENGINEERING COMPANY
WO2020099561A1	Generation of drinking water from air by means of a box, comprising at least one sorption material	2020-05-22	BASF SE THE REGENTS OF THE UNIVERSITY OF CALIFORNIA
US20190240645A1	High porosity metal oxide catalyst coatings	2019-08-08	BASF CORPORATION
WO2020101906A1	Adsorbent matrix as propellant in aerosol package	2020-05-22	THE PROCTER & GAMBLE COMPANY
US20200052330A1	Sulfide-based solid electrolyte for lithium battery, method of preparing the same, and lithium battery including the sulfide-based solid electrolyte	2020-02-13	SAMSUNG ELECTRONICS CO., LTD. SAMSUNG SDI CO., LTD.
WO2020004197A1	Fluorescin-containing bakeable powder coating composition and liquid coating composition, and coating and coated body comprising this bakeable powder coating composition or liquid coating composition	2020-01-02	NIPPON FUSO CO., LTD
US20190376154A1	Filter media for the removal of particles, ions, and biological materials, and decolorization in a sugar purification process, and use thereof	2019-12-12	GRAVER TECHNOLOGIES LLC
US20190241270A1	Catalytic ozone removal	2019-08-08	HAMILTON SUNDRAND CORPORATION
WO2019201829A1	Method for storing a gaseous medium, and storage tank	2019-10-24	ROBERT BOSCH GMBH
IN201937001053A	Method for enhancing volumetric capacity in gas storage and release systems	2019-03-08	INGEVITY SOUTH CAROLINA, LLC
US20190194232A1	Metal-organic framework and method of producing the same	2019-06-27	TOYOTA JIDOSHA KABUSHIKI KAISHA
US20190300548A1	Desulfurizer, hydrogen generation device, and fuel cell system	2019-10-03	PANASONIC INTELLECTUAL PROPERTY MANAGEMENT CO., LTD.
WO2019130187A1	Flexible thermoelectric device	2019-07-04	3M INNOVATIVE PROPERTIES COMPANY
US20200147424A1	Fire suppressing device	2020-05-14	THE BOEING COMPANY
US20190105598A1	Electronic gas in-situ purification	2019-04-11	NUMAT TECHNOLOGIES, INC.,
US20190091620A1	Adsorbent-assisted stabilization of highly reactive gases	2019-03-28	NUMAT TECHNOLOGIES, INC.

B

Representative Companies	Location	MOF Activity Description
Atomis	Japan	MOF R&D services and synthesis
BASF	Germany	Large scale production
Bosch	Germany	Sensors
Exxon Mobile	United States	Catalysts, CO2 Sequestration
Framergy	United States	MOF R&D services and synthesis
Immaterial	United Kingdom	MOF R&D services and synthesis
Johnson Matthey	United Kingdom	Gas filtration
Lantha Sensors	United States	Chemical sensors
Matrix Sensors	United States	Chemical sensors
Merck KGaA	Germany	Crystallography
MOF Technologies	United Kingdom	MOF R&D services and synthesis
MOFAPPS	Norway	MOF R&D services and synthesis
MOFWORX	Australia	CO2 Sequestration
Molecule	United Kingdom	Atmospheric water harvesting
Mosaic Materials	United States	CO2 Sequestration
novoMOF	Switzerland	R&D services and synthesis
NuMat Technologies	United States	Integrated MOF solutions provider
ProfMOF	Norway	R&D services and synthesis
Rimo Therapeutics	United States	Therapeutics
Sikemia	France	MOF ligand supplier
SyncMOF	Japan	MOFs and new gas utilization systems
Taiyo Nippon Sanso Corporation	Japan	Nitrogen sensor
Total S.A.	France	CO2 Sequestration
Water Harvesting Inc	United States	Atmospheric water harvesting

Fig. 28 Representative patent publications by private sector assignees where “MOFs” or “Metal Organic Framework” are mentioned in the Title, Abstract or Claims (Source: PatSnap), and B) Selected companies in the MOF ecosystem.

Challenges to Broader Adoption

Application Fit & Material Design Complexity

Today, there are over 200 known zeolite structures and at least 2 million hypothetical structures, but after seven decades of intensive work, approximately only 20 zeolite structures are used in commercial applications.⁴³⁶ Compare this to MOFs, where there are nearly infinite combinatorial possibilities, and already over 14,000 synthesized to date.⁴³⁷ Given the large and rapidly-growing number of synthesized MOF structures, trial-and-error screening of MOFs for any particular application is becoming increasingly impractical. In this sense, we might think of MOFs as taking a personalized medicine approach to chemistry, where a unique MOF can be tailored for a specific problem or application. The downside of this bespoke approach to material design is that it is challenging to realize the economies of scale with any single MOF. For this reason, MOFs will continue to be more expensive (at least for the foreseeable future) than conventional adsorbents such as zeolites and carbons, which are currently produced in massive quantities. In the near to medium term, MOFs will be best applied in solving problems which are either impossible or extremely expensive to address with conventional technologies, or where the value delivered through performance improvements dramatically offsets incremental costs. Below we highlight three case studies of companies that have taken just such an approach to commercializing MOF-enabled solutions.

Fragmented Industrial Base & Expert Networks

While the MOF field is generating significant research output, including over 4,200 publications in 2019 alone,⁴³⁸ a fragmented industrial base with distributed functional capability systems makes research transition challenging. As we will discuss in the BASF case study, efforts

have already addressed several perceived challenges related to MOF scale-up. That is to say, supply-chains exist, or can be established to satisfy volume demand should it materialize. The greater commercialization challenge relates to application development and integration—linking materials discovery to end-products and system performance. Doing so requires cross-disciplinary expertise and an integrated R&D workflow, from discovery through end-product manufacture. For example, successful commercialization of one product may require expert networks from academia, application integrators, chemical suppliers, and channel partners or customers. Put differently, it will remain challenging for even sophisticated companies to replicate published results, let alone transition technologies to market without expanded collaboration networks. One model that we are familiar with will be discussed in the NuMat case study below.

NuMat Technologies Case Study: An “end-to-end” commercialization framework for MOFs

NuMat Technologies, Inc. uses computationally-guided discovery, sophisticated chemistry, and advanced process engineering to build advanced materials and products that drive the industries of tomorrow. NuMat is a recognized pioneer in the field of MOFs, focused on delivering solutions to innovation challenges in the electronics, defense, specialty chemicals, and life science industries.

In NuMat's experience, the successful commercialization of MOFs has required the development of "end-to-end" capabilities: from sophisticated computational modeling through end-product manufacturing (**Fig. 29**). At NuMat, computational scientists, chemists, and engineers work side-by-side to design, validate, and scale-up MOFs to then integrate them into novel products and processes. Unifying these functions into an integrated commercialization workflow is a pathway to addressing the industrial-based challenges tied to capability gaps and fragmented expertise. The increasing knowledge of MOFs will be instrumental in the development of new technologies,

which in turn, will loop back into growing the collective knowledge of these materials. Through this cyclic approach, we could greatly benefit from economies of scale to maximize output while minimizing production cost, all of which are crucial for the commercialization of complex MOF-based systems.

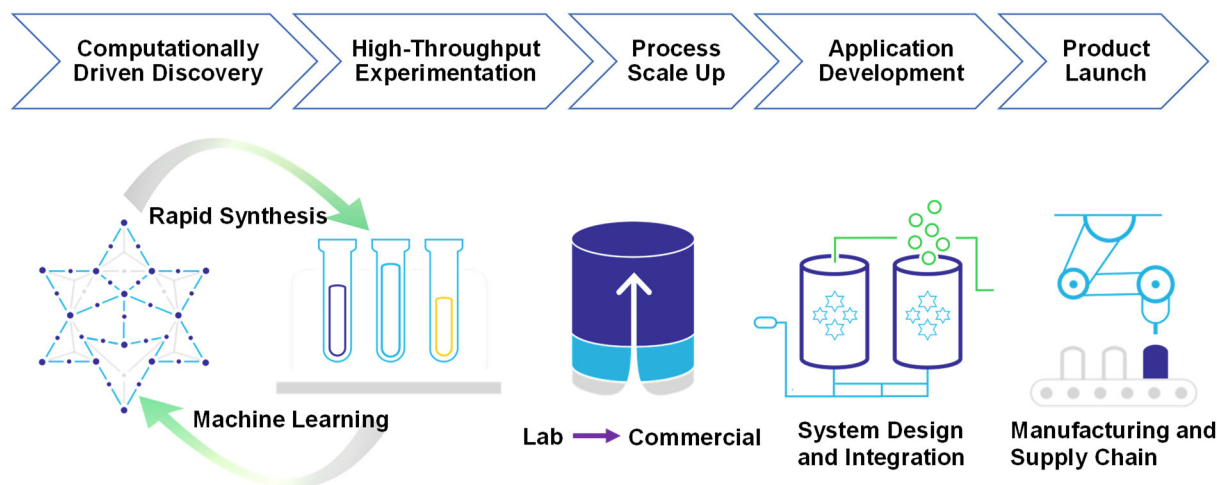


Fig. 29 An “end-to-end” approach to MOF commercialization.

Pairing Computationally-guided Discovery with Rapid Experimentation and Scale-up

As cloud computing has become more affordable, the process of screening hypothetical structures has subsequently become significantly cheaper and faster. Whereas 10 years ago it may have taken a team of computational scientists months to run limited simulations, complex simulations on millions of structures can now be done in just days at a fraction of the cost. Computationally-guided material selection will play an increasingly critical role in accelerating R&D outcomes and reducing MOF selection complexity. At NuMat, this workflow includes discovering new materials through high-powered atomistic simulations, identifying and testing new properties through material informatics, predicting performance through first-principles

modeling, and modeling complex interactions at a system-level all before materials are synthesized in the lab. After initial computational screening, candidate materials are synthesized, characterized, and experimentally validated at lab scale. While computational tools are a powerful R&D accelerator, material selection is ultimately an iterative process that requires human intuition and experimental validation. This is especially true when an application involves complex chemical interactions where model refinement requires experimental input.

After experimental validation, materials are transitioned to a pilot or commercial plant (**Fig. 30**), where a team of process engineers scale materials from the kilogram- to ton-scale while optimizing synthetic recipes, yields, and crystal size distributions. Depending on the application, these materials are then functionalized or formed into highly engineered shapes. Application engineers integrate these materials into pilot-scale process systems or commercial product prototypes for validation. This can take the form of separation, purification, packaging, or catalytic units at 1/100th of full scale. Customer-specific qualification testing may include cycle, purity, and yield testing under a range of real-world operating conditions, all conducted in dedicated application laboratories. Based on performance data, the design of a material and system will be further optimized, which may include going several steps back in the process. This feedback-driven, iterative loop is key to enabling real-time optimization of both the chemistry and the process. After validation, dedicated manufacturing and quality organizations work to transition prototypes into integrated solutions that meet regulatory and quality requirements. In NuMat's experience, integrating capability systems into one unified workflow dramatically reduces development cycles, while significantly improving outcomes at a fraction of the cost. A case study describing this approach is discussed below.



Fig. 30 One of NuMat's pilot plant units used for process scale-up optimization.

ION-X Case Study: The Future of Electronic Chemical Delivery

The Need: Safe Delivery of Dangerous Electronic Gases

The semiconductor industry uses a variety of ultra-high-purity, highly-toxic, and often unstable gases as key raw materials for the manufacture of integrated circuits. Historically, for safety purposes, these dangerous gases were supplied as 1% mixtures in high-pressure cylinders, with 99% of the volume being inert gas. Later, solid adsorbents (first zeolites and then activated carbon) were introduced to enable safe storage and delivery of 100% neat gases at sub-atmospheric pressure. While adsorbent-based storage and delivery provided significant productivity improvements (reduced cylinder change-outs) and safety benefits (sub-atmospheric-pressure storage), activated carbon is inherently an amorphous material with limited surface area, a wide distribution of pore sizes, high chemical reactivity, and kinetic flow rate restrictions; all of which limit its application to a small subset of gases.

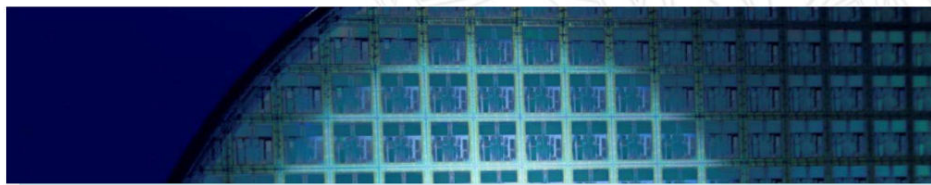
Next Generation Electronic Gas Delivery: ION-X[®]

NuMat's ION-X[®] product line represents a new generation of delivery systems based on MOF adsorbents which have been custom-designed to safely store, stabilize, and release dangerous electronic gases on demand (**Fig. 31**). The ION-X[®] product line provides safe, customized, high-capacity solutions for arsine (AsH₃), phosphine (PH₃), and isotopically-enriched boron trifluoride (¹¹BF₃) gases. Engineered as a packaged solution, ION-X[®] integrates MOFs into specialty gas cylinders, which are designed to be installed inside the gas boxes of ion implant tools within a semiconductor fab. The gases inside ION-X[®] cylinders are transported and delivered below atmospheric pressure, which significantly reduces the health and environmental impact of an accidental gas release. The higher surface area and design flexibility of MOFs provide significant advantages over previous carbon adsorbents. The pore size of a MOF can be precisely tuned to match the molecular sizes of the gas to be stored. This parameter impacts adsorption capacities (how much gas can be loaded), desorption characteristics (how much can be delivered as a function of pressure), and enables self-reacting gases to be stabilized within the pores of the MOF. The technological innovations and capabilities that have enabled ION-X[®] will continue to open new pathways for the electronics industry in its push for total-fab solutions, as well as other industries that rely on safe, performance-driven chemical delivery.⁴³⁹

AsH₃ (Arsine) ION-X[®] Dopant Gas Storage and Delivery System



Next-Generation Adsorbent Technology of Sub-Atmospheric Dopant Gases



Versum Materials and NuMat Technologies announce a global alliance to bring ION-X[®] sub-atmospheric gas storage and delivery system solutions to our worldwide customers.



BENEFITS

New line of products for the safe storage and delivery of toxic dopant gases, using state-of-the-art MOF (Metal Organic Framework) technology as adsorbent

Delivers ultrahigh purity dopant gases at sub-atmospheric pressures

Best true sub-atmospheric solution

100% Plug and Play with existing implant machines

Delivers capacity premium to SDS3 with AsH₃ and BF₃

Reduced change-outs and cost-of-ownership

Favorable desorption and flow characteristics supporting ease of gas extraction

Superior cylinder construction with the least failure modes



SPECIFICATIONS

(Shelf life: 5 years)

Arsine (AsH ₃)	≥ 99.9995%
Carbon Dioxide (CO ₂)	≤ 0.5 ppmv
Carbon Monoxide (CO)	≤ 0.1 ppmv
Methane (CH ₄)	≤ 0.5 ppmv
Nitrogen (N ₂)	≤ 2.0 ppmv
Oxygen (O ₂)	≤ 1.0 ppmv
Water (H ₂ O)	≤ 2.0 ppmv

SAFETY INFORMATION

Formula	AsH ₃
Physical Description	Colorless gas with a mild, garlic-like odor
CAS Number	7784-42-1
OSHA PEL	TWA 0.05 ppm
NIOSH PEL	0.002 mg/m ³ (15 min. ceiling)
ACGIH-TLV	0.05 ppm
NIOSH-IDLH	Ca (3 ppm)

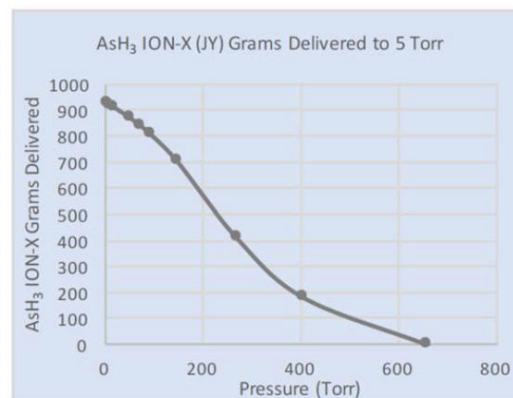


Fig. 31 ION-X[®] specification sheet from Versum Materials website.

The Path to Commercialization

Using NuMat's integrated workflow, ION-X[®] was developed in approximately 18 months—from design inception to initial product qualification. NuMat used high-performance

computing paired with high-throughput experimentation to select the ideal MOF candidate for each gas. Each MOF was then further refined to control complex interactions and performance requirements for each gas. For example, modifying the pore size of one MOF by 2 Å resulted in a 25% improvement in delivered gas capacity. This iterative optimization process took approximately 14 days from computational modeling to synthesis and experimental validation. A portfolio of MOFs were then scaled from the gram- to the metric ton-scale, integrated into an engineered system, qualified in a specialized electronic chemicals applications laboratory, and then transitioned to an assembly line meeting the quality standards of the semiconductor industry – all within NuMat. In 2017, NuMat announced a global alliance with Versum Materials, a subsidiary of Merck KGaA, Darmstadt Germany, to distribute ION-X[®] products to semiconductor manufacturers worldwide. In this agreement, NuMat manufactures the ION-X[®] product, and then ships it to a dedicated plant in South Korea for gas filling and final distribution to customers.⁴⁴⁰ This collaboration model is an example of how parties can partner to leverage their respective capability systems and infrastructure for MOF products. Here, beyond material discovery or synthesis, NuMat forward integrated to become a solutions provider, and then partnered with a global company with the existing infrastructure and distribution channels to sell into the semiconductor industry. NuMat and their partners have successfully replicated this model across multiple application and market segments.

Case Study: Crystalline Sponge Technology - A Breakthrough in Molecular Structure Analysis (Merck KGaA, Darmstadt, Germany)

Merck KGaA, Darmstadt Germany is a leading science and technology company, operating in Healthcare, Life Science and Performance Materials. The company has approximately 57,000 employees around the world and generated sales of € 16.2 billion in 2019.

MilliporeSigma, the company's Life Science business in the U.S., and Versum Materials are affiliates of Merck KGaA, Darmstadt, Germany. An innovation project at the company's Innovation Center works on a highly innovative technology to make molecular structure analysis faster, more direct, and applicable to samples on sub-microgram-scale.

The Need: An Extension of X-ray Crystallography

Conventional X-ray crystallography is the method of choice for determining molecular structures completely and with absolute certainty. While this is a powerful technique, it typically requires milligram quantities of analyte to produce a perfect crystal, which can be synthetically challenging and costly.

The Solution: Crystalline Sponge Technology

A special group of MOF structures, invented by Professor Makoto Fujita of Tokyo University and licensed by Merck KGaA, Darmstadt, Germany for their crystalline sponge technology, enables nanogram to microgram quantities of analyte to be used in the X-ray crystallography process, without the need for direct crystallization.¹²³ Crystalline sponge technology combines the information density of X-ray crystallography and the sensitivity needed to facilitate analysis of natural substances and impurities – without requiring crystallization of the target molecule. Crystals or “hosts” are three-dimensional porous metal complexes containing either solvent molecules or analyte in their pores. During soaking, the target “guest” is absorbed into the sponge pores and regularly ordered by the intermolecular, non-covalent interactions with the MOF. The guest molecules, once oriented in the crystal host pores, can be analyzed by X-ray diffraction. These ‘instant crystals’ can be created rapidly and with an extremely small quantity of analyte, resulting in an order of magnitude improvement in the time and cost required for

conventional crystallography. Of note, when using the crystal sponge method, cooperative framework transformation can occur upon adsorption of guest molecules. Being a major supplier to the pharmaceutical industry, Merck KGaA, Darmstadt, Germany takes a particular interest in pharma-related applications of the technology, as illustrated by the following use case.

A Sensitive and Rapid Method for Metabolite Identification

During the drug discovery process, the structure of compounds resulting from the metabolism of drug candidates must be elucidated as they may contribute to efficacy, safety, toxicity, and drug-drug interactions. Metabolites generated in *in-vitro* systems are typically analyzed using configurations of liquid chromatography-mass spectrometry (LC-MS) by drawing inferences from fragmentation patterns. While MS techniques offer high sensitivity, these approaches often fail to provide complete metabolite structure identification. Alternatively, nuclear magnetic resonance (NMR) can be used, but this is a less sensitive approach and typically requires milligram amounts of pure starting material. SCXRD can provide structural information at the atomic level but involves the time-consuming process of crystallization, requires a relatively large amount of starting material, and cannot be performed with liquid or volatile analytes. Use of crystalline sponge technology combines the information density of SCXRD and a sensitivity approaching MS to enable structural elucidation of human metabolites from nanogram amounts of analyte.⁴⁴¹ The ability to significantly reduce substance requirements from milligram to nano or microgram quantities provides the opportunity to dramatically accelerate early stage drug development processes, enabling researchers to identify toxic metabolites earlier in the development cycle. In addition, the technology offers a multitude of applications also in general chemistry, as illustrated in **Fig. 32**. Here, the absolute structure of a molecule was obtained that

would not be easily accessible by conventional SCXRD due to the difficulty in crystallizing the analyte.

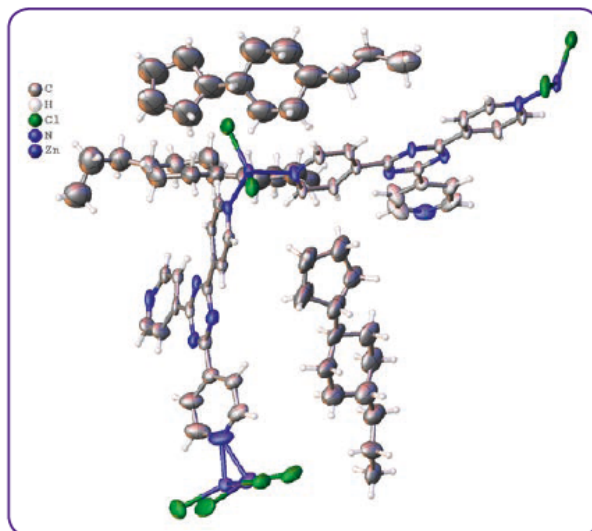


Fig. 32 Definitive identification of the chemical structure and configuration of a liquid crystal compound by crystalline sponge technology. Two molecules in trans configuration are shown within the crystalline sponge.

The Path to Commercialization

Use of crystalline sponge technology overcomes the limitations of conventional X-ray crystallography which can be a bottleneck in the analysis of molecular structures. Innovative “crystal-free” crystallography requires only nanogram to microgram quantities of sample, can be performed on liquid and volatile compounds, and rapidly provides conclusive structures. Given the power of this technology to rapidly and definitively identify molecular structures of compounds and impurities, its applications will be many and diverse. From pharmaceuticals to performance chemicals, fragrance, food, and more, we have only begun to tap the full potential of crystalline sponge technology. In June 2019, Merck KGaA, Darmstadt, Germany and Rigaku Corporation

(Tokyo, Japan), a key leader in scientific equipment instrumentation, announced a partnership to commercialize the crystalline sponge technology as part of an integrated, turn-key solution for customers. Under this partnership, Rigaku will customize their X-ray systems to accommodate crystalline sponge consumables developed by Merck KGaA, Darmstadt, Germany. This integrated solution will be deployed as a next generation analytical platform to rapidly determine chemical structures of pharmaceuticals, fine chemicals, and natural compounds.

As of the date of this publication, Merck KGaA, Darmstadt, Germany is using crystalline sponge technology as an internal service across the organization. The project is hosted at the company's Innovation Center. For more information, please visit crystallinesponge.emdgroup.com.

BASF: A Pathway to MOF Scale-up and Commercialization

BASF is a German chemical company and the largest chemical producer in the world. The BASF Group comprises subsidiaries and joint ventures in more than 80 countries and operates six integrated production sites and 390 other production sites in Europe, Asia, Australia, the Americas, and Africa.

In comparison to the 200 years in between the first description of zeolites in the 18th century to their first application in the 1950's, MOFs have achieved tremendous progress within their short history of only 20 years. Beyond discovery, key milestones in the field have included commercialization in specialty applications and significant de-risking of process scale-up. Several of the early challenges around material robustness have also been addressed leading the way to broader adoption.

Compared to incumbent porous materials, MOFs offer a level of design flexibility which creates differentiation and potential for their novel application in new market platforms (**Fig. 33**). This includes emerging opportunities in chemical and biological protection, biomedical products, and sensor applications.

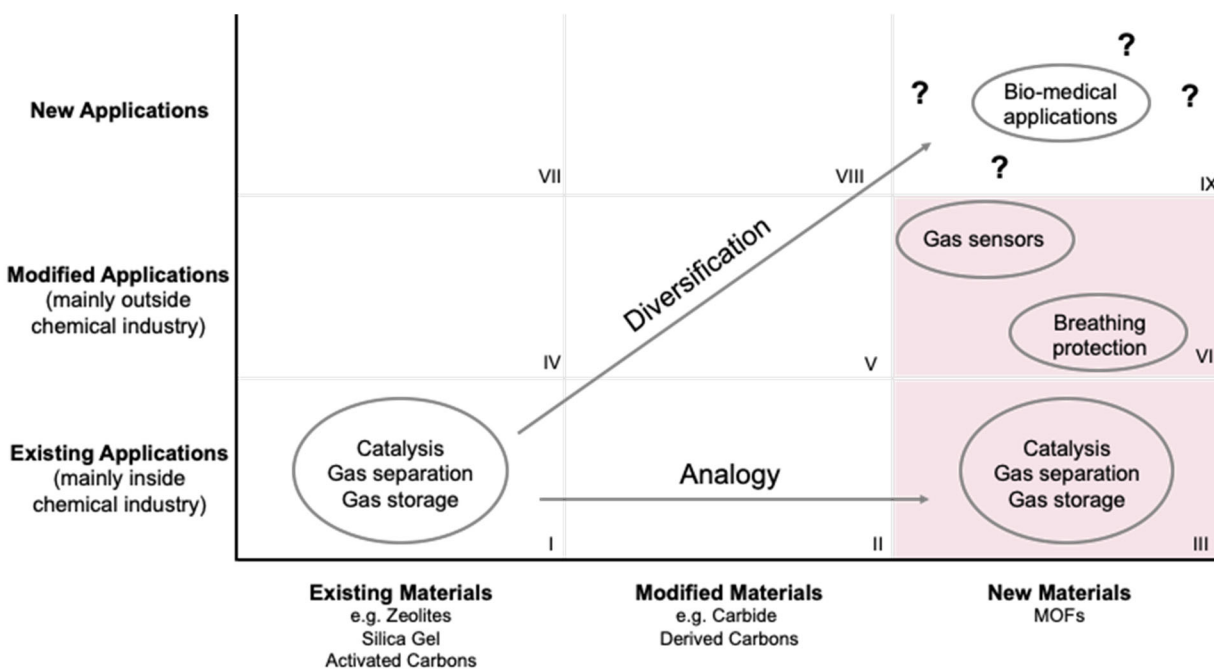


Fig. 33 Representative application roadmap and fit by porous material class.

Key learnings in industrial scale-up:

As of this publication date, MOFs have been applied commercially and many more applications are on the verge of commercialization. While MOFs will continue to find commercially viable opportunities as premium, specialty additive materials, their economic synthesis is critical for broader adoption in markets where incumbent materials and solutions are well established.

For example, a MOF that offers higher adsorption capacity for a component in a gas stream, thus leading to a reduced adsorbent bed size or prolonged maintenance intervals, can perhaps support a cost (and price) of 2-3× an existing adsorbent solution. However, for the same application, but where space or form factor limitations on bed size exist (e.g. an offshore platform or mobile application), the price multiple for a MOF can be significantly higher. Although MOFs are still recognized to be relatively expensive, and volumes too low to fully displace incumbent adsorbents in industrial scale markets, several companies have already proven that some MOFs can be produced in commercially relevant scales (tons) and manufactured at costs below 20 €/kg at those scales. In this sense, the cost curve of MOFs is similar to that of other adsorbents—driven by raw material inputs and production scale.

According to BASF's experience, the main cost drivers of MOFs are: 1. linker costs, 2. space time yield, 3. down-stream processing effort, and 4. solvents used (**Fig. 34**).

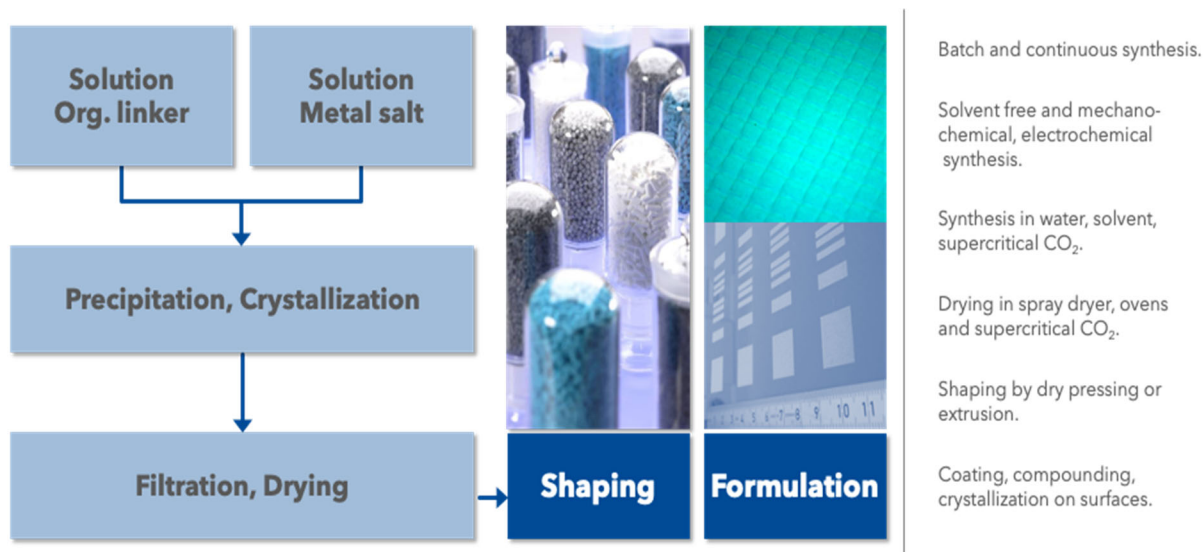


Fig. 34 Key process steps in MOF production.

Linker selection is often the key success factor in scale-up feasibility. Ideally, the linker is a commodity and globally available without long transportation distances. But as stated above, depending on the application, the linker can also be more complex and scale-up of sophisticated structures such as MOF-174 and MOF-184 have been successfully demonstrated at BASF. Thus, linker cost can vary over a broad range from less than 5 €/kg up to several 100 €/kg. Selection will depend on the application and resultant performance, cost, and pricing requirements for adoption.

In addition to raw material costs, space time yield is an important factor in controlling synthesis costs. Twenty years ago, the first synthetic recipes from academia resulted in space time yields of 10 kg MOF per m³ of reaction volume and day. In the past years, impressive process improvements have taken place to increase the concentration and reduce reaction times, resulting in space time yields of >1,000 kg m⁻³d⁻¹. For continuous MOF synthesis, space time yields of more than 10,000 kg m⁻³d⁻¹ have been achieved at BASF. Unfortunately, this impressive number is only true for the precipitation of the MOF itself. If downstream processes like filtration, washing, and drying are taken into consideration, the space time yield is often reduced. Nevertheless, when compared to modern zeolite synthesis, space time yield of MOF synthesis can be a factor of 10x higher, holding promise for cost advantaged production economics at industrial scale.

Besides the precipitation, further unit operations like filtration, washing, drying, milling and shaping (e.g. pelletization and extrusion) may be required. BASF has worked on those process steps for a portfolio of MOFs to understand the impact of each of these process steps on the quality of the end product. Specific surface area is a valid indicator across process step to evaluate if, for example, washing of the filter cake was successful, or if the mechanical force applied during shaping has negatively impacted material performance.

Finally, continued optimization work has led to synthetic recipes that have replaced organic solvents with water, or removed the need for organic solvents altogether, further improving safety and reducing costs.

In sum, enormous progress has been made in driving the process improvements which have reduced MOF manufacturing cost and de-risked industrial scale production. MOFs have left the laboratory and are on the edge of becoming industrially relevant materials. In BASF's experience, the challenge for the future is more related to the identification of the right MOF for the application of interest, as opposed to the ability to scale MOFs. Due to the huge number of available MOFs (and an even higher number of theoretical MOF structures) computer-based simulations will play an increasingly important role in the material selection process, helping condense development cycles and increase the probability of success.^{442, 443}

Commercialization Case Study: Dehumidification

As an early entrant in the field of MOFs, BASF has had a unique perspective from which to view the evolution of the field. BASF's work in the field has spanned gas packaging and separations to more recent work on complex encapsulation and controlled release applications – an area of significant promise (**Fig. 35**).

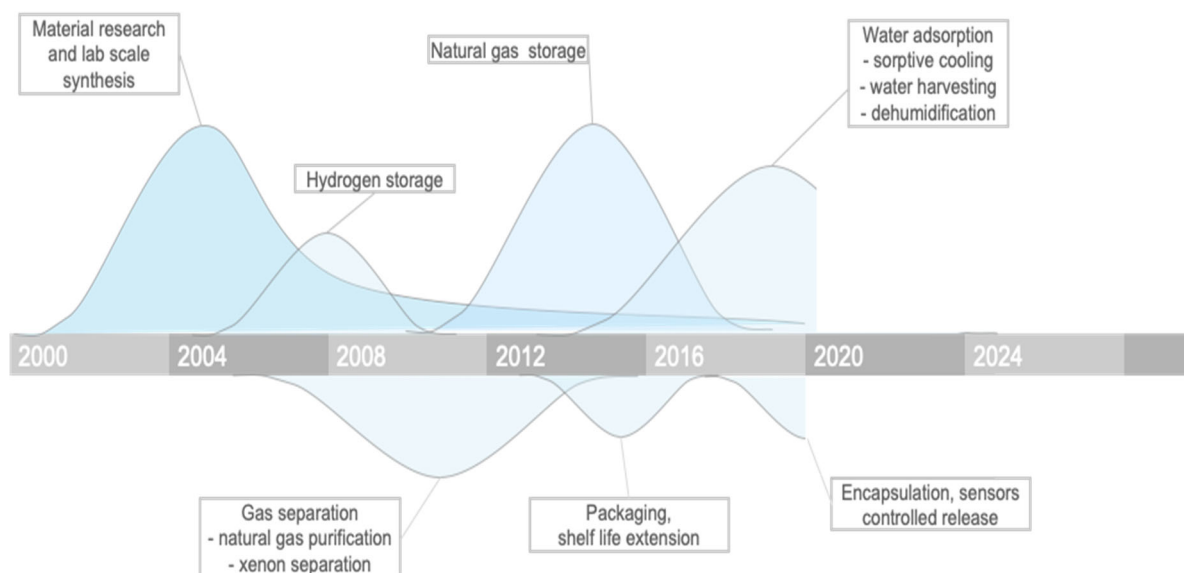


Fig. 35 Evolution of BASF's MOF development activities.

One example of BASF's recent work in the field involves adsorptive dehumidification. An air-conditioner must fulfill two tasks. The obvious one is to cool external air to a comfortable level. However, humidity control is as important as temperature. In a standard compression-based air-conditioner, external air is cooled to a target temperature level, whereby the humidity then begins to condensate. Dew pointing of air is energy intensive and depending on climatic conditions can be responsible for up to 60% of total unit energy draw.

An energy-efficient alternative would entail an adsorption-based system. Here, humidity would be selectively adsorbed by a MOF, resulting in reduced electricity consumption of the device. Under the right conditions, a MOF-based air-drying system could lead to 50-60% reduced energy draw, equivalent to savings of thousands of kWh per year in standard office units. When compared to silica gels (the incumbent adsorption material), MOFs are capable of achieving 1.5–2 × higher volumetric energy density (enabling device miniaturization), while also achieving a 27% higher coefficient of performance.⁴⁴⁴

However, adsorption systems have their own energy penalty. After saturation of the MOF with water, a desorption step must be taken to regenerate the MOF and release the water. This thermal energy can come from any low temperature heat source, such as a solar thermal supply, or waste heat from the compressor of the air conditioner system itself.

Applications such as this show that the unique properties of MOFs cannot be addressed by state-of-the-art materials or technologies. New applications will follow, and costs will continue to drop tied to economies of scale, which will support an expansion of additional use-cases.

Future direction of MOFs

Understanding mechanical properties is important for both fundamental illustration of structure-property relationship and the further processing of MOFs, which is highly relevant to industrial application.⁴⁴⁵ It is desirable to study the impact of mechanical stress on the structures and functionalities of MOFs. The other long-term stabilities^{445, 446} (e.g., hydrolytic stability and chemical stability) of MOFs are also crucial for many practical applications, although not required in some niche areas such as the destruction of highly toxic nerve agents or capture of toxic gases with protective masks. Both experimental and theoretical approaches are suggested to identify materials with the best compromise between the property and stability.

The assembly mechanism of MOFs is still not well understood. It is of great interest to illustrate the growth of MOF crystals, identify polymorphism of MOFs, and understand the insight of the thermodynamic versus kinetic products. During this process, it is favorable to introduce new techniques to study and characterize MOFs such as atomic force microscopy (AFM),⁴⁴⁷⁻⁴⁴⁹ high-resolution transmission electron microscopy (HRTEM),⁴⁵⁰⁻⁴⁵² cryogenic electron microscopy (cryo-EM),⁴⁵³ isothermal titration calorimetry (ITC),^{454, 455} Atom probe tomography (APT),⁴⁵⁶ etc.

Some new techniques can be applied to study emerging scientific phenomena such as unique dynamism or flexibility within MOFs, and we believe this is essential for the further development of the field.

Greener, safer, and more efficient methods for synthesizing MOFs are crucial to realize the large-scale production of MOFs as adsorbents for gas separation or storage processes. Different approaches including water-based synthesis,⁴⁵⁷⁻⁴⁵⁹ room temperature methods,⁴⁶⁰ and mechanochemical strategies^{461, 462} may provide future paths for optimizing the production of the high-performing MOFs.

The Future of MOF Commercialization

As the MOF industrial base continues to mature, commercialization activity will increasingly track with the rate of new patent filings. Continuing with the “personalized medicine” approach to chemistry, near-term opportunities will expand for MOFs as ultra-premium consumable materials in markets that provide an innovation premium. Opportunities will be particularly robust in industries where MOFs’ current scale and cost position are generally acceptable, including the semiconductor, biopharmaceutical, defense, and specialty chemical sectors. Delivering solutions in these segments will be complex, requiring novel development models where capability and knowledge networks are consolidated within organizations or through collaboration.

Medium-term, MOFs may very well begin to challenge the cost-performance position of incumbent materials such as activated carbons, zeolites, and silica, or at a minimum be an integral part of multi-material solutions (e.g. polishing layers). This will depend on application, and

similarly require dedicated capability and supply-chain networks capable of executing against opportunities as they emerge.

Longer-term, we may very well find that MOFs become the plastics of the 21st century, ubiquitous across industries, products and daily life.⁴⁶³ While it will take decades to see if this prediction comes to pass, what we can confidentially state today is that MOFs have left academia and their broader commercial adoption is not a question of “what if?”, but of “what next?”, and of who is positioned *today* to capitalize on the opportunities of *tomorrow*.

Acknowledgements

Authors gratefully acknowledge support from the Defense Threat Reduction Agency (HDTRA1-18-1-0003, HDTRA1-19-1-0010, and HDTRA1-19-1-0007); the U. S. Department of Energy’s Office of Energy Efficiency and Renewable Energy(EERE) under award no. DE-EE0008816; the U. S. Department of Energy (DOE) Office of Science, Basic Energy Sciences Program for Separation (DE-FG02-08ER15967); the Army Research Office, under Award Number W911NF1910340; the Inorganometallic Catalyst Design Center, an EFRC funded by the DOE, Office of Science, Basic Energy Sciences (DE-SC0012702); the U.S. Department of Energy, National Nuclear Security Administration, under Award Number DE-NA0003763; the Air Force Research Laboratory (FA8650-15-2-5518); the Northwestern University Institute for Catalysis in Energy Processes (ICEP), funded by the DOE, Office of Basic Energy Sciences (Award Number DE-FG02-03ER15457). M.C.W. and J.G.K are supported by the National Science Foundation Graduate Research Fellowship under grant DGE-1842165. R.J.D. appreciates the support of the Ryan Fellowship funded by Northwestern's Graduate School and the International Institute for Nanotechnology. F.A.S. is supported by the Department of Defense (DoD) through the National Defense Science & Engineering Graduate (NDSEG) Fellowship Program.

Competing interests

Omar K. Farha and Benjamin Hernandez are founders of NuMat Technologies. Stefan Marx is an employee of BASF SE. Wolfgang Hierse and Clemens Kühn are employees of Merck KGaA, Darmstadt, Germany.

References

- 1 A. Corma, *J. Catal.*, 2003, **216**, 298-312.
- 2 M. E. Davis, *Nature*, 2002, **417**, 813-821.
- 3 D. W. Breck, *J. Chem. Educ.*, 1964, **41**, 678.
- 4 J. Rouquerol, D. Avnir, C. W. Fairbridge, D. H. Everett, J. M. Haynes, N. Pernicone, J. D. F. Ramsay, K. S. W. Sing and K. K. Unger, *Pure Appl. Chem.*, 1994, **66**, 1739.
- 5 R. M. Barrer, *Discuss. Faraday Soc.*, 1949, **7**, 135-141.
- 6 T. Wigmans, *Carbon*, 1989, **27**, 13-22.
- 7 H. Furukawa, K. E. Cordova, M. O’Keeffe and O. M. Yaghi, *Science*, 2013, **341**, 1230444.
- 8 S. Kitagawa, R. Kitaura and S. Noro, *Angew. Chem. Int. Ed.*, 2004, **43**, 2334-2375.
- 9 G. Ferey, *Chem. Soc. Rev.*, 2008, **37**, 191-214.
- 10 H.-C. Zhou, J. R. Long and O. M. Yaghi, *Chem. Rev.*, 2012, **112**, 673-674.
- 11 H. Furukawa, U. Müller and M. Yaghi Omar, *Angew. Chem. Int. Ed.*, 2015, **54**, 3417-3430.
- 12 J. R. Long and O. M. Yaghi, *Chem. Soc. Rev.*, 2009, **38**, 1213-1214.
- 13 H.-C. J. Zhou and S. Kitagawa, *Chem. Soc. Rev.*, 2014, **43**, 5415-5418.
- 14 S. Kitagawa, *Acc. Chem. Res.*, 2017, **50**, 514-516.
- 15 M. Kondo, T. Yoshitomi, H. Matsuzaka, S. Kitagawa and K. Seki, *Angew. Chem. Int. Ed.*, 1997, **36**, 1725-1727.
- 16 H. Li, M. Eddaoudi, T. L. Groy and O. M. Yaghi, *J. Am. Chem. Soc.*, 1998, **120**, 8571-8572.
- 17 M. Eddaoudi, J. Kim, N. Rosi, D. Vodak, J. Wachter, M. O’Keeffe and O. M. Yaghi, *Science*, 2002, **295**, 469-472.
- 18 H. Deng, S. Grunder, K. E. Cordova, C. Valente, H. Furukawa, M. Hmadeh, F. Gándara, A. C. Whalley, Z. Liu, S. Asahina, H. Kazumori, M. O’Keeffe, O. Terasaki, J. F. Stoddart and O. M. Yaghi, *Science*, 2012, **336**, 1018-1023.
- 19 D.-X. Xue, A. J. Cairns, Y. Belmabkhout, L. Wojtas, Y. Liu, M. H. Alkordi and M. Eddaoudi, *J. Am. Chem. Soc.*, 2013, **135**, 7660-7667.
- 20 P. Li, Q. Chen, T. C. Wang, N. A. Vermeulen, B. L. Mehdi, A. Dohnalkova, N. D. Browning, D. Shen, R. Anderson, D. A. Gómez-Gualdrón, F. M. Cetin, J. Jagiello, A. M. Asiri, J. F. Stoddart and O. K. Farha, *Chem*, 2018, **4**, 1022-1034.
- 21 O. K. Farha, I. Eryazici, N. C. Jeong, B. G. Hauser, C. E. Wilmer, A. A. Sarjeant, R. Q. Snurr, S. T. Nguyen, A. Ö. Yazaydın and J. T. Hupp, *J. Am. Chem. Soc.*, 2012, **134**, 15016-15021.

- 22 I. M. Honicke, I. Senkowska, V. Bon, I. A. Baburin, N. Bonisch, S. Raschke, J. D. Evans and S. Kaskel, *Angew. Chem. Int. Ed.*, 2018, **57**, 13780-13783.
- 23 H. Furukawa, N. Ko, Y. B. Go, N. Aratani, S. B. Choi, E. Choi, A. Ö. Yazaydin, R. Q. Snurr, M. O’Keeffe, J. Kim and O. M. Yaghi, *Science*, 2010, **329**, 424-428.
- 24 H. K. Chae, D. Y. Siberio-Pérez, J. Kim, Y. Go, M. Eddaoudi, A. J. Matzger, M. O’Keeffe, O. M. Yaghi, D. Materials and G. Discovery, *Nature*, 2004, **427**, 523-527.
- 25 Z. Chen, P. Li, R. Anderson, X. Wang, X. Zhang, L. Robison, L. R. Redfern, S. Moribe, T. Islamoglu, D. A. Gómez-Gualdrón, T. Yildirim, J. F. Stoddart and O. K. Farha, *Science*, 2020, **368**, 297-303.
- 26 Y. Bai, Y. Dou, L.-H. Xie, W. Rutledge, J.-R. Li and H.-C. Zhou, *Chem. Soc. Rev.*, 2016, **45**, 2327-2367.
- 27 Z. Chen, Ł. J. Weseliński, K. Adil, Y. Belmabkhout, A. Shkurenko, H. Jiang, P. M. Bhatt, V. Guillermin, E. Dauzon, D.-X. Xue, M. O’Keeffe and M. Eddaoudi, *J. Am. Chem. Soc.*, 2017, **139**, 3265-3274.
- 28 H. Jiang, J. Jia, A. Shkurenko, Z. Chen, K. Adil, Y. Belmabkhout, L. J. Weselinski, A. H. Assen, D.-X. Xue, M. O’Keeffe and M. Eddaoudi, *J. Am. Chem. Soc.*, 2018, **140**, 8858-8867.
- 29 Z. Chen, H. Jiang, M. O’Keeffe and M. Eddaoudi, *Faraday Discuss.*, 2017, **201**, 127-143.
- 30 L. Liu, K. Konstas, M. R. Hill and S. G. Telfer, *J. Am. Chem. Soc.*, 2013, **135**, 17731-17734.
- 31 J. Jiang, F. Gándara, Y.-B. Zhang, K. Na, O. M. Yaghi and W. G. Klemperer, *J. Am. Chem. Soc.*, 2014, **136**, 12844-12847.
- 32 J. Jiang and O. M. Yaghi, *Chem. Rev.*, 2015, **115**, 6966-6997.
- 33 A. C. H. Sue, R. V. Mannige, H. Deng, D. Cao, C. Wang, F. Gándara, J. F. Stoddart, S. Whitelam and O. M. Yaghi, *Proc. Natl. Acad. Sci. U.S.A.*, 2015, **112**, 5591.
- 34 Y.-B. Zhang, H. Furukawa, N. Ko, W. Nie, H. J. Park, S. Okajima, K. E. Cordova, H. Deng, J. Kim and O. M. Yaghi, *J. Am. Chem. Soc.*, 2015, **137**, 2641-2650.
- 35 H. Deng, C. J. Doonan, H. Furukawa, R. B. Ferreira, J. Towne, C. B. Knobler, B. Wang and O. M. Yaghi, *Science*, 2010, **327**, 846.
- 36 H. Furukawa, J. Kim, N. W. Ockwig, M. O’Keeffe and O. M. Yaghi, *J. Am. Chem. Soc.*, 2008, **130**, 11650-11661.
- 37 Z. Ji, H. Wang, S. Canossa, S. Wuttke and O. M. Yaghi, *Adv. Funct. Mater.*, 2020, **n/a**, 2000238.
- 38 J. E. Mondloch, M. J. Katz, W. C. Isley Iii, P. Ghosh, P. Liao, W. Bury, G. W. Wagner, M. G. Hall, J. B. DeCoste, G. W. Peterson, R. Q. Snurr, C. J. Cramer, J. T. Hupp and O. K. Farha, *Nat. Mater.*, 2015, **14**, 512-516.
- 39 S.-Y. Moon, Y. Liu, J. T. Hupp and O. K. Farha, *Angew. Chem. Int. Ed.*, 2015, **54**, 6795-6799.
- 40 Y. Liu, W. Xuan and Y. Cui, *Adv. Mater.*, 2010, **22**, 4112-4135.
- 41 T. Zhang and W. Lin, *Chem. Soc. Rev.*, 2014, **43**, 5982-5993.
- 42 M. Yoon, R. Srirambalaji and K. Kim, *Chem. Rev.*, 2012, **112**, 1196-1231.
- 43 N. Kornienko, Y. Zhao, C. S. Kley, C. Zhu, D. Kim, S. Lin, C. J. Chang, O. M. Yaghi and P. Yang, *J. Am. Chem. Soc.*, 2015, **137**, 14129-14135.
- 44 S. M. J. Rogge, A. Bavykina, J. Hajek, H. Garcia, A. I. Olivos-Suarez, A. Sepúlveda-Escribano, A. Vimont, G. Clet, P. Bazin, F. Kapteijn, M. Daturi, E. V. Ramos-Fernandez,

- F. X. Llabrés i Xamena, V. Van Speybroeck and J. Gascon, *Chem. Soc. Rev.*, 2017, **46**, 3134-3184.
- 45 J. S. Lee, E. A. Kapustin, X. Pei, S. Llopis, O. M. Yaghi and F. D. Toste, *Chem*, 2020, **6**, 142-152.
- 46 H. Zhong, M. Ghorbani-Asl, K. H. Ly, J. Zhang, J. Ge, M. Wang, Z. Liao, D. Makarov, E. Zschech, E. Brunner, I. M. Weidinger, J. Zhang, A. V. Krasheninnikov, S. Kaskel, R. Dong and X. Feng, *Nat. Commun.*, 2020, **11**, 1409.
- 47 L. E. Kreno, K. Leong, O. K. Farha, M. Allendorf, R. P. Van Duyne and J. T. Hupp, *Chem. Rev.*, 2012, **112**, 1105-1125.
- 48 Z. Hu, B. J. Deibert and J. Li, *Chem. Soc. Rev.*, 2014, **43**, 5815-5840.
- 49 Y. Cui, Y. Yue, G. Qian and B. Chen, *Chem. Rev.*, 2012, **112**, 1126-1162.
- 50 T.-Y. Luo, P. Das, D. L. White, C. Liu, A. Star and N. L. Rosi, *J. Am. Chem. Soc.*, 2020, **142**, 2897-2904.
- 51 L. Sun, T. Miyakai, S. Seki and M. Dincă, *J. Am. Chem. Soc.*, 2013, **135**, 8185-8188.
- 52 L. Sun, M. G. Campbell and M. Dincă, *Angew. Chem. Int. Ed.*, 2016, **55**, 3566-3579.
- 53 M. Ko, L. Mendecki and K. A. Mirica, *Chem. Commun.*, 2018, **54**, 7873-7891.
- 54 W. Xu, X. Pei, C. S. Diercks, H. Lyu, Z. Ji and O. M. Yaghi, *J. Am. Chem. Soc.*, 2019, **141**, 17522-17526.
- 55 M. D. Allendorf, R. Dong, X. Feng, S. Kaskel, D. Matoga and V. Stavila, *Chem. Rev.*, 2020, DOI: 10.1021/acs.chemrev.0c00033.
- 56 R. C. Huxford, J. Della Rocca and W. Lin, *Curr. Opin. Chem. Biol.*, 2010, **14**, 262-268.
- 57 P. Horcajada, R. Gref, T. Baati, P. K. Allan, G. Maurin, P. Couvreur, G. Férey, R. E. Morris and C. Serre, *Chem. Rev.*, 2012, **112**, 1232-1268.
- 58 Y. Chen, P. Li, J. A. Modica, R. J. Drout and O. K. Farha, *J. Am. Chem. Soc.*, 2018, **140**, 5678-5681.
- 59 M.-X. Wu and Y.-W. Yang, *Adv. Mater.*, 2017, **29**, 1606134.
- 60 K. J. Hartlieb, D. P. Ferris, J. M. Holcroft, I. Kandela, C. L. Stern, M. S. Nassar, Y. Y. Botros and J. F. Stoddart, *Mol. Pharmaceutics*, 2017, **14**, 1831-1839.
- 61 S. Rojas, T. Baati, L. Njim, L. Manchego, F. Neffati, N. Abdeljelil, S. Saguem, C. Serre, M. F. Najjar, A. Zakhama and P. Horcajada, *J. Am. Chem. Soc.*, 2018, **140**, 9581-9586.
- 62 L. Cooper, T. Hidalgo, M. Gorman, T. Lozano-Fernández, R. Simón-Vázquez, C. Olivier, N. Guillou, C. Serre, C. Martineau, F. Taulelle, D. Damasceno-Borges, G. Maurin, Á. González-Fernández, P. Horcajada and T. Devic, *Chem. Commun.*, 2015, **51**, 5848-5851.
- 63 H. Kim, S. Yang, S. R. Rao, S. Narayanan, E. A. Kapustin, H. Furukawa, A. S. Umans, O. M. Yaghi and E. N. Wang, *Science*, 2017, **356**, 430-434.
- 64 N. Hanikel, M. S. Prévot, F. Fathieh, E. A. Kapustin, H. Lyu, H. Wang, N. J. Diercks, T. G. Glover and O. M. Yaghi, *ACS Cent. Sci.*, 2019, **5**, 1699-1706.
- 65 M. J. Kalmutzki, C. S. Diercks and O. M. Yaghi, *Adv. Mater.*, 2018, **30**, 1704304.
- 66 A. J. Rieth, A. M. Wright and M. Dincă, *Nat Rev Mater.*, 2019, **4**, 708-725.
- 67 J. Canivet, A. Fateeva, Y. Guo, B. Coasne and D. Farrusseng, *Chem. Soc. Rev.*, 2014, **43**, 5594-5617.
- 68 N. C. Burtch, H. Jasuja and K. S. Walton, *Chem. Rev.*, 2014, **114**, 10575-10612.
- 69 N. Hanikel, M. S. Prévot and O. M. Yaghi, *Nat. Nanotechnol.*, 2020, **15**, 348-355.
- 70 F. Fathieh, M. J. Kalmutzki, E. A. Kapustin, P. J. Waller, J. Yang and O. M. Yaghi, *Sci. Adv.*, 2018, **4**.

- 71 G. Akiyama, R. Matsuda and S. Kitagawa, *Chem. Lett.*, 2010, **39**, 360-361.
- 72 S. Wang, J. S. Lee, M. Wahiduzzaman, J. Park, M. Muschi, C. Martineau-Corcoss, A. Tissot, K. H. Cho, J. Marrot, W. Shepard, G. Maurin, J.-S. Chang and C. Serre, *Nat. Energy*, 2018, **3**, 985-993.
- 73 D. O’Nolan, A. Kumar and M. J. Zaworotko, *J. Am. Chem. Soc.*, 2017, **139**, 8508-8513.
- 74 P. Kusgens, M. Rose, I. Senkovska, H. Frode, A. Henschel, S. Siegle and S. Kaskel, *Microporous Mesoporous Mater.*, 2009, **120**, 325-330.
- 75 F.-X. Coudert, *Acc. Chem. Res.*, 2020, **53**, 1342-1350.
- 76 M. J. Katz, J. E. Mondloch, R. K. Totten, J. K. Park, S. T. Nguyen, O. K. Farha and J. T. Hupp, *Angew. Chem. Int. Ed.*, 2014, **53**, 497-501.
- 77 Z. Chen, K. Ma, J. J. Mahle, H. Wang, Z. H. Syed, A. Atilgan, Y. Chen, J. H. Xin, T. Islamoglu, G. W. Peterson and O. K. Farha, *J. Am. Chem. Soc.*, 2019, **141**, 20016-20021.
- 78 K. O. Kirlikovali, Z. Chen, T. Islamoglu, J. T. Hupp and O. K. Farha, *ACS Appl. Mater. Interfaces*, 2020, **12**, 14702-14720.
- 79 J. M. Palomba, S. P. Harvey, M. Kalaj, B. R. Pimentel, J. B. DeCoste, G. W. Peterson and S. M. Cohen, *ACS Appl. Mater. Interfaces*, 2020, **12**, 14672-14677.
- 80 A. Evans, R. Luebke and C. Petit, *J. Mater. Chem. A*, 2018, **6**, 10570-10594.
- 81 H. Li, K. Wang, Y. Sun, C. T. Lollar, J. Li and H.-C. Zhou, *Materials Today*, 2018, **21**, 108-121.
- 82 T. Islamoglu, Z. Chen, M. C. Wasson, C. T. Buru, K. O. Kirlikovali, U. Afrin, M. R. Mian and O. K. Farha, *Chem. Rev.*, 2020, **120**, 8130-8160.
- 83 D. Britt, D. Tranchemontagne and O. M. Yaghi, *Proc. Natl. Acad. Sci. U.S.A.*, 2008, **105**, 11623.
- 84 C. Wang, J. Kim, V. Malgras, J. Na, J. Lin, J. You, M. Zhang, J. Li and Y. Yamauchi, *Small*, 2019, **15**, 1970085.
- 85 S. Dhaka, R. Kumar, A. Deep, M. B. Kurade, S.-W. Ji and B.-H. Jeon, *Coord. Chem. Rev.*, 2019, **380**, 330-352.
- 86 R. J. Drout, L. Robison, Z. Chen, T. Islamoglu and O. K. Farha, *Trends Chem.*, 2019, **1**, 304-317.
- 87 Z. Ajoyan, P. Marino and A. J. Howarth, *CrystEngComm*, 2018, **20**, 5899-5912.
- 88 B. Li, H.-M. Wen, W. Zhou, Jeff Q. Xu and B. Chen, *Chem*, 2016, **1**, 557-580.
- 89 Y. Peng, V. Krungleviciute, I. Eryazici, J. T. Hupp, O. K. Farha and T. Yildirim, *J. Am. Chem. Soc.*, 2013, **135**, 11887-11894.
- 90 J. A. Mason, J. Oktawiec, M. K. Taylor, M. R. Hudson, J. Rodriguez, J. E. Bachman, M. I. Gonzalez, A. Cervellino, A. Guagliardi, C. M. Brown, P. L. Llewellyn, N. Masciocchi and J. R. Long, *Nature*, 2015, **527**, 357-361.
- 91 J. Jiang, H. Furukawa, Y.-B. Zhang and O. M. Yaghi, *J. Am. Chem. Soc.*, 2016, **138**, 10244-10251.
- 92 O. K. Farha, A. O. Yazaydin, I. Eryazici, C. D. Malliakas, B. G. Hauser, M. G. Kanatzidis, S. T. Nguyen, R. Q. Snurr and J. T. Hupp, *Nat. Chem.*, 2010, **2**, 944-948.
- 93 D. Alezi, Y. Belmabkhout, M. Suyetin, P. M. Bhatt, Ł. J. Weseliński, V. Solovyeva, K. Adil, I. Spanopoulos, P. N. Trikalitis, A.-H. Emwas and M. Eddaoudi, *J. Am. Chem. Soc.*, 2015, **137**, 13308-13318.
- 94 A. Ahmed, S. Seth, J. Purewal, A. G. Wong-Foy, M. Veenstra, A. J. Matzger and D. J. Siegel, *Nat. Commun.*, 2019, **10**, 1568.

- 95 M. T. Kapelewski, T. Runčevski, J. D. Tarver, H. Z. H. Jiang, K. E. Hurst, P. A. Parilla, A. Ayala, T. Gennett, S. A. FitzGerald, C. M. Brown and J. R. Long, *Chem. Mater.*, 2018, **30**, 8179-8189.
- 96 P. García-Holley, B. Schweitzer, T. Islamoglu, Y. Liu, L. Lin, S. Rodriguez, M. H. Weston, J. T. Hupp, D. A. Gómez-Gualdrón, T. Yildirim and O. K. Farha, *ACS Energy Lett.*, 2018, **3**, 748-754.
- 97 M. D. Allendorf, Z. Hulvey, T. Gennett, A. Ahmed, T. Autrey, J. Camp, E. Seon Cho, H. Furukawa, M. Haranczyk, M. Head-Gordon, S. Jeong, A. Karkamkar, D.-J. Liu, J. R. Long, K. R. Meihaus, I. H. Nayyar, R. Nazarov, D. J. Siegel, V. Stavila, J. J. Urban, S. P. Veccham and B. C. Wood, *Energy Environ. Sci.*, 2018, **11**, 2784-2812.
- 98 M. P. Suh, H. J. Park, T. K. Prasad and D.-W. Lim, *Chem. Rev.*, 2012, **112**, 782-835.
- 99 S. S. Kaye, A. Dailly, O. M. Yaghi and J. R. Long, *J. Am. Chem. Soc.*, 2007, **129**, 14176-14177.
- 100 X. Zhang, R.-B. Lin, J. Wang, B. Wang, B. Liang, T. Yildirim, J. Zhang, W. Zhou and B. Chen, *Adv. Mater.*, 2020, **32**, 1907995.
- 101 B. Li, H.-M. Wen, H. Wang, H. Wu, M. Tyagi, T. Yildirim, W. Zhou and B. Chen, *J. Am. Chem. Soc.*, 2014, **136**, 6207-6210.
- 102 K. Adil, Y. Belmabkhout, R. S. Pillai, A. Cadiau, P. M. Bhatt, A. H. Assen, G. Maurin and M. Eddaoudi, *Chem. Soc. Rev.*, 2017, **46**, 3402-3430.
- 103 A. Cadiau, K. Adil, P. M. Bhatt, Y. Belmabkhout and M. Eddaoudi, *Science*, 2016, **353**, 137-140.
- 104 E. D. Bloch, W. L. Queen, R. Krishna, J. M. Zadrozny, C. M. Brown and J. R. Long, *Science*, 2012, **335**, 1606-1610.
- 105 H. Wu, Q. Gong, D. H. Olson and J. Li, *Chem. Rev.*, 2012, **112**, 836-868.
- 106 X. Cui, K. Chen, H. Xing, Q. Yang, R. Krishna, Z. Bao, H. Wu, W. Zhou, X. Dong, Y. Han, B. Li, Q. Ren, M. J. Zaworotko and B. Chen, *Science*, 2016, **353**, 141-144.
- 107 O. Shekhah, Y. Belmabkhout, Z. Chen, V. Guillerm, A. Cairns, K. Adil and M. Eddaoudi, *Nat. Commun.*, 2014, **5**, 4228.
- 108 J. W. Yoon, H. Chang, S.-J. Lee, Y. K. Hwang, D.-Y. Hong, S.-K. Lee, J. S. Lee, S. Jang, T.-U. Yoon, K. Kwac, Y. Jung, R. S. Pillai, F. Faucher, A. Vimont, M. Daturi, G. Férey, C. Serre, G. Maurin, Y.-S. Bae and J.-S. Chang, *Nat. Mater.*, 2016, **16**, 526.
- 109 Z. R. Herm, B. M. Wiers, J. A. Mason, J. M. van Baten, M. R. Hudson, P. Zajdel, C. M. Brown, N. Masciocchi, R. Krishna and J. R. Long, *Science*, 2013, **340**, 960-964.
- 110 P.-Q. Liao, W.-X. Zhang, J.-P. Zhang and X.-M. Chen, *Nat. Commun.*, 2015, **6**, 8697.
- 111 Z. Chen, L. Feng, L. Liu, P. M. Bhatt, K. Adil, A.-H. Emwas, A. H. Assen, Y. Belmabkhout, Y. Han and M. Eddaoudi, *Langmuir*, 2018, **34**, 14546-14551.
- 112 P. A. P. Mendes, P. Horcajada, S. Rives, H. Ren, A. E. Rodrigues, T. Devic, E. Magnier, P. Trens, H. Jobic, J. Ollivier, G. Maurin, C. Serre and J. A. C. Silva, *Adv. Funct. Mater.*, 2014, **24**, 7666-7673.
- 113 B. Zheng, J. Bai, J. Duan, L. Wojtas and M. J. Zaworotko, *J. Am. Chem. Soc.*, 2010, **133**, 748-751.
- 114 J. Liu, P. K. Thallapally, B. P. McGrail, D. R. Brown and J. Liu, *Chem. Soc. Rev.*, 2012, **41**, 2308-2322.
- 115 S. Mukherjee, N. Sikdar, D. O’Nolan, D. M. Franz, V. Gascón, A. Kumar, N. Kumar, H. S. Scott, D. G. Madden, P. E. Kruger, B. Space and M. J. Zaworotko, *Sci. Adv.*, 2019, **5**, eaax9171.

- 116 R.-B. Lin, L. Li, H.-L. Zhou, H. Wu, C. He, S. Li, R. Krishna, J. Li, W. Zhou and B. Chen, *Nat. Mater.*, 2018, **17**, 1128-1133.
- 117 X. Cui, Q. Yang, L. Yang, R. Krishna, Z. Zhang, Z. Bao, H. Wu, Q. Ren, W. Zhou, B. Chen and H. Xing, *Adv. Mater.*, 2017, **29**, 1606929.
- 118 Z. Bao, G. Chang, H. Xing, R. Krishna, Q. Ren and B. Chen, *Energy Environ. Sci.*, 2016, **9**, 3612-3641.
- 119 B. Li, H. Wang and B. Chen, *Chemistry – An Asian Journal*, 2014, **9**, 1474-1498.
- 120 J. Wang, Y. Zhang, P. Zhang, J. Hu, R.-B. Lin, Q. Deng, Z. Zeng, H. Xing, S. Deng and B. Chen, *J. Am. Chem. Soc.*, 2020, **142**, 9744-9751.
- 121 M. H. Mohamed, Y. Yang, L. Li, S. Zhang, J. P. Ruffley, A. G. Jarvi, S. Saxena, G. Veser, J. K. Johnson and N. L. Rosi, *J. Am. Chem. Soc.*, 2019, **141**, 13003-13007.
- 122 Y. Inokuma, T. Arai and M. Fujita, *Nat. Chem.*, 2010, **2**, 780-783.
- 123 Y. Inokuma, S. Yoshioka, J. Ariyoshi, T. Arai, Y. Hitora, K. Takada, S. Matsunaga, K. Rissanen and M. Fujita, *Nature*, 2013, **495**, 461-466.
- 124 S. Lee, E. A. Kapustin and O. M. Yaghi, *Science*, 2016, **353**, 808.
- 125 S.-Y. Zhang, D. Fairen-Jimenez and M. J. Zaworotko, *Angew. Chem. Int. Ed.*, 2020, **n/a**.
- 126 NuMat Technologies, <https://www.numat-tech.com/>, (accessed 25 September 2019).
- 127 T. Faust, *Nat. Chem.*, 2016, **8**, 990-991.
- 128 O. M. Yaghi, G. Li and H. Li, *Nature*, 1995, **378**, 703-706.
- 129 A. Werner, *Z. Anorg. Allg. Chem.*, 1893, **3**, 267-330.
- 130 B. Rungtaweeworanit, C. S. Diercks, M. J. Kalmutzki and O. M. Yaghi, *Faraday Discuss.*, 2017, **201**, 9-45.
- 131 H. Li, M. Eddaoudi, M. O'Keeffe and O. M. Yaghi, *Nature*, 1999, **402**, 276-279.
- 132 K. A. Hofmann and F. Küspert, *Z. Anorg. Allg. Chem.*, 1897, **15**, 204-207.
- 133 H. M. Powell and J. H. Rayner, *Nature*, 1949, **163**, 566-567.
- 134 H. J. Buser, A. Ludi, W. Petter and D. Schwarzenbach, *J. Chem. Soc., Chem. Commun.*, 1972, DOI: 10.1039/C39720001299, 1299-1299.
- 135 H. J. Buser, D. Schwarzenbach, W. Petter and A. Ludi, *Inorg. Chem.*, 1977, **16**, 2704-2710.
- 136 J. H. Cavka, S. Jakobsen, U. Olsbye, N. Guillou, C. Lamberti, S. Bordiga and K. P. Lillerud, *J. Am. Chem. Soc.*, 2008, **130**, 13850-13851.
- 137 C. S. Campos-Fernández, R. Clérac, J. M. Koomen, D. H. Russell and K. R. Dunbar, *J. Am. Chem. Soc.*, 2001, **123**, 773-774.
- 138 S. Alvarez, *Dalton Trans.*, 2005, DOI: 10.1039/B503582C, 2209-2233.
- 139 S. R. Batten, S. M. Neville and D. R. Turner, in *Coordination Polymers: Design, Analysis and Application*, The Royal Society of Chemistry, 2009, DOI: 10.1039/9781847558862-00144, pp. 144-190.
- 140 B. Moulton and M. J. Zaworotko, *Chem. Rev.*, 2001, **101**, 1629-1658.
- 141 K. R. Dunbar; and R. A. Heintz, in *Progress in Inorganic Chemistry*, DOI: 10.1002/9780470166468.ch4, pp. 283-391.
- 142 Y. Kinoshita, I. Matsubara and Y. Saito, *Bull. Chem. Soc. Jpn.*, 1959, **32**, 741-747.
- 143 A. Aumüller, P. Erk, G. Klebe, S. Hünig, J. U. von Schütz and H.-P. Werner, *Angew. Chem. Int. Ed.*, 1986, **25**, 740-741.
- 144 B. F. Hoskins and R. Robson, *J. Am. Chem. Soc.*, 1989, **111**, 5962-5964.
- 145 R. Kato, H. Kobayashi and A. Kobayashi, *J. Am. Chem. Soc.*, 1989, **111**, 5224-5232.
- 146 B. F. Hoskins and R. Robson, *J. Am. Chem. Soc.*, 1990, **112**, 1546-1554.

- 147 B. F. Abrahams, B. F. Hoskins, D. M. Michail and R. Robson, *Nature*, 1994, **369**, 727-729.
- 148 S. Subramanian and M. J. Zaworotko, *Angew. Chem. Int. Ed.*, 1995, **34**, 2127-2129.
- 149 B. F. Abrahams, B. F. Hoskins and R. Robson, *J. Am. Chem. Soc.*, 1991, **113**, 3606-3607.
- 150 M. Fujita, Y. J. Kwon, S. Washizu and K. Ogura, *J. Am. Chem. Soc.*, 1994, **116**, 1151-1152.
- 151 S. Kitagawa, M. Munakata and T. Tanimura, *Inorg. Chem.*, 1992, **31**, 1714-1717.
- 152 S. i. Noro, S. Kitagawa, M. Kondo and K. Seki, *Angew. Chem. Int. Ed.*, 2000, **39**, 2081-2084.
- 153 P. Nugent, Y. Belmabkhout, S. D. Burd, A. J. Cairns, R. Luebke, K. Forrest, T. Pham, S. Ma, B. Space, L. Wojtas, M. Eddaoudi and M. J. Zaworotko, *Nature*, 2013, **495**, 80-84.
- 154 S. D. Burd, S. Ma, J. A. Perman, B. J. Sikora, R. Q. Snurr, P. K. Thallapally, J. Tian, L. Wojtas and M. J. Zaworotko, *J. Am. Chem. Soc.*, 2012, **134**, 3663-3666.
- 155 M. Eddaoudi, D. B. Moler, H. Li, B. Chen, T. M. Reineke, M. O'Keeffe and O. M. Yaghi, *Acc. Chem. Res.*, 2001, **34**, 319-330.
- 156 M. J. Kalmutzki, N. Hanikel and O. M. Yaghi, *Sci. Adv.*, 2018, **4**, eaat9180.
- 157 M. O'Keeffe and O. M. Yaghi, *Chem. Rev.*, 2012, **112**, 675-702.
- 158 O. M. Yaghi and Q. Li, *MRS Bulletin*, 2011, **34**, 682-690.
- 159 M. O'Keeffe, M. A. Peskov, S. J. Ramsden and O. M. Yaghi, *Acc. Chem. Res.*, 2008, **41**, 1782-1789.
- 160 O. Delgado-Friedrichs, M. O'Keeffe and O. M. Yaghi, *Phys. Chem. Chem. Phys.*, 2007, **9**, 1035-1043.
- 161 O. Delgado-Friedrichs, M. O'Keeffe and O. M. Yaghi, *Acta Cryst. A*, 2006, **62**, 350-355.
- 162 N. W. Ockwig, O. Delgado-Friedrichs, M. O'Keeffe and O. M. Yaghi, *Acc. Chem. Res.*, 2005, **38**, 176-182.
- 163 S. S.-Y. Chui, S. M.-F. Lo, J. P. H. Charmant, A. G. Orpen and I. D. Williams, *Science*, 1999, **283**, 1148-1150.
- 164 K. Barthelet, J. Marrot, D. Riou and G. Férey, *Angew. Chem. Int. Ed.*, 2002, **41**, 281-284.
- 165 N. L. Rosi, M. Eddaoudi, J. Kim, M. O'Keeffe and O. M. Yaghi, *Angew. Chem. Int. Ed.*, 2002, **41**, 284-287.
- 166 O. M. Yaghi, M. O'Keeffe and M. Kanatzidis, *J. Solid State Chem.*, 2000, **152**, 1-2.
- 167 B. Chen, M. Eddaoudi, T. M. Reineke, J. W. Kampf, M. O'Keeffe and O. M. Yaghi, *J. Am. Chem. Soc.*, 2000, **122**, 11559-11560.
- 168 M. Dan-Hardi, C. Serre, T. Frot, L. Rozes, G. Maurin, C. Sanchez and G. Férey, *J. Am. Chem. Soc.*, 2009, **131**, 10857-10859.
- 169 G. Férey, C. Mellot-Draznieks, C. Serre, F. Millange, J. Dutour, S. Surblé and I. Margiolaki, *Science*, 2005, **309**, 2040-2042.
- 170 G. Férey, *J. Solid State Chem.*, 2000, **152**, 37-48.
- 171 J.-P. Zhang, Y.-B. Zhang, J.-B. Lin and X.-M. Chen, *Chem. Rev.*, 2012, **112**, 1001-1033.
- 172 F. A. Almeida Paz, J. Klinowski, S. M. F. Vilela, J. P. C. Tomé, J. A. S. Cavaleiro and J. Rocha, *Chem. Soc. Rev.*, 2012, **41**, 1088-1110.
- 173 D. Zhao, D. J. Timmons, D. Yuan and H.-C. Zhou, *Acc. Chem. Res.*, 2011, **44**, 123-133.
- 174 F. C. Hawthorne, *Nature*, 1990, **345**, 297-297.
- 175 J. Maddox, *Nature*, 1988, **335**, 201-201.
- 176 O. M. Yaghi, M. O'Keeffe, N. W. Ockwig, H. K. Chae, M. Eddaoudi and J. Kim, *Nature*, 2003, **423**, 705-714.

- 177 Z. Chen, Z. Thiam, A. Shkurenko, L. J. Weselinski, K. Adil, H. Jiang, D. Alezi, A. H. Assen, M. O'Keeffe and M. Eddaoudi, *J. Am. Chem. Soc.*, 2019, **141**, 20480-20489.
- 178 I. Spanopoulos, C. Tsangarakis, E. Klontzas, E. Tylianakis, G. Froudakis, K. Adil, Y. Belmabkhout, M. Eddaoudi and P. N. Trikalitis, *J. Am. Chem. Soc.*, 2016, **138**, 1568-1574.
- 179 Z. Chen, P. Li, X. Zhang, P. Li, M. C. Wasson, T. Islamoglu, J. F. Stoddart and O. K. Farha, *J. Am. Chem. Soc.*, 2019, **141**, 2900-2905.
- 180 Z. Chen, H. Jiang, M. Li, M. O'Keeffe and M. Eddaoudi, *Chem. Rev.*, 2020, **120**, 8039-8065.
- 181 M. Eddaoudi, J. Kim, M. O'Keeffe and O. M. Yaghi, *J. Am. Chem. Soc.*, 2002, **124**, 376-377.
- 182 F. Nouar, J. F. Eubank, T. Bousquet, L. Wojtas, M. J. Zaworotko and M. Eddaoudi, *J. Am. Chem. Soc.*, 2008, **130**, 1833-1835.
- 183 P. Li, N. A. Vermeulen, C. D. Malliakas, D. A. Gómez-Gualdrón, A. J. Howarth, B. L. Mehdi, A. Dohnalkova, N. D. Browning, M. O'Keeffe and O. K. Farha, *Science*, 2017, **356**, 624-627.
- 184 Z. Chen, P. Li, X. Zhang, M. R. Mian, X. Wang, P. Li, Z. Liu, M. O'Keeffe, J. F. Stoddart and O. K. Farha, *Nano Res.*, 2020, DOI: 10.1007/s12274-020-2690-3.
- 185 W. Morris, B. Voloskiy, S. Demir, F. Gándara, P. L. McGrier, H. Furukawa, D. Cascio, J. F. Stoddart and O. M. Yaghi, *Inorg. Chem.*, 2012, **51**, 6443-6445.
- 186 U. Stoeck, I. Senkovska, V. Bon, S. Krause and S. Kaskel, *Chem. Commun.*, 2015, **51**, 1046-1049.
- 187 F. Gándara, H. Furukawa, S. Lee and O. M. Yaghi, *J. Am. Chem. Soc.*, 2014, **136**, 5271-5274.
- 188 T. Devic and C. Serre, *Chem. Soc. Rev.*, 2014, **43**, 6097-6115.
- 189 C. Serre, F. Millange, C. Thouvenot, M. Noguès, G. Marsolier, D. Louër and G. Férey, *J. Am. Chem. Soc.*, 2002, **124**, 13519-13526.
- 190 G. Férey, C. Serre, C. Mellot-Draznieks, F. Millange, S. Surblé, J. Dutour and I. Margiolaki, *Angewandte Chemie*, 2004, **116**, 6456-6461.
- 191 T.-F. Liu, L. Zou, D. Feng, Y.-P. Chen, S. Fordham, X. Wang, Y. Liu and H.-C. Zhou, *J. Am. Chem. Soc.*, 2014, **136**, 7813-7816.
- 192 S. M. Towsif Abtab, D. Alezi, P. M. Bhatt, A. Shkurenko, Y. Belmabkhout, H. Aggarwal, Ł. J. Weseliński, N. Alsadun, U. Samin, M. N. Hedhili and M. Eddaoudi, *Chem*, 2018, **4**, 94-105.
- 193 D. Feng, Z.-Y. Gu, J.-R. Li, H.-L. Jiang, Z. Wei and H.-C. Zhou, *Angew. Chem. Int. Ed.*, 2012, **51**, 10307-10310.
- 194 J. E. Mondloch, W. Bury, D. Fairen-Jimenez, S. Kwon, E. J. DeMarco, M. H. Weston, A. A. Sarjeant, S. T. Nguyen, P. C. Stair, R. Q. Snurr, O. K. Farha and J. T. Hupp, *J. Am. Chem. Soc.*, 2013, **135**, 10294-10297.
- 195 S. Vaesen, V. Guillerm, Q. Yang, A. D. Wiersum, B. Marszalek, B. Gil, A. Vimont, M. Daturi, T. Devic, P. L. Llewellyn, C. Serre, G. Maurin and G. De Weireld, *Chem. Commun.*, 2013, **49**, 10082-10084.
- 196 S. Yuan, T.-F. Liu, D. Feng, J. Tian, K. Wang, J. Qin, Q. Zhang, Y.-P. Chen, M. Bosch, L. Zou, S. J. Teat, S. J. Dalgarno and H.-C. Zhou, *Chem. Sci.*, 2015, **6**, 3926-3930.
- 197 H. L. Nguyen, F. Gándara, H. Furukawa, T. L. H. Doan, K. E. Cordova and O. M. Yaghi, *J. Am. Chem. Soc.*, 2016, **138**, 4330-4333.

- 198 H. L. Nguyen, *New J. Chem.*, 2017, **41**, 14030-14043.
- 199 S. Wang, T. Kitao, N. Guillou, M. Wahiduzzaman, C. Martineau-Corcros, F. Nouar, A. Tissot, L. Binet, N. Ramsahye, S. Devautour-Vinot, S. Kitagawa, S. Seki, Y. Tsutsui, V. Briois, N. Steunou, G. Maurin, T. Uemura and C. Serre, *Nat. Commun.*, 2018, **9**, 1660.
- 200 Z. Chen, S. L. Hanna, L. R. Redfern, D. Alezi, T. Islamoglu and O. K. Farha, *Coord. Chem. Rev.*, 2019, **386**, 32-49.
- 201 Z. Chen, P. Li, X. Wang, K.-i. Otake, X. Zhang, L. Robison, A. Atilgan, T. Islamoglu, M. G. Hall, G. W. Peterson, J. F. Stoddart and O. K. Farha, *J. Am. Chem. Soc.*, 2019, **141**, 12229-12235.
- 202 V. Colombo, C. Montoro, A. Maspero, G. Palmisano, N. Masciocchi, S. Galli, E. Barea and J. A. R. Navarro, *J. Am. Chem. Soc.*, 2012, **134**, 12830-12843.
- 203 A. Schoedel, A. J. Cairns, Y. Belmabkhout, L. Wojtas, M. Mohamed, Z. Zhang, D. M. Proserpio, M. Eddaoudi and M. J. Zaworotko, *Angew. Chem. Int. Ed.*, 2013, **125**, 2974-2977.
- 204 S. K. Elsaidi, M. H. Mohamed, L. Wojtas, A. J. Cairns, M. Eddaoudi and M. J. Zaworotko, *Chem. Commun.*, 2013, **49**, 8154-8156.
- 205 A. Schoedel, L. Wojtas, S. P. Kelley, R. D. Rogers, M. Eddaoudi and M. J. Zaworotko, *Angew. Chem. Int. Ed.*, 2011, **50**, 11421-11424.
- 206 A. J. Cairns, J. A. Perman, L. Wojtas, V. C. Kravtsov, M. H. Alkordi, M. Eddaoudi and M. J. Zaworotko, *J. Am. Chem. Soc.*, 2008, **130**, 1560-1561.
- 207 Z. Chen, K. Adil, L. J. Weselinski, Y. Belmabkhout and M. Eddaoudi, *J. Mater. Chem. A*, 2015, **3**, 6276-6281.
- 208 V. Guillerm, Ł. Weseliński, J., Y. Belmabkhout, A. J. Cairns, V. D'Elia, Ł. Wojtas, K. Adil and M. Eddaoudi, *Nat. Chem.*, 2014, **6**, 673-680.
- 209 V. Guillerm, D. Kim, J. F. Eubank, R. Luebke, X. Liu, K. Adil, M. S. Lah and M. Eddaoudi, *Chem. Soc. Rev.*, 2014, **43**, 6141-6172.
- 210 J. F. Eubank, Ł. Wojtas, M. R. Hight, T. Bousquet, V. C. Kravtsov and M. Eddaoudi, *J. Am. Chem. Soc.*, 2011, **133**, 17532-17535.
- 211 D. Yuan, D. Zhao, D. Sun and H.-C. Zhou, *Angew. Chem. Int. Ed.*, 2010, **49**, 5357-5361.
- 212 S. Krause, V. Bon, I. Senkovska, U. Stoeck, D. Wallacher, D. M. Töbrens, S. Zander, R. S. Pillai, G. Maurin, F. o.-X. Coudert and S. Kaskel, *Nature*, 2016, **532**, 348-352.
- 213 U. Stoeck, S. Krause, V. Bon, I. Senkovska and S. Kaskel, *Chem. Commun.*, 2012, **48**, 10841-10843.
- 214 O. Delgado Friedrichs, M. O'Keeffe and O. M. Yaghi, *Acta Cryst. A*, 2003, **59**, 22-27.
- 215 O. Delgado Friedrichs, M. O'Keeffe and O. M. Yaghi, *Acta Crystallogr A*, 2003, **59**, 515-525.
- 216 M. Li, D. Li, M. O'Keeffe and O. M. Yaghi, *Chem. Rev.*, 2014, **114**, 1343-1370.
- 217 J. J. Perry Iv, J. A. Perman and M. J. Zaworotko, *Chem. Soc. Rev.*, 2009, **38**, 1400-1417.
- 218 M. O'Keeffe, M. Eddaoudi, H. Li, T. Reineke and O. M. Yaghi, *J. Solid State Chem.*, 2000, **152**, 3-20.
- 219 Q. Lin, X. Bu, A. Kong, C. Mao, X. Zhao, F. Bu and P. Feng, *J. Am. Chem. Soc.*, 2015, **137**, 2235-2238.
- 220 T.-F. Liu, D. Feng, Y.-P. Chen, L. Zou, M. Bosch, S. Yuan, Z. Wei, S. Fordham, K. Wang and H.-C. Zhou, *J. Am. Chem. Soc.*, 2015, **137**, 413-419.

- 221 T. C. Wang, W. Bury, D. A. Gómez-Gualdrón, N. A. Vermeulen, J. E. Mondloch, P. Deria, K. Zhang, P. Z. Moghadam, A. A. Sarjeant, R. Q. Snurr, J. F. Stoddart, J. T. Hupp and O. K. Farha, *J. Am. Chem. Soc.*, 2015, **137**, 3585-3591.
- 222 J. Zheng, M. Wu, F. Jiang, W. Su and M. Hong, *Chem. Sci.*, 2015, **6**, 3466-3470.
- 223 S. M. Cohen, *J. Am. Chem. Soc.*, 2017, **139**, 2855-2863.
- 224 L. Feng, S. Yuan, J.-S. Qin, Y. Wang, A. Kirchon, D. Qiu, L. Cheng, S. T. Madrahimov and H.-C. Zhou, *Matter*, 2019, **1**, 156-167.
- 225 Z. Yin, S. Wan, J. Yang, M. Kurmoo and M.-H. Zeng, *Coord. Chem. Rev.*, 2019, **378**, 500-512.
- 226 O. Karagiari, W. Bury, J. E. Mondloch, J. T. Hupp and O. K. Farha, *Angew. Chem. Int. Ed.*, 2014, **53**, 4530-4540.
- 227 R. J. Marshall and R. S. Forgan, *Eur. J. Inorg. Chem.*, 2016, **2016**, 4310-4331.
- 228 M. Taddei, R. J. Wakeham, A. Koutsianos, E. Andreoli and A. R. Barron, *Angew. Chem. Int. Ed.*, 2018, **57**, 11706-11710.
- 229 C.-X. Chen, Z.-W. Wei, J.-J. Jiang, S.-P. Zheng, H.-P. Wang, Q.-F. Qiu, C.-C. Cao, D. Fenske and C.-Y. Su, *J. Am. Chem. Soc.*, 2017, **139**, 6034-6037.
- 230 Z. Wang and S. M. Cohen, *J. Am. Chem. Soc.*, 2007, **129**, 12368-12369.
- 231 T. Ishiwata, Y. Furukawa, K. Sugikawa, K. Kokado and K. Sada, *J. Am. Chem. Soc.*, 2013, **135**, 5427-5432.
- 232 Y. Zhang, X. Feng, H. Li, Y. Chen, J. Zhao, S. Wang, L. Wang and B. Wang, *Angew. Chem. Int. Ed.*, 2015, **54**, 4259-4263.
- 233 T. Li, M. T. Kozłowski, E. A. Doud, M. N. Blakely and N. L. Rosi, *J. Am. Chem. Soc.*, 2013, **135**, 11688-11691.
- 234 B. J. Burnett, P. M. Barron, C. Hu and W. Choe, *J. Am. Chem. Soc.*, 2011, **133**, 9984-9987.
- 235 C. Liu, T.-Y. Luo, E. S. Feura, C. Zhang and N. L. Rosi, *J. Am. Chem. Soc.*, 2015, **137**, 10508-10511.
- 236 S. Yuan, P. Zhang, L. Zhang, A. T. Garcia-Esparza, D. Sokaras, J.-S. Qin, L. Feng, G. S. Day, W. Chen, H. F. Drake, P. Elumalai, S. T. Madrahimov, D. Sun and H.-C. Zhou, *J. Am. Chem. Soc.*, 2018, **140**, 10814-10819.
- 237 M. Dincă and J. R. Long, *J. Am. Chem. Soc.*, 2007, **129**, 11172-11176.
- 238 M. J. Ingleson, J. Perez Barrio, J.-B. Guilhaud, Y. Z. Khimyak and M. J. Rosseinsky, *Chem. Commun.*, 2008, DOI: 10.1039/B718367D, 2680-2682.
- 239 C. J. Doonan, W. Morris, H. Furukawa and O. M. Yaghi, *J. Am. Chem. Soc.*, 2009, **131**, 9492-9493.
- 240 W. Morris, C. J. Doonan and O. M. Yaghi, *Inorg. Chem.*, 2011, **50**, 6853-6855.
- 241 S. Das, H. Kim and K. Kim, *J. Am. Chem. Soc.*, 2009, **131**, 3814-3815.
- 242 K. K. Tanabe and S. M. Cohen, *Chem. Soc. Rev.*, 2011, **40**, 498-519.
- 243 S. M. Cohen, *Chem. Rev.*, 2012, **112**, 970-1000.
- 244 M. Kim, J. F. Cahill, H. Fei, K. A. Prather and S. M. Cohen, *J. Am. Chem. Soc.*, 2012, **134**, 18082-18088.
- 245 T. Islamoglu, S. Goswami, Z. Li, A. J. Howarth, O. K. Farha and J. T. Hupp, *Acc. Chem. Res.*, 2017, **50**, 805-813.
- 246 C. K. Brozek and M. Dincă, *Chem. Soc. Rev.*, 2014, **43**, 5456-5467.
- 247 C. K. Brozek, L. Bellarosa, T. Soejima, T. V. Clark, N. López and M. Dincă, *Chem. Eur. J.*, 2014, **20**, 6871-6874.

- 248 L. Zou, D. Feng, T.-F. Liu, Y.-P. Chen, S. Yuan, K. Wang, X. Wang, S. Fordham and H.-C. Zhou, *Chem. Sci.*, 2016, **7**, 1063-1069.
- 249 J. Park, D. Feng and H.-C. Zhou, *J. Am. Chem. Soc.*, 2015, **137**, 11801-11809.
- 250 D. Denysenko, J. Jelic, K. Reuter and D. Volkmer, *Chem. Eur. J.*, 2015, **21**, 8188-8199.
- 251 M. Lalonde, W. Bury, O. Karagiari, Z. Brown, J. T. Hupp and O. K. Farha, *J. Mater. Chem. A*, 2013, **1**, 5453-5468.
- 252 M. Bosch, S. Yuan, W. Rutledge and H.-C. Zhou, *Acc. Chem. Res.*, 2017, **50**, 857-865.
- 253 X. Lian, D. Feng, Y.-P. Chen, T.-F. Liu, X. Wang and H.-C. Zhou, *Chem. Sci.*, 2015, **6**, 7044-7048.
- 254 C. Cuadrado-Collados, G. Mouchaham, L. Daemen, Y. Cheng, A. Ramirez-Cuesta, H. Aggarwal, A. Missyul, M. Eddaoudi, Y. Belmabkhout and J. Silvestre-Albero, *J. Am. Chem. Soc.*, 2020, **142**, 13391-13397.
- 255 M. B. Lalonde, J. E. Mondloch, P. Deria, A. A. Sarjeant, S. S. Al-Juaid, O. I. Osman, O. K. Farha and J. T. Hupp, *Inorg. Chem.*, 2015, **54**, 7142-7144.
- 256 M. Kim, J. F. Cahill, Y. Su, K. A. Prather and S. M. Cohen, *Chem. Sci.*, 2012, **3**, 126-130.
- 257 X. Zhao, Z. Zhang, X. Cai, B. Ding, C. Sun, G. Liu, C. Hu, S. Shao and M. Pang, *ACS Appl. Mater. Interfaces*, 2019, **11**, 7884-7892.
- 258 G. C. Shearer, J. G. Vitillo, S. Bordiga, S. Svelle, U. Olsbye and K. P. Lillerud, *Chem. Mater.*, 2016, **28**, 7190-7193.
- 259 C. Tan, X. Han, Z. Li, Y. Liu and Y. Cui, *J. Am. Chem. Soc.*, 2018, **140**, 16229-16236.
- 260 W. Bury, D. Fairen-Jimenez, M. B. Lalonde, R. Q. Snurr, O. K. Farha and J. T. Hupp, *Chem. Mater.*, 2013, **25**, 739-744.
- 261 F. A. Son, A. Atilgan, K. B. Idrees, T. Islamoglu and O. K. Farha, *Inorg. Chem. Front.*, 2020, **7**, 984-990.
- 262 H. Fei and S. M. Cohen, *J. Am. Chem. Soc.*, 2015, **137**, 2191-2194.
- 263 H. Fei, J. Shin, Y. S. Meng, M. Adelhart, J. Sutter, K. Meyer and S. M. Cohen, *J. Am. Chem. Soc.*, 2014, **136**, 4965-4973.
- 264 S. Jeong, D. Kim, X. Song, M. Choi, N. Park and M. S. Lah, *Chem. Mater.*, 2013, **25**, 1047-1054.
- 265 W. Wu, J. Su, M. Jia, Z. Li, G. Liu and W. Li, *Sci. Adv.*, 2020, **6**, eaax7270.
- 266 P. Deria, J. E. Mondloch, E. Tylianakis, P. Ghosh, W. Bury, R. Q. Snurr, J. T. Hupp and O. K. Farha, *J. Am. Chem. Soc.*, 2013, **135**, 16801-16804.
- 267 P. Deria, W. Bury, I. Hod, C.-W. Kung, O. Karagiari, J. T. Hupp and O. K. Farha, *Inorg. Chem.*, 2015, **54**, 2185-2192.
- 268 J. Liu, J. Ye, Z. Li, K.-i. Otake, Y. Liao, A. W. Peters, H. Noh, D. G. Truhlar, L. Gagliardi, C. J. Cramer, O. K. Farha and J. T. Hupp, *J. Am. Chem. Soc.*, 2018, **140**, 11174-11178.
- 269 D. Sun, P. R. Adiyala, S.-J. Yim and D.-P. Kim, *Angew. Chem. Int. Ed.*, 2019, **58**, 7405-7409.
- 270 J. Liu, Z. Li, X. Zhang, K.-i. Otake, L. Zhang, A. W. Peters, M. J. Young, N. M. Bedford, S. P. Letourneau, D. J. Mandia, J. W. Elam, O. K. Farha and J. T. Hupp, *ACS Catal.*, 2019, **9**, 3198-3207.
- 271 L. Robison, R. J. Drout, L. R. Redfern, F. A. Son, M. C. Wasson, S. Goswami, Z. Chen, A. Olszewski, K. B. Idrees, T. Islamoglu and O. K. Farha, *Chem. Mater.*, 2020, **32**, 3545-3552.

- 272 A. Bétard and R. A. Fischer, *Chem. Rev.*, 2012, **112**, 1055-1083.
- 273 J. Liu and C. Wöll, *Chem. Soc. Rev.*, 2017, **46**, 5730-5770.
- 274 O. Shekhah, H. Wang, S. Kowarik, F. Schreiber, M. Paulus, M. Tolan, C. Sternemann, F. Evers, D. Zacher, R. A. Fischer and C. Woll, *J. Am. Chem. Soc.*, 2007, **129**, 15118-15119.
- 275 O. Shekhah, H. Wang, M. Paradinas, C. Ocal, B. Schüpbach, A. Terfort, D. Zacher, R. A. Fischer and C. Wöll, *Nat. Mater.*, 2009, **8**, 481-484.
- 276 M. C. So, S. Jin, H.-J. Son, G. P. Wiederrecht, O. K. Farha and J. T. Hupp, *J. Am. Chem. Soc.*, 2013, **135**, 15698-15701.
- 277 Y. Zhong, B. Cheng, C. Park, A. Ray, S. Brown, F. Mujid, J.-U. Lee, H. Zhou, J. Suh, K.-H. Lee, A. J. Mannix, K. Kang, S. J. Sibener, D. A. Muller and J. Park, *Science*, 2019, DOI: 10.1126/science.aax9385, eaax9385.
- 278 S. Qiu, M. Xue and G. Zhu, *Chem. Soc. Rev.*, 2014, **43**, 6116-6140.
- 279 A. J. Brown, N. A. Brunelli, K. Eum, F. Rashidi, J. R. Johnson, W. J. Koros, C. W. Jones and S. Nair, *Science*, 2014, **345**, 72.
- 280 X. Ma, P. Kumar, N. Mittal, A. Khlyustova, P. Daoutidis, K. A. Mkhoyan and M. Tsapatsis, *Science*, 2018, **361**, 1008.
- 281 J. Zhao, D. T. Lee, R. W. Yaga, M. G. Hall, H. F. Barton, I. R. Woodward, C. J. Oldham, H. J. Walls, G. W. Peterson and G. N. Parsons, *Angew. Chem. Int. Ed.*, 2016, **55**, 13224-13228.
- 282 Y. Zhang, S. Yuan, X. Feng, H. Li, J. Zhou and B. Wang, *J. Am. Chem. Soc.*, 2016, **138**, 5785-5788.
- 283 K. Ma, Y. Wang, Z. Chen, T. Islamoglu, C. Lai, X. Wang, B. Fei, O. K. Farha and J. H. Xin, *ACS Appl. Mater. Interfaces*, 2019, **11**, 22714-22721.
- 284 K. Ma, T. Islamoglu, Z. Chen, P. Li, M. C. Wasson, Y. Chen, Y. Wang, G. W. Peterson, J. H. Xin and O. K. Farha, *J. Am. Chem. Soc.*, 2019, **141**, 15626-15633.
- 285 D. T. Lee, J. D. Jamir, G. W. Peterson and G. N. Parsons, *Matter*, 2020, **2**, 404-415.
- 286 X. Zhang, Z. Chen, X. Liu, S. L. Hanna, X. Wang, R. Taheri-Ledari, A. Maleki, P. Li and O. K. Farha, *Chem. Soc. Rev.*, 2020, DOI: 10.1039/D0CS00997K.
- 287 S. Brunauer, P. H. Emmett and E. Teller, *J. Am. Chem. Soc.*, 1938, **60**, 309-319.
- 288 J. L. Rouquerol, P.; Rouquerol, F., ed. P. L. R.-R. Llewellyn, F.; Rouquerol, J.; Seaton, N., Eds, Elsevier, Amsterdam, 2007, vol. 160, p. 49.
- 289 D. A. Gómez-Gualdrón, P. Z. Moghadam, J. T. Hupp, O. K. Farha and R. Q. Snurr, *J. Am. Chem. Soc.*, 2016, **138**, 215-224.
- 290 A. P. Nelson, O. K. Farha, K. L. Mulfort and J. T. Hupp, *J. Am. Chem. Soc.*, 2009, **131**, 458-460.
- 291 O. K. Farha and J. T. Hupp, *Acc. Chem. Res.*, 2010, **43**, 1166-1175.
- 292 I. Senkovska and S. Kaskel, *Chem. Commun.*, 2014, **50**, 7089-7098.
- 293 L. Ma, A. Jin, Z. Xie and W. Lin, *Angew. Chem. Int. Ed.*, 2009, **48**, 9905-9908.
- 294 S. Horike, S. Shimomura and S. Kitagawa, *Nat. Chem.*, 2009, **1**, 695-704.
- 295 A. Schneemann, V. Bon, I. Schwedler, I. Senkovska, S. Kaskel and R. A. Fischer, *Chem. Soc. Rev.*, 2014, **43**, 6062-6096.
- 296 Z.-J. Lin, J. Lu, M. Hong and R. Cao, *Chem. Soc. Rev.*, 2014, **43**, 5867-5895.
- 297 J.-P. Zhang, H.-L. Zhou, D.-D. Zhou, P.-Q. Liao and X.-M. Chen, *Natl. Sci. Rev.*, 2017, **5**, 907-919.

- 298 K. C. Stylianou, J. Rabone, S. Y. Chong, R. Heck, J. Armstrong, P. V. Wiper, K. E. Jelfs, S. Zlatogorsky, J. Bacsá, A. G. McLennan, C. P. Ireland, Y. Z. Khimiyak, K. M. Thomas, D. Bradshaw and M. J. Rosseinsky, *J. Am. Chem. Soc.*, 2012, **134**, 20466-20478.
- 299 J. H. Lee, S. Jeoung, Y. G. Chung and H. R. Moon, *Coord. Chem. Rev.*, 2019, **389**, 161-188.
- 300 M. Shivanna, Q.-Y. Yang, A. Bajpai, S. Sen, N. Hosono, S. Kusaka, T. Pham, K. A. Forrest, B. Space, S. Kitagawa and M. J. Zaworotko, *Sci. Adv.*, 2018, **4**, 1636.
- 301 M. L. Foo, R. Matsuda and S. Kitagawa, *Chem. Mater.*, 2014, **26**, 310-322.
- 302 Y. Sakata, S. Furukawa, M. Kondo, K. Hirai, N. Horike, Y. Takashima, H. Uehara, N. Louvain, M. Meilikhov, T. Tsuruoka, S. Isoda, W. Kosaka, O. Sakata and S. Kitagawa, *Science*, 2013, **339**, 193.
- 303 R. Matsuda, R. Kitaura, S. Kitagawa, Y. Kubota, R. V. Belosludov, T. C. Kobayashi, H. Sakamoto, T. Chiba, M. Takata, Y. Kawazoe and Y. Mita, *Nature*, 2005, **436**, 238.
- 304 R. Kitaura, K. Seki, G. Akiyama and S. Kitagawa, *Angew. Chem. Int. Ed.*, 2003, **42**, 428-430.
- 305 S. Krause, N. Hosono and S. Kitagawa, *Angew. Chem. Int. Ed.*, 2020, **59**, 15325.
- 306 K. C. Stylianou, R. Heck, S. Y. Chong, J. Bacsá, J. T. A. Jones, Y. Z. Khimiyak, D. Bradshaw and M. J. Rosseinsky, *J. Am. Chem. Soc.*, 2010, **132**, 4119-4130.
- 307 A. Knebel, B. Geppert, K. Volgmann, D. I. Kolokolov, A. G. Stepanov, J. Twiefel, P. Heitjans, D. Volkmer and J. Caro, *Science*, 2017, **358**, 347.
- 308 F. X. Coudert, M. Jeffroy, A. H. Fuchs, A. Boutin and C. Mellot-Draznieks, *J. Am. Chem. Soc.*, 2008, **130**, 14294-14302.
- 309 F.-X. Coudert, *Chem. Mater.*, 2015, **27**, 1905-1916.
- 310 L. Li, R.-B. Lin, R. Krishna, X. Wang, B. Li, H. Wu, J. Li, W. Zhou and B. Chen, *J. Am. Chem. Soc.*, 2017, **139**, 7733-7736.
- 311 D. Tanaka, *Angew. Chem. Int. Ed.*, 2008, **47**, 3914-3918.
- 312 K. Uemura, R. Matsuda and S. Kitagawa, *J. Solid State Chem.*, 2005, **178**, 2420-2429.
- 313 J. Y. Kim, L. Zhang, R. Balderas-Xicohténcatl, J. Park, M. Hirscher, H. R. Moon and H. Oh, *J. Am. Chem. Soc.*, 2017, **139**, 17743-17746.
- 314 P. Lama and L. J. Barbour, *J. Am. Chem. Soc.*, 2018, **140**, 2145-2150.
- 315 Q. Chen, Z. Chang, W.-C. Song, H. Song, H.-B. Song, T.-L. Hu and X.-H. Bu, *Angew. Chem. Int. Ed.*, 2013, **52**, 11550-11553.
- 316 G. Férey and C. Serre, *Chem. Soc. Rev.*, 2009, **38**, 1380-1399.
- 317 P. Horcajada, *J. Am. Chem. Soc.*, 2008, **130**, 6774-6780.
- 318 C. Gu, N. Hosono, J.-J. Zheng, Y. Sato, S. Kusaka, S. Sakaki and S. Kitagawa, *Science*, 2019, **363**, 387.
- 319 S. Wannapaiboon, A. Schneemann, I. Hante, M. Tu, K. Epp, A. L. Semrau, C. Sternemann, M. Paulus, S. J. Baxter, G. Kieslich and R. A. Fischer, *Nat. Commun.*, 2019, **10**, 346.
- 320 S. Ma and H.-C. Zhou, *Chem. Commun.*, 2010, **46**, 44-53.
- 321 Z. Guo, H. Wu, G. Srinivas, Y. Zhou, S. Xiang, Z. Chen, Y. Yang, W. Zhou, M. O'Keeffe and B. Chen, *Angew. Chem. Int. Ed.*, 2011, **50**, 3178-3181.
- 322 Y. He, W. Zhou, G. Qian and B. Chen, *Chem. Soc. Rev.*, 2014, **43**, 5657-5678.
- 323 Y. Fang, S. Banerjee, E. A. Joseph, G. S. Day, M. Bosch, J. Li, Q. Wang, H. Drake, O. K. Ozdemir, J. M. Ornstein, Y. Wang, T.-B. Lu and H.-C. Zhou, *Chem. Eur. J.*, 2018, **24**, 16977-16982.

- 324 R. Grönker, V. Bon, P. Müller, U. Stoeck, S. Krause, U. Mueller, I. Senkovska and S. Kaskel, *Chem. Commun.*, 2014, **50**, 3450-3452.
- 325 J. A. Mason, M. Veenstra and J. R. Long, *Chem. Sci.*, 2014, **5**, 32-51.
- 326 T. Kundu, M. Wahiduzzaman, B. B. Shah, G. Maurin and D. Zhao, *Angew. Chem. Int. Ed.*, 2019, **58**, 8073-8077.
- 327 C.-C. Liang, Z.-L. Shi, C.-T. He, J. Tan, H.-D. Zhou, H.-L. Zhou, Y. Lee and Y.-B. Zhang, *J. Am. Chem. Soc.*, 2017, **139**, 13300-13303.
- 328 S. Kitagawa and M. Kondo, *Bull. Chem. Soc. Jpn*, 1998, **71**, 1739-1753.
- 329 M. Shivanna, Q.-Y. Yang, A. Bajpai, E. Patyk-Kazmierczak and M. J. Zaworotko, *Nat. Commun.*, 2018, **9**, 3080.
- 330 T. M. McDonald, J. A. Mason, X. Kong, E. D. Bloch, D. Gygi, A. Dani, V. Crocellà, F. Giordanino, S. O. Odoh, W. S. Drisdell, B. Vlasisavljevich, A. L. Dzubak, R. Poloni, S. K. Schnell, N. Planas, K. Lee, T. Pascal, L. F. Wan, D. Prendergast, J. B. Neaton, B. Smit, J. B. Kortright, L. Gagliardi, S. Bordiga, J. A. Reimer and J. R. Long, *Nature*, 2015, **519**, 303-308.
- 331 M. Z. Jacobson, W. G. Colella and D. M. Golden, *Science*, 2005, **308**, 1901-1905.
- 332 I. Staffell, D. Scamman, A. Velazquez Abad, P. Balcombe, P. E. Dodds, P. Ekins, N. Shah and K. R. Ward, *Energy Environ. Sci.*, 2019, **12**, 463-491.
- 333 Target Explanation Document: Onboard Hydrogen Storage for Light-Duty Fuel Cell Vehicles, U.S. Department of Energy, https://www.energy.gov/sites/prod/files/2017/05/f34/fcto_targets_onboard_hydro_storage_explanation.pdf, accessed May 2020.
- 334 D. A. Gómez-Gualdrón, T. C. Wang, P. García-Holley, R. M. Sawelewa, E. Argueta, R. Q. Snurr, J. T. Hupp, T. Yildirim and O. K. Farha, *ACS Appl. Mater. Interfaces*, 2017, **9**, 33419-33428.
- 335 A. Ahmed, Y. Liu, J. Purewal, L. D. Tran, A. G. Wong-Foy, M. Veenstra, A. J. Matzger and D. J. Siegel, *Energy Environ. Sci.*, 2017, **10**, 2459-2471.
- 336 *Journal*, 2016.
- 337 U. S. G. Survey, *Mineral Commodity Summaries* 2019.
- 338 S. N. Behera, M. Sharma, V. P. Aneja and R. Balasubramanian, *Environ Sci Pollut Res*, 2013, **20**, 8092-8131.
- 339 A. J. Rieth and M. Dincă, *J. Am. Chem. Soc.*, 2018, **140**, 3461-3466.
- 340 J. Sculley, D. Yuan and H.-C. Zhou, *Energy Environ. Sci.*, 2011, **4**, 2721-2735.
- 341 D. S. Sholl and R. P. Lively, *Nature News*, 2016, **532**, 435.
- 342 P. Angelini, T. Armstrong, R. Counce, W. Griffith, T. LKlasson, G. Muralidharan, C. Narula, V. Sikka, G. Closset and G. Keller, *DOE, EERE Office, Washington, DC*, 2005, 103.
- 343 K. Sumida, D. L. Rogow, J. A. Mason, T. M. McDonald, E. D. Bloch, Z. R. Herm, T. H. Bae and J. R. Long, *Chem. Rev.*, 2012, **112**, 724-781.
- 344 P. M. Bhatt, V. Guillermin, S. J. Datta, A. Shkurenko and M. Eddaoudi, *Chem*, 2020, **6**, 1613-1633.
- 345 J.-R. Li, J. Sculley and H.-C. Zhou, *Chem. Rev.*, 2012, **112**, 869-932.
- 346 K. Sumida, D. L. Rogow, J. A. Mason, T. M. McDonald, E. D. Bloch, Z. R. Herm, T.-H. Bae and J. R. Long, *Chem. Rev.*, 2012, **112**, 724-781.
- 347 H. K. Abdel-Aal, M. A. Aggour and M. A. Fahim, *Petroleum and gas field processing*, CRC press, 2015.

- 348 N. S. Bobbitt, M. L. Mendonca, A. J. Howarth, T. Islamoglu, J. T. Hupp, O. K. Farha and R. Q. Snurr, *Chem. Soc. Rev.*, 2017, **46**, 3357-3385.
- 349 S. R. Caskey, A. G. Wong-Foy and A. J. Matzger, *J. Am. Chem. Soc.*, 2008, **130**, 10870-10871.
- 350 S. Xiang, Y. He, Z. Zhang, H. Wu, W. Zhou, R. Krishna and B. Chen, *Nat. Commun.*, 2012, **3**, 954.
- 351 H. K. Izumi, J. E. Kirsch, C. L. Stern and K. R. Poeppelmeier, *Inorg. Chem.*, 2005, **44**, 884-895.
- 352 R. Gautier, M. D. Donakowski and K. R. Poeppelmeier, *J. Solid State Chem.*, 2012, **195**, 132-139.
- 353 P. M. Bhatt, Y. Belmabkhout, A. Cadiau, K. Adil, O. Shekhah, A. Shkurenko, L. J. Barbour and M. Eddaoudi, *J. Am. Chem. Soc.*, 2016, **138**, 9301-9307.
- 354 N. L. Rosi, J. Kim, M. Eddaoudi, B. Chen, M. O'Keeffe and O. M. Yaghi, *J. Am. Chem. Soc.*, 2005, **127**, 1504-1518.
- 355 P. D. C. Dietzel, Y. Morita, R. Blom and H. Fjellvåg, *Angew. Chem. Int. Ed.*, 2005, **44**, 6354-6358.
- 356 D. Britt, H. Furukawa, B. Wang, T. G. Glover and O. M. Yaghi, *Proc. Natl. Acad. Sci. U.S.A.*, 2009, **106**, 20637.
- 357 T. M. McDonald, W. R. Lee, J. A. Mason, B. M. Wiers, C. S. Hong and J. R. Long, *J. Am. Chem. Soc.*, 2012, **134**, 7056-7065.
- 358 R. L. Siegelman, T. M. McDonald, M. I. Gonzalez, J. D. Martell, P. J. Milner, J. A. Mason, A. H. Berger, A. S. Bhowan and J. R. Long, *J. Am. Chem. Soc.*, 2017, **139**, 10526-10538.
- 359 E. J. Kim, R. L. Siegelman, H. Z. H. Jiang, A. C. Forse, J.-H. Lee, J. D. Martell, P. J. Milner, J. M. Falkowski, J. B. Neaton, J. A. Reimer, S. C. Weston and J. R. Long, *Science*, 2020, **369**, 392.
- 360 Y. Belmabkhout, P. M. Bhatt, K. Adil, R. S. Pillai, A. Cadiau, A. Shkurenko, G. Maurin, G. Liu, W. J. Koros and M. Eddaoudi, *Nat. Energy*, 2018, **3**, 1059-1066.
- 361 S. H. Schneider and F. K. Hare, *Encyclopedia of climate and weather*, Oxford university press New York, 1996.
- 362 A. M. Wright, A. J. Rieth, S. Yang, E. N. Wang and M. Dincă, *Chem. Sci.*, 2018, **9**, 3856-3859.
- 363 A. J. Rieth, S. Yang, E. N. Wang and M. Dincă, *ACS Cent. Sci.*, 2017, **3**, 668-672.
- 364 D. Ma, P. Li, X. Duan, J. Li, P. Shao, Z. Lang, L. Bao, Y. Zhang, Z. Lin and B. Wang, *Angew. Chem. Int. Ed.*, 2020, **59**, 3905-3909.
- 365 C. R. Second, E. Edition, G. Ertl, H. Knözinger, F. Schüth, J. Weitkamp, W.-V. V. G. KGaA and Co, *Journal*, 2008.
- 366 C. Copéret, A. Comas-Vives, M. P. Conley, D. P. Estes, A. Fedorov, V. Mougel, H. Nagee, F. Núñez-Zarur and P. A. Zhizhko, *Chem. Rev.*, 2016, **116**, 323-421.
- 367 X.-F. Yang, A. Wang, B. Qiao, J. Li, J. Liu and T. Zhang, *Acc. Chem. Res.*, 2013, **46**, 1740-1748.
- 368 J. Höcker, J.-O. Krispeneit, T. Schmidt, J. Falta and J. I. Flege, *Nanoscale*, 2017, **9**, 9352-9358.
- 369 H. Ha, S. Yoon, K. An and H. Y. Kim, *ACS Catal.*, 2018, **8**, 11491-11501.
- 370 M. Nolan and G. W. Watson, *J. Phys. Chem. B*, 2006, **110**, 16600-16606.

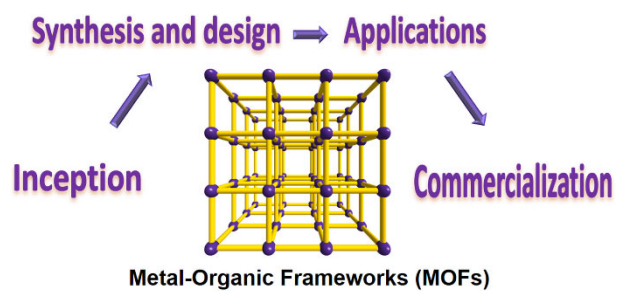
- 371 K.-i. Otake, Y. Cui, C. T. Buru, Z. Li, J. T. Hupp and O. K. Farha, *J. Am. Chem. Soc.*, 2018, **140**, 8652-8656.
- 372 S. Øien-Ødegaard, G. C. Shearer, D. S. Wragg and K. P. Lillerud, *Chem. Soc. Rev.*, 2017, **46**, 4867-4876.
- 373 J. M. Thomas, R. Raja and D. W. Lewis, *Angew. Chem. Int. Ed.*, 2005, **44**, 6456-6482.
- 374 M. C. Wasson, C. T. Buru, Z. Chen, T. Islamoglu and O. K. Farha, *Appl. Catal., A.*, 2019, **586**, 117214.
- 375 J. Lee, O. K. Farha, J. Roberts, K. A. Scheidt, S. T. Nguyen and J. T. Hupp, *Chem. Soc. Rev.*, 2009, **38**, 1450-1459.
- 376 D. Farrusseng, S. Aguado and C. Pinel, *Angew. Chem. Int. Ed.*, 2009, **48**, 7502-7513.
- 377 A. Corma, H. García and F. X. Llabrés i Xamena, *Chem. Rev.*, 2010, **110**, 4606-4655.
- 378 P. Horcajada, S. Surblé, C. Serre, D.-Y. Hong, Y.-K. Seo, J.-S. Chang, J.-M. Grenèche, I. Margiolaki and G. Férey, *Chem. Commun.*, 2007, DOI: 10.1039/B704325B, 2820-2822.
- 379 Y. Liu, J. F. Eubank, A. J. Cairns, J. Eckert, V. C. Kravtsov, R. Luebke and M. Eddaoudi, *Angew. Chem. Int. Ed.*, 2007, **46**, 3278-3283.
- 380 M. Pang, A. J. Cairns, Y. Liu, Y. Belmabkhout, H. C. Zeng and M. Eddaoudi, *J. Am. Chem. Soc.*, 2013, **135**, 10234-10237.
- 381 Y. Belmabkhout, R. S. Pillai, D. Alezi, O. Shekhah, P. M. Bhatt, Z. Chen, K. Adil, S. Vaesen, G. De Weireld, M. Pang, M. Suetin, A. J. Cairns, V. Solovyeva, A. Shkurenko, O. El Tall, G. Maurin and M. Eddaoudi, *J. Mater. Chem. A*, 2017, **5**, 3293-3303.
- 382 H. Chevreau, A. Permyakova, F. Nouar, P. Fabry, C. Livage, F. Ragon, A. Garcia-Marquez, T. Devic, N. Steunou, C. Serre and P. Horcajada, *CrystEngComm*, 2016, **18**, 4094-4101.
- 383 A. Dhakshinamoorthy, M. Alvaro, H. Chevreau, P. Horcajada, T. Devic, C. Serre and H. Garcia, *Catal. Sci. Technol.*, 2012, **2**, 324-330.
- 384 D. Feng, K. Wang, Z. Wei, Y.-P. Chen, C. M. Simon, R. K. Arvapally, R. L. Martin, M. Bosch, T.-F. Liu, S. Fordham, D. Yuan, M. A. Omary, M. Haranczyk, B. Smit and H.-C. Zhou, *Nat. Commun.*, 2014, **5**, 5723.
- 385 H. F. Drake, G. S. Day, S. W. Vali, Z. Xiao, S. Banerjee, J. Li, E. A. Joseph, J. E. Kuszynski, Z. T. Perry, A. Kirchon, O. K. Ozdemir, P. A. Lindahl and H.-C. Zhou, *Chem. Commun.*, 2019, **55**, 12769-12772.
- 386 M. C. Simons, J. G. Vitillo, M. Babucci, A. S. Hoffman, A. Boubnov, M. L. Beauvais, Z. Chen, C. J. Cramer, K. W. Chapman, S. R. Bare, B. C. Gates, C. C. Lu, L. Gagliardi and A. Bhan, *J. Am. Chem. Soc.*, 2019, **141**, 18142-18151.
- 387 M. Barona, S. Ahn, W. Morris, W. Hoover, J. M. Notestein, O. K. Farha and R. Q. Snurr, *ACS Catal.*, 2020, **10**, 1460-1469.
- 388 A. Friboulet, F. Rieger, D. Goudou, G. Amitai and P. Taylor, *Biochemistry*, 1990, **29**, 914-920.
- 389 K. Kim, O. G. Tsay, D. A. Atwood and D. G. Churchill, *Chem. Rev.*, 2011, **111**, 5345-5403.
- 390 Y. Zhang, X. Zhang, J. Lyu, K.-i. Otake, X. Wang, L. R. Redfern, C. D. Malliakas, Z. Li, T. Islamoglu, B. Wang and O. K. Farha, *J. Am. Chem. Soc.*, 2018, **140**, 11179-11183.
- 391 H. Furukawa, F. Gándara, Y.-B. Zhang, J. Jiang, W. L. Queen, M. R. Hudson and O. M. Yaghi, *J. Am. Chem. Soc.*, 2014, **136**, 4369-4381.
- 392 A. M. Rice, G. A. Leith, O. A. Ejegbavwo, E. A. Dolgoplova and N. B. Shustova, *ACS Energy Lett.*, 2019, **4**, 1938-1946.

- 393 X. Cao, C. Tan, M. Sindoro and H. Zhang, *Chem. Soc. Rev.*, 2017, **46**, 2660-2677.
- 394 A. M. Appel, J. E. Bercaw, A. B. Bocarsly, H. Dobbek, D. L. DuBois, M. Dupuis, J. G. Ferry, E. Fujita, R. Hille, P. J. A. Kenis, C. A. Kerfeld, R. H. Morris, C. H. F. Peden, A. R. Portis, S. W. Ragsdale, T. B. Rauchfuss, J. N. H. Reek, L. C. Seefeldt, R. K. Thauer and G. L. Waldrop, *Chem. Rev.*, 2013, **113**, 6621-6658.
- 395 M. Aresta, A. Dibenedetto and A. Angelini, *Chem. Rev.*, 2014, **114**, 1709-1742.
- 396 E. E. Benson, C. P. Kubiak, A. J. Sathrum and J. M. Smieja, *Chem. Soc. Rev.*, 2009, **38**, 89-99.
- 397 E. V. Kondratenko, G. Mul, J. Baltrusaitis, G. O. Larrazábal and J. Pérez-Ramírez, *Energy Environ. Sci.*, 2013, **6**, 3112-3135.
- 398 M. K. Debe, *Nature*, 2012, **486**, 43-51.
- 399 Y. Jiao, Y. Zheng, M. Jaroniec and S. Z. Qiao, *Chem. Soc. Rev.*, 2015, **44**, 2060-2086.
- 400 M. Wang, K. Torbensen, D. Salvatore, S. Ren, D. Joulié, F. Dumoulin, D. Mendoza, B. Lassalle-Kaiser, U. Işci, C. P. Berlinguette and M. Robert, *Nat. Commun.*, 2019, **10**, 3602.
- 401 M. Schreier, F. Héroguel, L. Steier, S. Ahmad, J. S. Luterbacher, M. T. Mayer, J. Luo and M. Grätzel, *Nat. Energy*, 2017, **2**, 17087.
- 402 X.-M. Hu, H. H. Hval, E. T. Bjerglund, K. J. Dalgaard, M. R. Madsen, M.-M. Pohl, E. Welter, P. Lamagni, K. B. Buhl, M. Bremholm, M. Beller, S. U. Pedersen, T. Skrydstrup and K. Daasbjerg, *ACS Catal.*, 2018, **8**, 6255-6264.
- 403 M. R. Wasielewski, *Chem. Rev.*, 1992, **92**, 435-461.
- 404 D. Ravelli, D. Dondi, M. Fagnoni and A. Albini, *Chem. Soc. Rev.*, 2009, **38**, 1999-2011.
- 405 J. Schneider, M. Matsuoka, M. Takeuchi, J. Zhang, Y. Horiuchi, M. Anpo and D. W. Bahnemann, *Chem. Rev.*, 2014, **114**, 9919-9986.
- 406 F. E. Osterloh, *Chem. Mater.*, 2008, **20**, 35-54.
- 407 M. A. Fox and M. T. Dulay, *Chem. Rev.*, 1993, **93**, 341-357.
- 408 C. K. Prier, D. A. Rankic and D. W. C. MacMillan, *Chem. Rev.*, 2013, **113**, 5322-5363.
- 409 P. V. Kamat, *J. Phys. Chem. B*, 2002, **106**, 7729-7744.
- 410 L. Zeng, X. Guo, C. He and C. Duan, *ACS Catal.*, 2016, **6**, 7935-7947.
- 411 J.-L. Wang, C. Wang and W. Lin, *ACS Catal.*, 2012, **2**, 2630-2640.
- 412 A. Dhakshinamoorthy, A. M. Asiri and H. García, *Angew. Chem. Int. Ed.*, 2016, **55**, 5414-5445.
- 413 M. A. Nasalevich, M. van der Veen, F. Kapteijn and J. Gascon, *CrystEngComm*, 2014, **16**, 4919-4926.
- 414 C. Wang, Z. Xie, K. E. deKrafft and W. Lin, *J. Am. Chem. Soc.*, 2011, **133**, 13445-13454.
- 415 J. Liu, L. Chen, H. Cui, J. Zhang, L. Zhang and C.-Y. Su, *Chem. Soc. Rev.*, 2014, **43**, 6011-6061.
- 416 Y.-B. Huang, J. Liang, X.-S. Wang and R. Cao, *Chem. Soc. Rev.*, 2017, **46**, 126-157.
- 417 L. Jiao and H.-L. Jiang, *Chem*, 2019, **5**, 786-804.
- 418 V. Pascanu, G. González Miera, A. K. Inge and B. Martín-Matute, *J. Am. Chem. Soc.*, 2019, **141**, 7223-7234.
- 419 T. A. Goetjen, J. Liu, Y. Wu, J. Sui, X. Zhang, J. T. Hupp and O. K. Farha, *Chem. Commun.*, 2020, **56**, 10409-10418.
- 420 C. Wang, B. An and W. Lin, *ACS Catal.*, 2019, **9**, 130-146.
- 421 F. Ke, Y.-P. Yuan, L.-G. Qiu, Y.-H. Shen, A.-J. Xie, J.-F. Zhu, X.-Y. Tian and L.-D. Zhang, *J. Mater. Chem.*, 2011, **21**, 3843-3848.

- 422 T. Kundu, S. Mitra, P. Patra, A. Goswami, D. Díaz Díaz and R. Banerjee, *Chem. Eur. J.*, 2014, **20**, 10514-10518.
- 423 X. Zhu, J. Gu, Y. Wang, B. Li, Y. Li, W. Zhao and J. Shi, *Chem. Commun.*, 2014, **50**, 8779-8782.
- 424 X.-G. Wang, Z.-Y. Dong, H. Cheng, S.-S. Wan, W.-H. Chen, M.-Z. Zou, J.-W. Huo, H.-X. Deng and X.-Z. Zhang, *Nanoscale*, 2015, **7**, 16061-16070.
- 425 F. Lyu, Y. Zhang, R. N. Zare, J. Ge and Z. Liu, *Nano Lett.*, 2014, **14**, 5761-5765.
- 426 V. Lykourinou, Y. Chen, X.-S. Wang, L. Meng, T. Hoang, L.-J. Ming, R. L. Musselman and S. Ma, *J. Am. Chem. Soc.*, 2011, **133**, 10382-10385.
- 427 Y. Chen, V. Lykourinou, C. Vetromile, T. Hoang, L.-J. Ming, R. W. Larsen and S. Ma, *J. Am. Chem. Soc.*, 2012, **134**, 13188-13191.
- 428 Y. Chen, V. Lykourinou, T. Hoang, L.-J. Ming and S. Ma, *Inorg. Chem.*, 2012, **51**, 9156-9158.
- 429 D. Feng, T.-F. Liu, J. Su, M. Bosch, Z. Wei, W. Wan, D. Yuan, Y.-P. Chen, X. Wang, K. Wang, X. Lian, Z.-Y. Gu, J. Park, X. Zou and H.-C. Zhou, *Nat. Commun.*, 2015, **6**, 5979.
- 430 X. Lian, Y.-P. Chen, T.-F. Liu and H.-C. Zhou, *Chem. Sci.*, 2016, **7**, 6969-6973.
- 431 X. Lian, Y. Fang, E. Joseph, Q. Wang, J. Li, S. Banerjee, C. Lollar, X. Wang and H.-C. Zhou, *Chem. Soc. Rev.*, 2017, **46**, 3386-3401.
- 432 M. B. Majewski, A. J. Howarth, P. Li, M. R. Wasielewski, J. T. Hupp and O. K. Farha, *CrystEngComm*, 2017, **19**, 4082-4091.
- 433 R. J. Drout, L. Robison and O. K. Farha, *Coord. Chem. Rev.*, 2019, **381**, 151-160.
- 434 J. Yang and Y.-W. Yang, *Small*, 2020, **16**, 1906846.
- 435 H. An, M. Li, J. Gao, Z. Zhang, S. Ma and Y. Chen, *Coord. Chem. Rev.*, 2019, **384**, 90-106.
- 436 Zeolites Statistics and Information, <https://www.usgs.gov/centers/nmic/zeolites-statistics-and-information#:~:text=Zeolites%20are%20hydrated%20aluminosilicates%20of,laumontite%2C%20mordenite%2C%20and%20phillipsite.>
- 437 Y. G. Chung, E. Haldoupis, B. J. Bucior, M. Haranczyk, S. Lee, H. Zhang, K. D. Vogiatzis, M. Milisavljevic, S. Ling, J. S. Camp, B. Slater, J. I. Siepmann, D. S. Sholl and R. Q. Snurr, *J. Chem. Eng. Data.*, 2019, **64**, 5985-5998.
- 438 Search "Metal–Organic Frameworks" and select the year of "2019", [https://academic.microsoft.com/topic/179366358/publication/search?q=Metal-organic%20framework&qe=And\(Composite\(F.FId%253D179366358\)%252CTy%253D%270%27\)&f=&orderBy=0](https://academic.microsoft.com/topic/179366358/publication/search?q=Metal-organic%20framework&qe=And(Composite(F.FId%253D179366358)%252CTy%253D%270%27)&f=&orderBy=0), (accessed 6 september 2020).
- 439 A new class of adsorbent materials offer high capacity storage and safe delivery of dopant gases, <https://www.numat-tech.com/ion-x-oem-data/>, (accessed 6 september 2020).
- 440 Versum Materials and NuMat Technologies to Commercialize Next-Generation Adsorbent Technology for Delivery of Dopant Gases, <https://www.businesswire.com/news/home/20170731005340/en/Versum-Materials-NuMat-Technologies-Commercialize-Next-Generation-Adsorbent>, (accessed 6 september 2020).
- 441 L. Rosenberger, C. von Essen, A. Khutia, C. Kühn, K. Urbahns, K. Georgi, R. W. Hartmann and L. Badolo, *Drug Metab. Dispos.*, 2020, **48**, 587.
- 442 R. B. Getman, Y.-S. Bae, C. E. Wilmer and R. Q. Snurr, *Chem. Rev.*, 2012, **112**, 703-723.

- 443 C. E. Wilmer, M. Leaf, C. Y. Lee, O. K. Farha, B. G. Hauser, J. T. Hupp and R. Q. Snurr, *Nat. Chem.*, 2012, **4**, 83-89.
- 444 Földner, G. (October, 2018). *Adsorptionskälte aus Abwärme flüssiggekühlter CPUs in HPC Rechenzentren - Material- und Komponentenentwicklung. D. Presentation given at Chillventa Congress 2018, Nürnberg, Germany.*
- 445 L. R. Redfern and O. K. Farha, *Chem. Sci.*, 2019, **10**, 10666-10679.
- 446 A. J. Howarth, Y. Liu, P. Li, Z. Li, T. C. Wang, J. T. Hupp and O. K. Farha, *Nat Rev Mater.*, 2016, **1**, 15018.
- 447 M. Shoaee, M. W. Anderson and M. P. Attfield, *Angew. Chem. Int. Ed.*, 2008, **47**, 8525-8528.
- 448 N. S. John, C. Scherb, M. Shöâèè, M. W. Anderson, M. P. Attfield and T. Bein, *Chem. Commun.*, 2009, 6294-6296.
- 449 N. Hosono, A. Terashima, S. Kusaka, R. Matsuda and S. Kitagawa, *Nat. Chem.*, 2019, **11**, 109-116.
- 450 D. Zhang, Y. Zhu, L. Liu, X. Ying, C.-E. Hsiung, R. Sougrat, K. Li and Y. Han, *Science*, 2018.
- 451 L. Liu, Z. Chen, J. Wang, D. Zhang, Y. Zhu, S. Ling, K.-W. Huang, Y. Belmabkhout, K. Adil, Y. Zhang, B. Slater, M. Eddaoudi and Y. Han, *Nat. Chem.*, 2019, **11**, 622-628.
- 452 Y. Zhu, J. Ciston, B. Zheng, X. Miao, C. Czarnik, Y. Pan, R. Sougrat, Z. Lai, C.-E. Hsiung, K. Yao, I. Pinnau, M. Pan and Y. Han, *Nat. Mater.*, 2017, **16**, 532-536.
- 453 Y. Li, K. Wang, W. Zhou, Y. Li, R. Vila, W. Huang, H. Wang, G. Chen, G.-H. Wu, Y. Tsao, H. Wang, R. Sinclair, W. Chiu and Y. Cui, *Matter*, 2019, **1**, 428-438.
- 454 S. Kato, R. J. Drout and O. K. Farha, *Cell Rep. Phys. Sci.*, 2020, **1**, 100006.
- 455 R. J. Drout, S. Kato, H. Chen, F. A. Son, K.-i. Otake, T. Islamoglu, R. Q. Snurr and O. K. Farha, *J. Am. Chem. Soc.*, 2020, **142**, 12357-12366.
- 456 Z. Ji, T. Li and O. M. Yaghi, *Science*, 2020, **369**, 674.
- 457 S. Wang and C. Serre, *ACS Sustain Chem Eng.*, 2019, **7**, 11911-11927.
- 458 C. Duan, Y. Yu, J. Xiao, X. Zhang, L. Li, P. Yang, J. Wu and H. Xi, *Sci. China Mater.*, 2020, **63**, 667-685.
- 459 Z. Chen, X. Wang, H. Noh, G. Ayoub, G. W. Peterson, C. T. Buru, T. Islamoglu and O. K. Farha, *CrystEngComm*, 2019, **21**, 2409-2415.
- 460 M. R. DeStefano, T. Islamoglu, S. J. Garibay, J. T. Hupp and O. K. Farha, *Chem. Mater.*, 2017, **29**, 1357-1361.
- 461 T. Stolar and K. Užarević, *CrystEngComm*, 2020, **22**, 4511-4525.
- 462 T. Frišćić, C. Mottillo and H. M. Titi, *Angew. Chem. Int. Ed.*, 2020, **59**, 1018-1029.
- 463 You've Probably Never Heard of MOFs, but..., <https://blogs.scientificamerican.com/observations/youve-probably-never-heard-of-mofs-but/>, (accessed 6 september 2020).

A table of contents entry



We provide a brief overview of the state of the MOF field from the inception, synthesis, potential applications, and finally, to their commercialization.